EXHUMATION MECHANISMS OF ECLOGITE IN THE SOUTHERN APPALACHIANS AND EVIDENCE FOR POST-CHEROKEE OROGENY MOVEMENT

James L. Bridgeman III

A thesis submitted to the faculty at the University of North Carolina at Chapel Hill in partial fulfillment of the requirements for the degree of Master of Science in the Department of Geological Sciences.

Chapel Hill
2015

Approved by:

Kevin G. Stewart

James P. Hibbard

Drew S. Coleman

ABSTRACT

James L. Bridgeman III: Exhumation Mechanisms of Eclogite in the Southern Appalachians and Evidence for Post-Cherokee Orogeny Movement
(Under the direction of Kevin G. Stewart)

The Bakersville, NC eclogite bodies in the southern Appalachians record peak metamorphic conditions of the Taconic orogeny. These high-pressure rocks are surrounded by amphibolite-facies rocks of the Ashe Metamorphic Suite. The eclogite zircons record ages of 460.7 ± 3.2 Ma, temperatures of 703-775 °C, and the zircon REE patterns indicate that they grew at eclogite-facies conditions. The amphibolite zircons record ages of 415 ± 3.8 Ma, temperatures of 614-669 °C, and their REE patterns indicate that the zircons did not grow in the presence of garnet, which are present at eclogite conditions. These differences suggest that the amphibolites are not retrograded eclogite and that the Bakersville eclogite was emplaced into lower-grade rocks during its exhumation, consistent with either driven cavity flow or plunger-driven exhumation models. The Silurian-Devonian age of the amphibolite zircon may record crustal thickening and burial related to post-Cherokee orogeny movement along the Burnsville fault.

ACKNOWLEDGEMENTS

I would like to thank my advisor, Kevin Stewart, his advice and guidance was invaluable to this thesis. My committee members, Drew Coleman and Jim Hibbard, also provided excellent feedback and conversations that have greatly improved this work. Thank you also to Jesse Hill and John DeDecker for their assistance with field work, as well as Connor Lawrence, Ryan Frasier and Ryan Mills for their help with zircon preparation and dating. This research was supported by the Martin fund and Jesse Davis travel funds.

I would also like to thank Mark Adams for providing me the opportunity to work in Spruce Pine, NC and his mentorship in Blue Ridge geology. He introduced me to the Bakersville eclogite roadcut several years ago, which sparked an interest that has culminated into this thesis.

Finally, I could not have completed this thesis without the love and support from my wife, Andrea. You give me purpose.

TABLE OF CONTENTS

LIST OF TABLES

LIST OF FIGURES

LIST OF ABBREVIATIONS

AMS ..... Ashe Metamorphic Suite

CL ..... Cathodoluminescence

Eu ..... Europium

GPa ..... Giga Pascal

HREE ..... Heavy rare earth elements

ICPMS ..... Inductively coupled plasma mass spectrometer

ID-TIMS ..... Isotopic Dilution Thermal Ionization Mass Spectrometry

Km ..... Kilometers

LASS ..... Laser-ablation split-stream

LREE ..... Light rare earth elements

m ..... meters

Ma ..... Million years

mm ..... Millimeters

MORB ..... Mid ocean ridge basalt

MREE ..... Middle rare earth elements

P ..... Pressure

Pb ..... Lead

REE ..... Rare earth elements

SEM ..... Scanning electron microscope

T ..... Temperature

Th ..... Thorium

Ti ..... Titanium

U.....Uranium

UHP..... Ultra-high pressure

XRF..... X-ray Fluorescence

Zr.....Zirconium

α .....activity

σ .....sigma or error

INTRODUCTION

The Ashe Metamorphic Suite is a metamorphosed accretionary wedge in the Eastern Blue Ridge province of the southern Appalachians (Rankin, 1970; Abbot and Raymond, 1984; Figure 1). It contains amphibolite-facies schist, gneiss, amphibolite, minor ultramafic bodies, and rare eclogite (Abbott and Raymond, 1984). Lenses of eclogite, as large as 1000 m by 100 m and up to 300 m thick, occur near Bakersville, NC (Willard and Adams, 1994; Adams et al., 1995). There are also small cm-scale layers of retrograded eclogite north of Boone, NC that lie in the same structural position in the Ashe Metamorphic Suite as the Bakersville eclogite, but are separated by the Grandfather Mountain window (Abbott and Greenwood, 2001). It remains unclear how these bodies of eclogite were exhumed to the surface.

There are many models of exhumation that have been proposed for eclogite bodies, which can be generally grouped into two types—those that exhume individual eclogite blocks into lower-grade rocks, and those that exhume large, regional-scale eclogite terranes. Mechanisms that bring up individual blocks of eclogite have circulatory flow within the accretionary wedge or subduction channel, which pushes the high-pressure rocks up into a lower-grade matrix. The exhumation of regional-scale eclogite terranes is caused by the reversal of subduction, driven by forces including buoyancy or slab breakoff.

One way to tell which exhumation style is more likely is to test the rocks surrounding the eclogite for evidence of eclogite-facies conditions. Eclogite exhumed within a high-pressure terrane will be surrounded by high-pressure rocks, whereas individual eclogite bodies exhumed through subduction channel circulation will be surrounded by lower-pressure rocks. However,

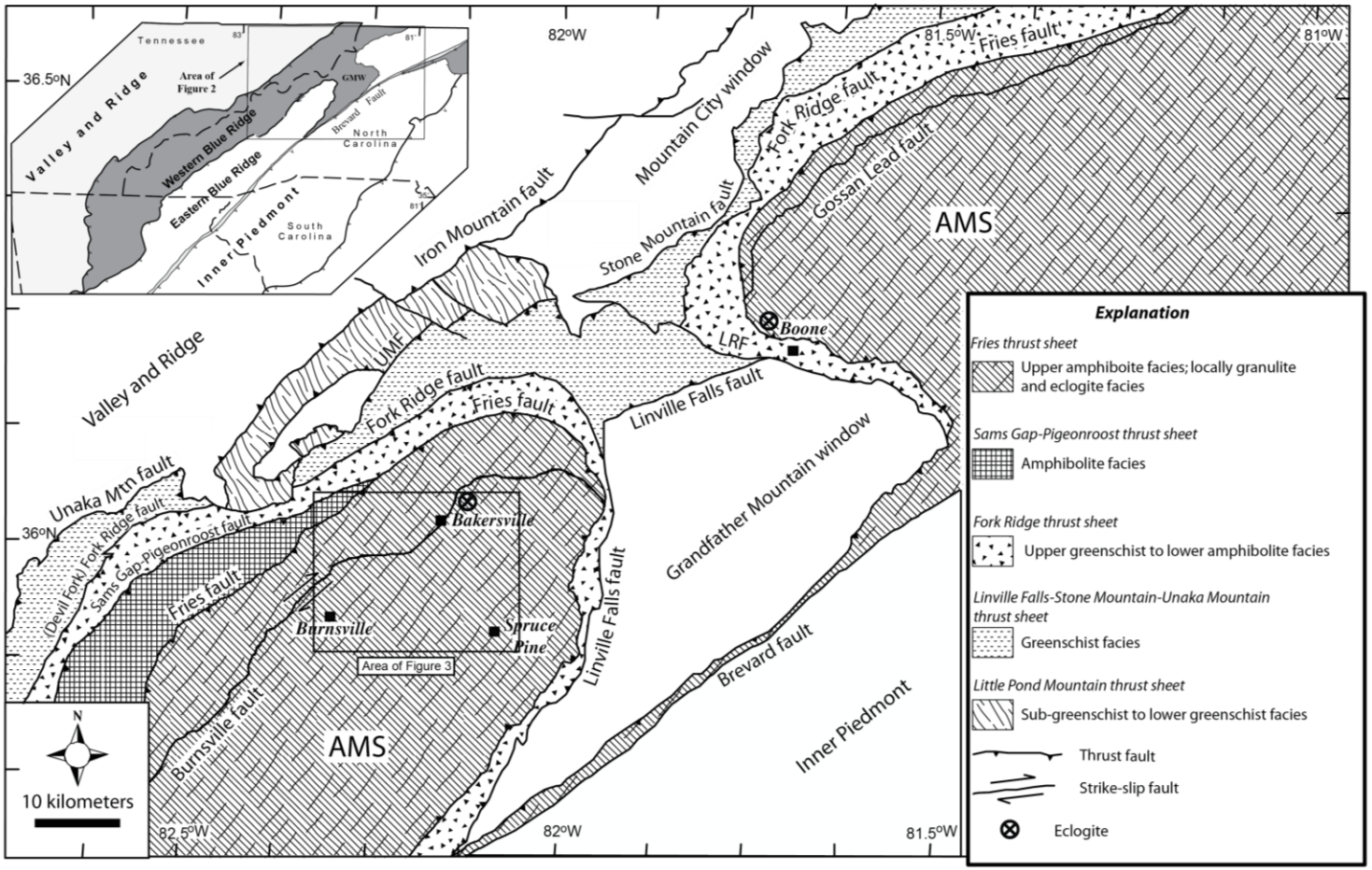

Figure 1. Geological map of the Blue Ridge Alleghanian thrust complex showing the locations of the Bakersville eclogite from Willard and Adams (1994) and the Boone retrograded eclogite from Abbott and Greenwood (2001). AMS- Ashe Metamorphic Suite. Modified from Trupe et al. (2004).

the relationship can become ambiguous if the high-pressure terranes experienced retrograde conditions. For example, the Pohorje Mountains in the Eastern Alps have *in situ* eclogite hosted by lower-grade metapelites and gneisses. The only evidence of previous eclogite-facies conditions in the lower-grade rocks are eclogite-facies mineral inclusions and REE patterns in the zircons (Janak et al., 2009).

The Bakersville eclogite has characteristics compatible with both sets of models that either exhume individual blocks or regional eclogite terranes. The accretionary-wedge setting supports subduction channel back-flow, but Syvertsen (2006) determined that the scattered eclogite blocks preserved parallel alignment of the eclogite-facies fabric. Her study found alignment within the blocks, which suggests they came up as a coherent slab, typical of exhumation within a larger terrane (Syvertsen, 2006). Retrograded eclogite near Boone, NC could represent another isolated block, or could suggest that a large area of the Ashe Metamorphic Suite experienced eclogite-facies conditions.

To test which exhumation style is most likely for the Bakersville eclogite, we examined the surrounding amphibolite bodies to see if they contain evidence of eclogite-facies conditions. Retrograded eclogite and amphibolite are petrologically indistinguishable in the Blue Ridge (Adams et al., 1995). Both rock types have similar mineralogy, MORB geochemical signature, and texture (Miller et al., 2010; Adams et al., 1995). To tell if the amphibolite bodies that surround the eclogite have retrograded from eclogite, we analyzed zircons from the amphibolites, zircons from the eclogite, and zircons from known retrograded eclogite. The zircons contain trace elements that can be measured to find U-Pb ages of the rocks, crystallization temperatures using Ti-in-zircon thermometry, and coexisting minerals during crystallization using the REE patterns. We compared the zircon signature of the amphibolite zircons to that of the eclogite zircons and known retrograded eclogite zircons to test whether the amphibolite zircons

crystallized at eclogite-facies conditions. If the amphibolite appears to be retrograded eclogite, then the region may have been part of a larger eclogite-facies terrane, brought to the surface by one of the large slab exhumation mechanisms. If the amphibolite is not retrograded eclogite and has a differing metamorphic history, then the eclogite is likely an isolated block exhumed through cyclic flow within the subduction channel.

EXHUMATION MODELS

Eclogite can be brought to the surface through combinations of subduction channel mechanisms, buoyancy forces, erosion, faulting, and slab breakoff (Platt, 1993; Warren, 2013). These exhumation mechanisms can be generally grouped into two types—those that bring up individual blocks of eclogite, and those that exhume regional eclogite-facies terranes. Models that explain the exhumation of individual blocks of eclogite include the corner-flow model (Cloos, 1982; Figure 2A), driven cavity flow (Burov et al., 2001; Figure 2B), and plunger expulsion (Warren et al., 2008; Figure 2C). Corner flow allows blocks of eclogite, plucked from the down-going slab, to get caught in circulatory flow within the accretionary wedge, and be carried up to the middle and upper crust (Warren, 2013). Driven cavity flow operates the same way, but occurs at greater depths within the subduction channel and involves the flow of serpentinite rather than accretionary wedge sediments (Burov et al., 2001; Guillot et al., 2001). Plunger expulsion is caused by the insertion of colder, stronger crust into the subduction channel that expels hotter, weaker material (Warren et al., 2008). All of these mechanisms emplace high-pressure rocks into lower-grade rocks, as in the Franciscan complex of California or the Lotru Metamorphic Suite in the South Carpathians of Romania (Ernst, 1984; Sabau and Massone, 2003). In the Lotru Metamorphic Suite, the eclogite pods show higher P-T conditions than the host rocks, suggesting they were emplaced in the subduction channel before a later amphibolite-facies metamorphic event (Sabau and Massonne, 2003).

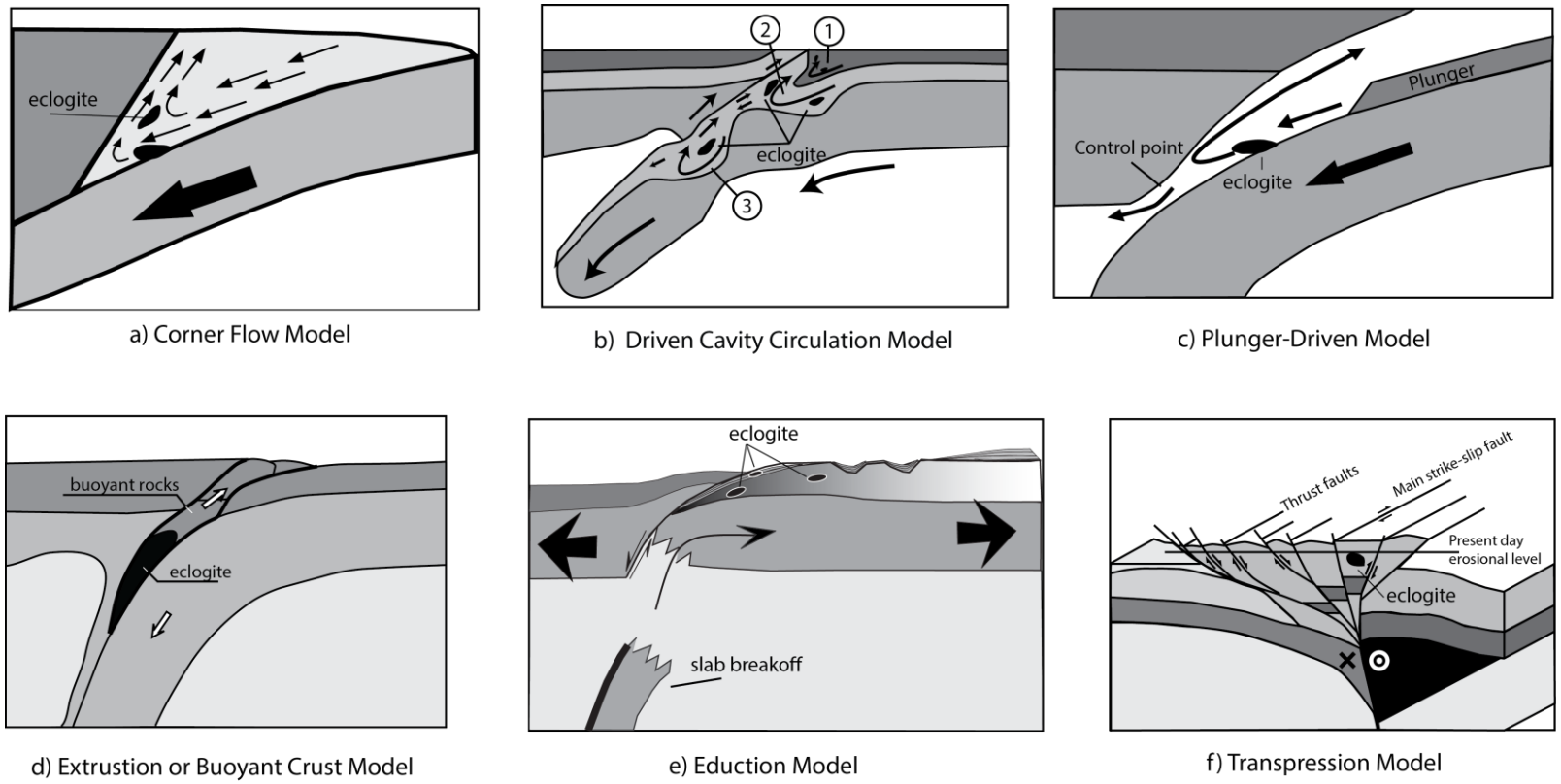

Figure 2. Diagrams showing models of exhumation. Models that bring up small eclogite blocks: (a) Corner flow model where the downgoing slab drives circulatory flow and carries blocks up in the accretionary mélange. Modified from Cloos (1982). (b) Driven cavity flow, where upward flow is driven by traction of the subducting plate. Driven cavity flow is similar to corner flow, but occurs at greater depths within the subduction channel and involves the flow of serpentinite rather than accretionary wedge sediments. The three eddy flows are at (1) 0-30 km, (2) 30-70 km, and (3) 80-120 km. Modified from Burov (2001). (c) Plunger-driven expulsion occurs when a more rigid body enters the subduction channel and expels hotter, weaker material. Modified from Warren et al. (2008). Models that exhume larger scale eclogite terranes: (d) Extrusion or buoyant crust model, where eclogite is surrounded by more buoyant rocks that pull the eclogite to the surface. Modified from Hacker et al. (2013). (E) Eduction occurs when slab breakoff triggers rebound of the subducting plate, pulling large eclogite facies terranes from depth. Modified from Brueckner and Cuthbert (2013). (F) Transpression occurs when high pressure material is squeezed upward from depth by oblique collision of strike-slipping plates. Modified from Camacho and McDougall (2000).

Regional eclogite-facies terranes, like the Western Gneiss region of Norway or the Dabie Sulu orogen in China expose >10,000 km^2 of eclogite-facies rocks (Sabau and Massonne, 2003; Kylander-Clark et al., 2012; Brueckner and Cuthbert, 2013) and cannot be exhumed by subduction channel cycling due to their large size. Mechanisms that have been proposed to exhume these large terranes include slab extrusion and eduction. Slab extrusion can occur when the eclogite is embedded within more-felsic crust and brought to the surface by the buoyancy of the surrounding rocks (Ernst, 1997; Figure 2D), and is sometimes driven by a slab-breakoff event (Hynes, 2002; Brueckner and Cuthbert, 2013). Eduction is the reversal in subduction direction of the slab, caused by isostatic rebound after slab-breakoff (Warren, 2013; Figure 2E). Eduction differs from slab extrusion in that the high-pressure terrane remains attached to its original substrate.

Transpression can also bring up eclogite as part of a large eclogite-facies terrane. Transpression commonly results from oblique collision of tectonic plates, which can exhume material that is forced up between the blocks (Thompson et al., 1997; Figure 2F). The Musgrave Range of central Australia is an inter-cratonic terrane that was uplifted through a crustal-scale transpressional flower-structure (Camocho and McDougall, 2000). Blocks of eclogite were brought to the surface from depths of at least 40 km through oblique collision and erosion along the Mann strike-slip fault (Camocho and McDougall, 2000). Another transpressionally exhumed eclogite body occurs on the Island of Margarita, Venezuela (Maresch et al., 2009). Here, the eclogites along with metapelites, marbles and gneisses were metamorphosed together, as shown by their matching P-T history, then exhumed at least 50 km as the Caribbean plate transpressionally collided with the South American plate (Maresch et al., 2009).

GEOLOGIC SETTING

The Blue Ridge of the southern Appalachians consists predominantly of Mesoproterozoic crystalline basement rocks with Neoproterozoic-to-early Paleozoic cover sequences that have been metamorphosed and deformed into a series of stacked thrust sheets through several major orogenic events (Horton et al., 1989; Trupe et al., 2004). The structurally highest Fries thrust sheet contains both 1.1 Ga Laurentian basement gneisses and younger metasedimentary-metavolcanic sequences, separated by the Burnsville fault, which is a Devonian dextral strike-slip fault (Adams et al., 1995; Trupe et al., 2003; Trupe et al., 2004; Figure 1). These metasedimentary and metavolcanic rocks make up the Ashe Metamorphic Suite (Rankin, 1970; Abbot and Raymond, 1984).

The protoliths for the Ashe Metamorphic Suite are an assemblage of basalt, shale, impure sandstone, and ultramafic rock of mantle origin (Abbott and Raymond, 1984). The basalts are geochemically diverse and include MORB-type oceanic crust, ocean island basalts, and subduction-related arc basalts (Misra and Conte, 1991). The eclogite and surrounding amphibolites have a MORB protolith (Miller et al., 2010). These protoliths, as well as local block-in-matrix structures, have led many workers to conclude that the Ashe Metamorphic Suite is an accretionary wedge (Abbott and Raymond, 1984; Raymond et al., 1989; Abbott and Greenwood, 2001; Willard and Adams, 1994).

The Ashe Metamorphic Suite has been affected by three major metamorphic events. During the Taconic orogeny, the Ashe Metamorphic Suite experienced amphibolite-to-granulite- and locally eclogite-facies metamorphism during the collision of the Piedmont terrane (Stewart

et al., 1997). The Cherokee orogeny occurred next, which marks the docking of Carolinia with the Laurentian margin (Hibbard et al., 2010). The Carboniferous-Permian Alleghanian orogeny was caused by the collision of Laurentia and Gondwana and resulted in greenschist-facies metamorphism and formation of thrust sheets that were stacked and imbricated into the Blue Ridge thrust complex (Stewart et al., 1997; Trupe et al., 2004; Miller et al., 2006).

Eclogite bodies occur near the structural base of Ashe Metamorphic Suite, interpreted from increasing P-T conditions along a traverse perpendicular to the regional strike of the Ashe Metamorphic Suite towards the Burnsville fault (Hewitt, 1999). The eclogite is surrounded by amphibolites and amphibolite-grade schists and gneiss (Willard and Adams, 1994). Retrograded eclogite was later mapped north of the Grandfather Mountain window, near Boone, NC (Abbott and Raymond, 1997). The Boone retrograded eclogites are garnet amphibolites that contain cm-scale layers of diopside and plagioclase symplectite (Adams et al., 1995; Abbott and Raymond, 1997). This symplectite formed from the breakdown of omphacite, which suggests that the rock was once eclogite (Abbott and Raymond, 1997). The Boone retrograded eclogite lies in the same structural position in the Ashe Metamorphic Suite as the Bakersville eclogite, but is separated from it by the Grandfather Mountain window (Bryant and Reed, 1970; Abbott and Greenwood, 2001).

The largest bodies of eclogite are on Lick Ridge, near Bakersville, NC (Adams et al., 1995). These Lick Ridge eclogite bodies retain some of the best-preserved peak mineral assemblages (omphacite+garnet+quartz+rutile), while other Bakersville eclogites have retrograded and include lower-grade minerals such as diopside+plagioclase symplectite, hornblende, and epidote (Willard and Adams, 1994; Anderson and Moecher, 2009). Previous workers have established P-T estimates of the Bakersville eclogite bodies at peak conditions of 1.3-1.7 GPa at 740-800 ºC (Willard and Adams, 1994; Page et al., 2003; Anderson and Moecher,

2007), and retrograde conditions of 0.85-1.2 GPa at 650-730 ºC (Willard and Adams, 1994). In contrast, the schists and amphibolites of the Ashe Metamorphic Suite record only upper amphibolite conditions with peak P-T estimates of 0.6–1.0 GPa and 580–750 °C (Abbott and Raymond, 1984; McSween et al., 1989; Willard and Adams, 1994; Adams et al., 1995; Adams and Trupe, 1997; Hewitt, 1999; Trupe et al., 2004).

Miller et al. (2010) dated zircons from the Bakersville eclogite and reported a crystallization age of 459 +1.5/–0.6 Ma, which fits into the timing of Taconic metamorphism (~460 to 455 Ma) in the southern Appalachians (Moecher et al., 2004; Hatcher, 2010). Farther southwest, near Franklin, NC, rocks from Winding Stair Gap record granulite-facies metamorphism with similar ages of 458 ± 1.0 Ma (Moecher et al., 2004). The Bakersville eclogite bodies also yielded U-Pb titanite ages of 393.5 ± 3.8 Ma and rutile ages of 333.7 ± 2.3 Ma (Miller et al., 2010). They interpreted the older titanite age as representing either late Taconic cooling or an amphibolite-facies event associated with the Acadian orogeny, and the 333.7 ± 2.3 Ma rutile age as recording cooling during the Alleghanian orogeny.

METHODS

In order to determine if the rocks surrounding the eclogite show evidence of eclogite-facies conditions, we collected and analyzed zircons from nearby amphibolite bodies. We sampled from amphibolite bodies for two reasons: First, the amphibolite bodies contain metamorphic zircons, whereas the schists and paragneisses contain detrital zircons with 1.1 Ga cores (Fullager, 2002). These detrital zircons have thin metamorphic rims that can be difficult to date separately from the cores. The metamorphic zircons in the amphibolites are more likely to only record ages and conditions of their metamorphism. Second, the amphibolites in the area are petrologically indistinguishable from retrograded eclogite, which makes them the best candidate to test for retrogression of a widespread eclogite-facies terrane (Adams et al., 1995). The eclogite and amphibolite both have MORB protoliths and similar geochemical signatures (Miller et al., 2010). During retrogression from eclogite to amphibolite, the eclogite-facies minerals recrystallize, but the zircons are preserved because they are stable over a wide range of pressure-temperature conditions. Therefore, the zircons can record the pressure-temperature path of their host rock through several metamorphic events.

To reveal their metamorphic histories, we separated the zircons from the eclogite and amphibolite samples, analyzed them with laser-ablation inductively coupled plasma mass spectrometry (LA-ICMPS), and measured their Ti concentration, U-Pb ages, and REE patterns. Eclogite zircons have a distinct REE pattern that includes pronounced flat HREE patterns, no Eu anomaly, a Ce spike, and U-shaped LREE patterns (Skublov et al., 2012). If we identify this pattern in REE concentrations in amphibolite zircons, we can suggest that the zircons grew in

eclogite before their host rock retrograded into amphibolite. Additionally, U-Pb ages can tell us when the zircon crystallized and the Ti concentrations can be used to find the temperature of crystallization. These data can be used together to define a time-temperature path.to determine whether the eclogite and surrounding rocks crystallized under the same conditions and the same times. A similar time-temperature path between the bodies would suggest that the eclogite was exhumed with the amphibolites but did not retrograde. Divergent time-temperature paths would indicate that the eclogite body crystallized separately and was later emplaced into the surrounding rocks.

Sampling Strategy

Four amphibolites were sampled along roadcuts to the southwest and southeast of the eclogite. The closest samples were collected 1.7 km from the Bakersville eclogites and the most distant were 16 km away. This sampling strategy allowed us to gauge the extent of previous eclogite-facies conditions. The sites are located within the Bakersville, Micaville and Burnsville, NC USGS 7.5' quadrangles (Figure 3). Of the four amphibolites, only two contained zircons abundant enough to be separated out. We also sampled a known retrograded eclogite from the margin of one of the Bakersville eclogite bodies, to further distinguish between the eclogite and amphibolite.

Zircon Preparation

Zircons were extracted by crushing, magnetic separation, heavy liquids separation, then handpicked under a microscope. To measure the Ti, U, and Pb, zircon and rutile were mounted in an epoxy disk and analyzed by laser-ablation split-stream inductively coupled plasma mass spectrometry (LASS-ICPMS) (Kylander et al., 2013) at University of California at Santa Barbara. The LASS lab at Santa Barbara uses an Analyte 193 ArF laser-ablation system and a

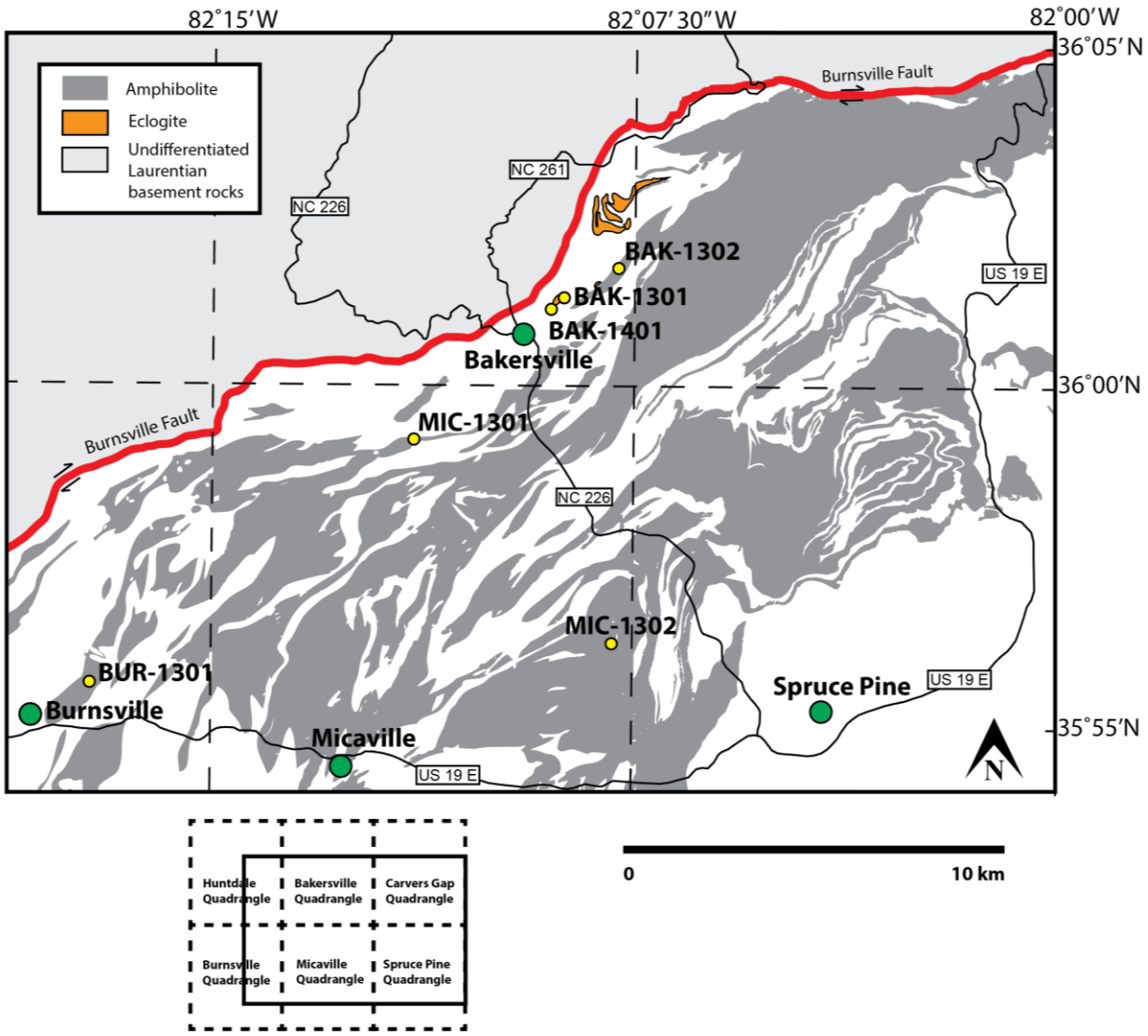

Figure 3. Map of sample locations and simplified geology. Geology from Adams (1995), Waters (1999), Borella (2000), and Brobst (1962).

Nu Plasma HR multi-collector ICPMS for U-Pb dating and a Nu AttoM single collector ICPMS for elemental abundances, including REEs and Ti content. Samples of known retrograded eclogite were analyzed at Virginia Polytechnic Institute and State University (VPI) using their GeoLas Pro laser and an Agilent 7500 ICPMS. Because laser ablation ages have large errors, additional zircons were analyzed with Isotopic Dilution Thermal Ionization Mass Spectrometry (ID-TIMS), which has a lower analytical error. ID-TIMS analyses were performed at the University of North Carolina at Chapel Hill on at VG Sector 54 mass spectrometer.

Samples for major- and trace-element geochemistry were crushed in a jaw crusher and then powdered in an aluminum-oxide ceramic rotary mill. The sample powders were fused using a Katanax K1 for major-element analysis, and powders were mixed with elvacite and pressed with 25 tons of pressure into disks for minor-element analysis. The disks were analyzed by x-ray fluorescence at UNC on a Rigaku Supermini 3230 XRF.

Thermometry

To calculate zircon crystallization temperature, we used the Ti-in-zircon thermometer of Ferry and Watson (2007). This thermometer has been calibrated through analysis of both natural and synthetic zircons (Watson et al., 2006), and is based on Ti exchange in the reaction:

$$\mathrm{ZrSiO_4} + \mathrm{TiO_2} = \mathrm{ZrTiO_4} + \mathrm{SiO_2} \quad (1)$$

Zircon, in the presence of Ti, will exchange a Si ion for a Ti ion, producing Ti-bearing zircon and quartz. The presence of rutile, or another Ti-bearing mineral, and quartz in the rock allows us to assume that the activities of quartz and rutile, a_{SiO2} and a_{TiO2}, are 1, meaning they are present in sufficient concentrations to readily substitute into the mineral structures. The relationship between Ti concentration and temperature is given by Ferry and Watson (2007) as:

$$\log(\mathrm{ppm\ Ti_{zircon}}) = (5.711 \pm 0.072) - \frac{4800 \pm 86}{T(K)} - \log a_{SiO2} + \log a_{TiO2} \quad (2)$$

The reference states for a_{SiO2} and a_{TiO2} are α-quartz and rutile at the P and T of interest (Ferry and Watson, 2007). A typical range of Ti concentration in zircons is around 0.3–50 ppm which would correspond to ~500–900°C (Watson et al., 2006). Our samples had Ti concentrations of 1.1-23.3 ppm. The thermometer has been calibrated at experimental conditions of 1 GPa and requires a pressure correction for higher-pressure rocks to account for the limited substitution caused by the lowered molar volume of the zircon (Ferriss et al., 2008).

Zr-in-rutile thermometry was applied to the eclogite sample, BAK-1301. The principles of this thermometer are similar to that of Ti-in-zircon, but a Zr ion substitutes for a Ti ion in the rutile structure (Watson et al., 2006). Ferry and Watson (2007) calibrated the relationship between Zr concentration and temperature as:

$$\log(\text{ppm Zr}_{\text{rutile}}) = (7.420 \pm 0.105) - \frac{4530 \pm 111}{T(K)} - \log a_{SiO2} \quad (3)$$

A pressure corrected Zr-in-rutile thermometer has been calibrated by Tomkins et al. (2007) through a wide range of experimental pressures. The equation under the α-quartz field is:

$$T(°C) = \frac{83.9 + 0.410P}{0.1428 - R\ln\phi} - 273 \quad (4)$$

and in the β-quartz field:

$$T(°C) = \frac{85.7 + 0.473P}{0.1453 - R\ln\phi} - 273 \quad (5)$$

where ϕ is ppm Zr, P is in kbar and R is the gas constant, 0.0083144 kJ K^{-1} (Tomkins et al. 2007).

Due to uncertainties inherent in the thermometry equations, as well as potential error in the measurement of the Ti-content, we used Monte Carlo simulations to estimate the standard deviation of the thermometry results. The Monte Carlo simulation populates variables with a uniform distribution of random numbers within that variable's error range, and then substitutes them into the original equation. This includes both sources of uncertainty in the temperature

equations and the standard error of the analysis, given by the ICPMS Iolite software. The LASS-ICPMS has a 2σ precision of 2-5% on elements in abundance greater than 100 ppm, 5-10% for elements as low as 1 ppm, and >10% for elements less than 1 ppm (Kylander-Clark et al., 2013). The temperature was then calculated from the equation with each variable assigned its randomly generated value. This simulation is performed over 1000 iterations, plotted on a histogram, and produces a normally distributed range of temperatures, confirmed using a Kurtosis test for normality. This normally distributed range is used to provide the mean temperature and standard deviation.

PETROLOGY

The eclogite, BAK-1301, is massive to weakly foliated with grain sizes up to 1.5 mm. It contains mostly garnet, omphacite and quartz, with minor rutile and retrograde amphibole and plagioclase (Figure 4A). Retrograded eclogite, BAK-1401, was collected near a pegmatite vein, which appears to have caused the retrogression. The sample contains poikiloblastic amphiboles up to 10 mm with inclusions of garnet, plagioclase and quartz. The amphiboles occur along discontinuous bands through the rock.

The amphibolite samples (BAK-1302, MIC-1301, MIC-1302, BUR-1301; Figures 4B-4E) are foliated and nematoblastic. Amphibolite mineralogy includes amphibole, plagioclase, and quartz. Grain size varies between 0.5-3 mm in the samples, with MIC-1301 containing layers of very coarse amphiboles up to 20 mm. Most samples have low felsic mineral content, but sample BUR-1301 is much lighter in color and contains ~20% plagioclase and quartz.

Major- and trace-element geochemistry for the eclogite and amphibolites (Table 1) are similar to other Eastern Blue Ridge amphibolites analyzed by Misra and Conte (1991) and Miller et al. (2010). Major- and trace-element concentrations for both amphibolite and eclogite samples suggest a MORB protolith (Figure 5).

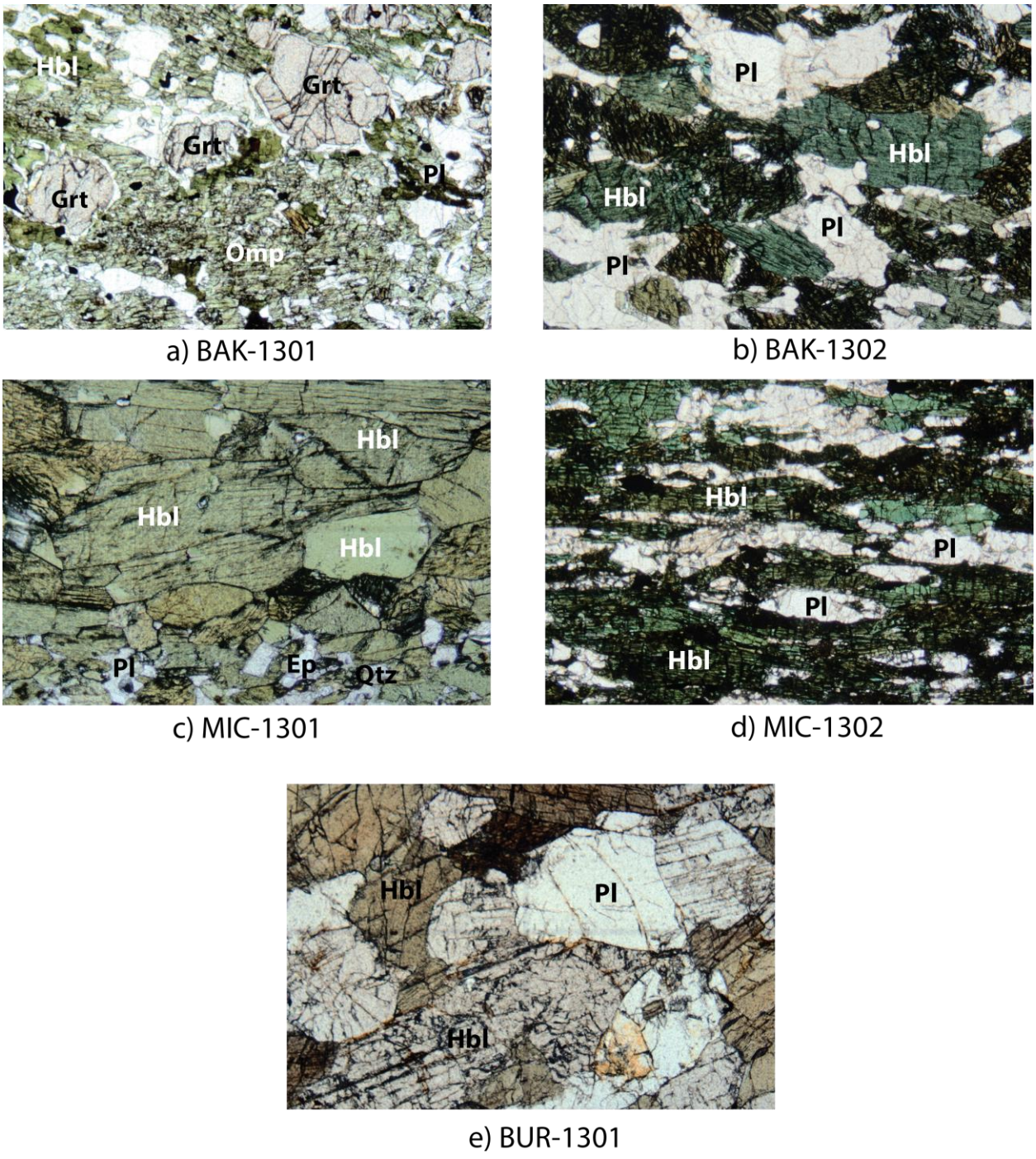

Figure 4. Photomicrographs of A) eclogite BAK-1301, B) amphibolite BAK-1302, C) amphibolite MIC-1301, D) amphibolite MIC-1302, E) amphibolite BUR-1301. Photomicrographs are in plane polarized light. Field of view is approximately 7mm horizontally. Mineral abbreviations: Hbl, hornblende; Pl, plagioclase; Grt, garnet; Omp, omphacite; Ep, epidote; and Qtz, quartz.

Table 1. Whole rock geochemistry						
(Wt%)	BAK-1301	BAK-1302	BAK-1401	MIC-1301	MIC-1302	BUR-1301
SiO2	50.44	48.76	50.60	47.88	49.05	48.37
Al2O3	14.05	13.63	14.29	14.40	13.10	16.10
CaO	10.74	11.41	10.77	12.42	9.59	11.23
MgO	7.42	8.71	8.35	10.44	6.35	8.77
Na2O	2.14	1.90	1.72	1.57	2.19	2.63
K2O	0.08	0.09	0.20	0.43	0.48	0.17
Fe2O3	14.42	13.88	13.44	11.73	16.06	10.98
MnO	0.20	0.23	0.23	0.19	0.22	0.20
TiO2	1.18	1.13	1.09	0.65	2.71	1.42
P2O5	0.12	0.14	0.12	0.09	0.25	0.24
LOI	0.07	0.04	0.10	0.05	0.09	0.05
SUM	100.86	99.93	100.89	99.84	100.08	100.15
(PPM)						
Ba	27	33	30	60	121	84
Rb	2	2	3	3	9	3
Sr	53	56	58	54	187	171
Y	32	29	21	17	34	35
Zr	60	56	57	26	131	96
Ni	101	133	91	218	131	107
V	243	218	226	174	350	237
Co	33	37	30	45	15	38
Cu	122	59	146	79	263	49
Zn	104	107	104	84	115	116
Sc	29	29	29	38	29	29

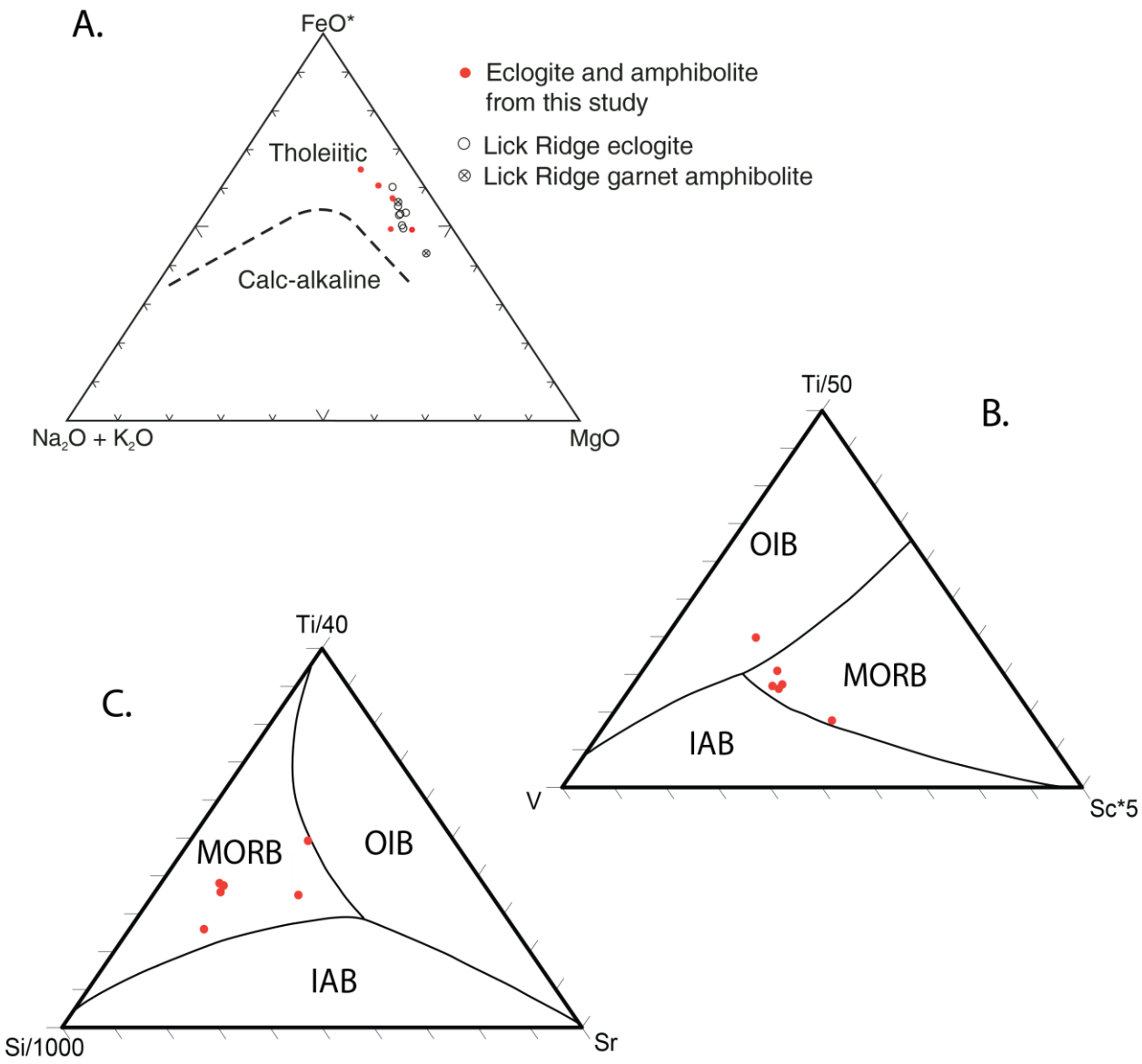

Figure 4. Tectonic discrimination diagrams. A) AFM diagram with data from this study and Miller et al. (2010) showing tholeiitic nature of the basalt protoliths. Modified from Miller et al. (2010). B) and C), discrimination diagrams of Vermeesch (2006) illustrating the MORB nature of the protolith. MORB- mid ocean ridge basalt, OIB- ocean island basalt, IAB- Island arc basalt.

Zircon Morphology

Zircons in the eclogite BAK-1301 and retrograded eclogite BAK-1401 are abundant and large—up to 300 μm in length. The crystals are commonly rounded with moderate-to-poor contrast between zones in cathodoluminescence (CL) images. Some zircons have sector zoning and bright patches (Figures 6B and 6D). Zircons in amphibolite MIC-1301 are less abundant and tend to be smaller (up to 200 μm in length) and more elongated than the eclogite zircons. Zones in the zircons are chaotic (Figures 6G and 6L) and include patches of fir-tree zoning (Figure 6I), sector zoning (Figure 6H) and some recrystallization (Figure 6J). Chaotic and fir tree zoning can be indicative of fluctuating growth rates (Corfu et al., 2003). Amphibolite sample BAK-1302 contains few zircons; only 10 were found after exhaustive searching. The zircons were small (up to 150 μm in length) and broken. Amphibolites MIC-1302 and BUR-1301 yielded no zircons.

U-Pb dates

The eclogite and amphibolite samples were dated by laser-ablation ICPMS to take advantage of the split-stream analysis capabilities at UC Santa Barbara. Additional zircons were dated with ID-TIMS at UNC to refine the dating precision. Eclogite BAK-1301 yielded laser-ablation ICPMS ages of 460.7 ± 3.2 Ma with Mean Square Weighted Deviation (MSWD) =0.95 (Figure 7A). These laser-ablation results overlap within error with the 459 +1.5/-0.6 Ma ID-TIMS ages from the same eclogite body reported by Miller et al. (2010). The retrograded eclogite, BAK-1401, was not dated as it is presumed to be the same age as the eclogite.

The amphibolites produced significantly younger ages than the eclogite. Amphibolite MIC-1301 yielded laser-ablation ICPMS ages of 424 ± 18 Ma with a MSWD=7.2 (Figure 7B). Small spot size and low U content in the zircons contributed to the large error. When the data were pared down to the 25 best measurements, which had lower error and higher U content, the

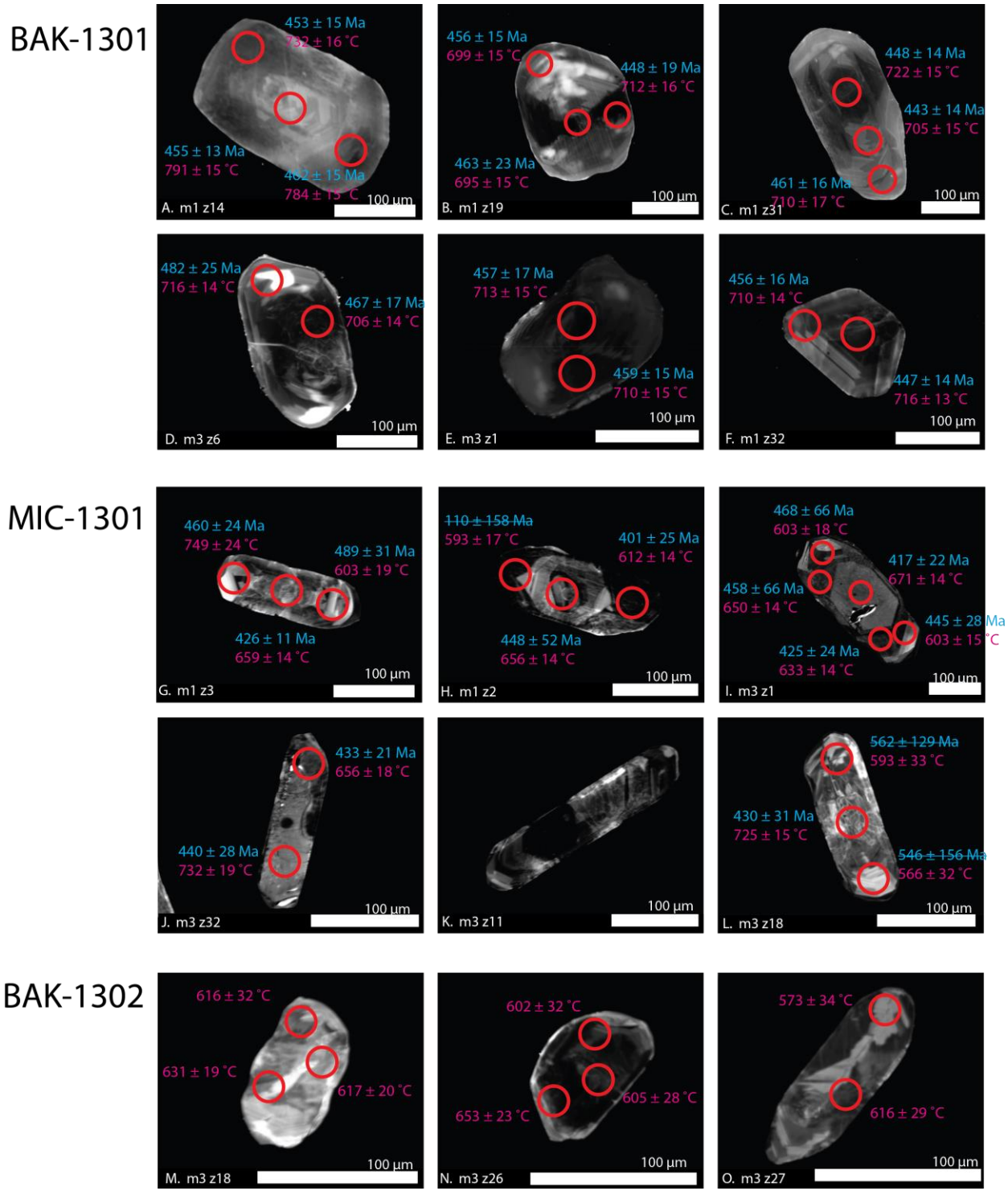

Figure 5. CL images showing the large, rounded zircons of the eclogite BAK-1301, compared to the more elongate zircons of the amphibolite MIC-1301. Amphibolite BAK-1302 has 3 small zircons. U-Pb ages are in blue and temperatures are in red. Spot sizes are approximately scaled.

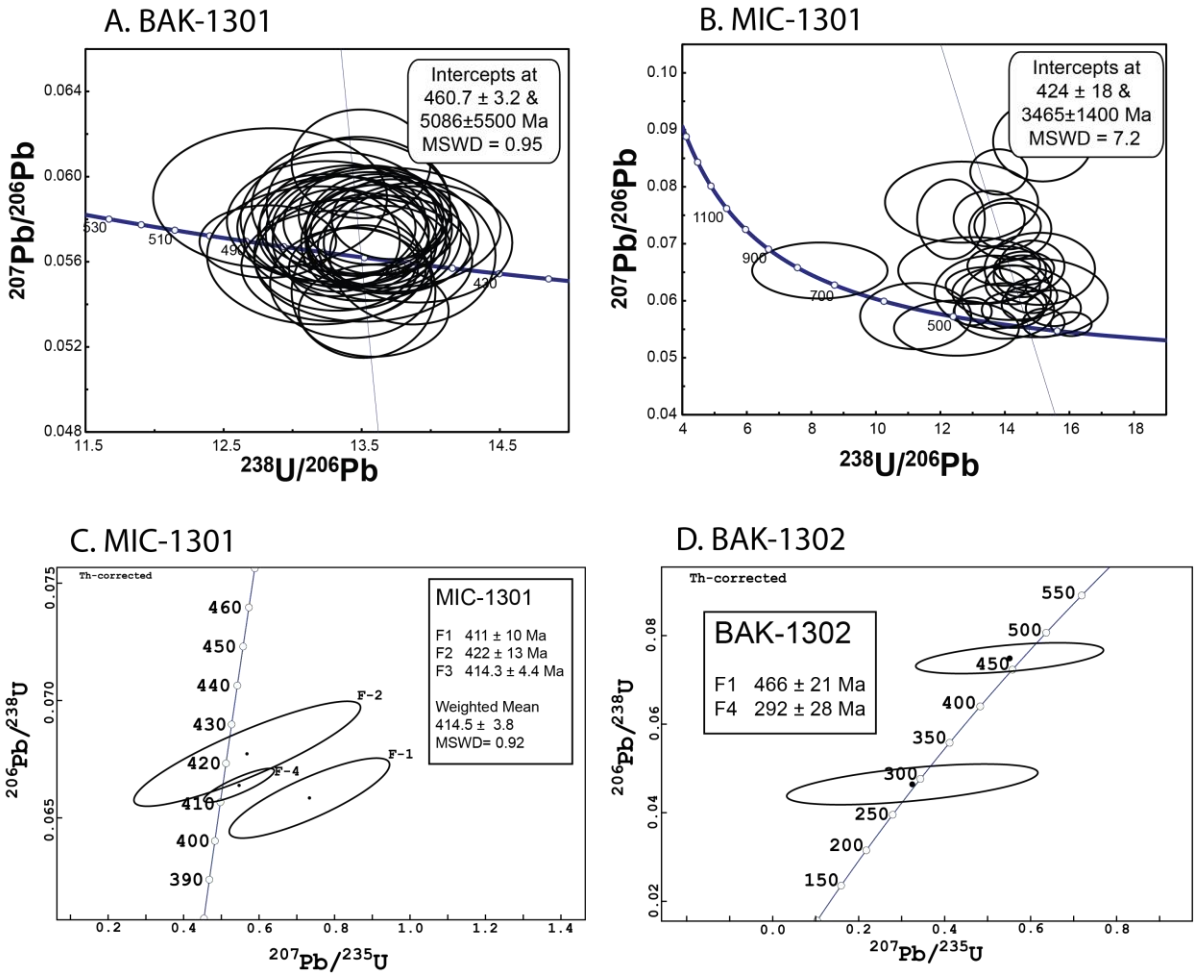

Figure 6. A-B) Tera-Wasserburg concordia plots of laser-ablation data for samples BAK-1301 and MIC-1301. C-D) Concordia plots of ID-TIMS data for samples MIC-1301 and BAK-1302. Error ellipses represent 2σ uncertainties. MSWD- mean square weighted deviation.

age becomes 418 ± 8 Ma with a MSWD=0.99. ID-TIMS dating of MIC-1301 yielded an age of 414.5 ± 3.8 Ma with a MSWD=0.92 (Figure 7C). Amphibolite BAK-1302 zircons did not have enough U or Pb to produce a reliable LASS-ICPMS age. Only two zircons from this sample yielded an ID-TIMS date, but with large errors. One zircon gave an age of 466 ± 21 Ma, and another 292 ± 28 Ma (Figure 7D). The younger age might indicate resetting or growth during Alleghanian thrusting, but we are hesitant to draw any conclusions from a single zircon measurement with such large error.

Th/U ratios can help distinguish between primary igneous zircons and metamorphic zircon (Hoskin and Ireland, 2000). Generally, zircons with Th/U ratios <0.1 are metamorphic and zircons with Th/U >0.1 crystallized from a melt (Williams et al., 1996; Hoskin and Ireland, 2000). In high-grade metamorphic rocks that have undergone partial melting, however, the Th/U ratio in zircon can vary widely, from < 0.1 to > 3.0 (Möller et al., 2002; Harley et al., 2007). The sampled zircons for this study have Th/U ratios ranging from 0.00 to 0.41, with the average at 0.07 and the majority < 0.1. The few outlier values that are > 0.1 may result from the low U content of the zircons. Overall, the Th/U values suggest that the zircons are metamorphic, which ensures that the ages and temperatures measured are representative of metamorphic conditions rather than their igneous protolith conditions.

Zircon REE patterns

The zircon REE patterns, normalized to chondrite, are clearly different between the amphibolite and eclogite bodies. The zircons from eclogite and retrograded eclogite bodies have a distinct pattern of U-shaped LREE with a Ce spike, no Eu anomaly, and a flat-to-decreasing values pattern of HREE (Figures 8A and 8B). This pattern is typical of eclogite zircons (Skublov et al., 2012), and seen in the REE patterns in the Midsund Bruk eclogite of the Western Gneiss

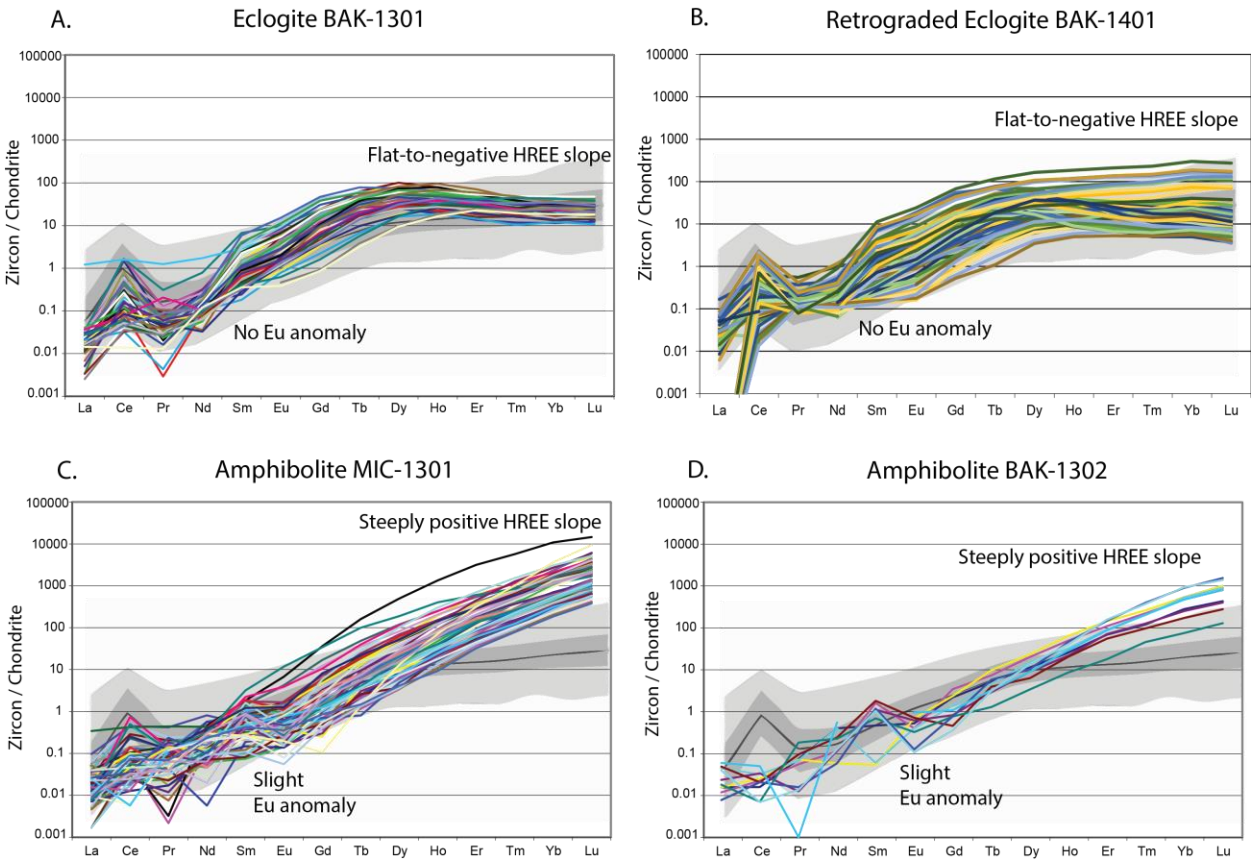

Figure 7. A-B, Eclogite and retrograded eclogite zircon REE patterns with low, flat HREE slopes suggesting concurrent growth with garnet at eclogite-facies conditions. C-D, Amphibolite MIC-1301 and BAK-1302 zircon REE patterns with high, steep HREE slopes and slight Eu anomaly. This pattern suggests zircon growth with plagioclase and no garnet present. All values are normalized to chondrite after McDonough and Sun (1995). The gray background pattern comes from a global average of 877 eclogite bodies compiled by Skublov et al. (2012). Light gray encompasses 95% of eclogite bodies, dark gray contains 90% of eclogite bodies, and the dark line is the average.

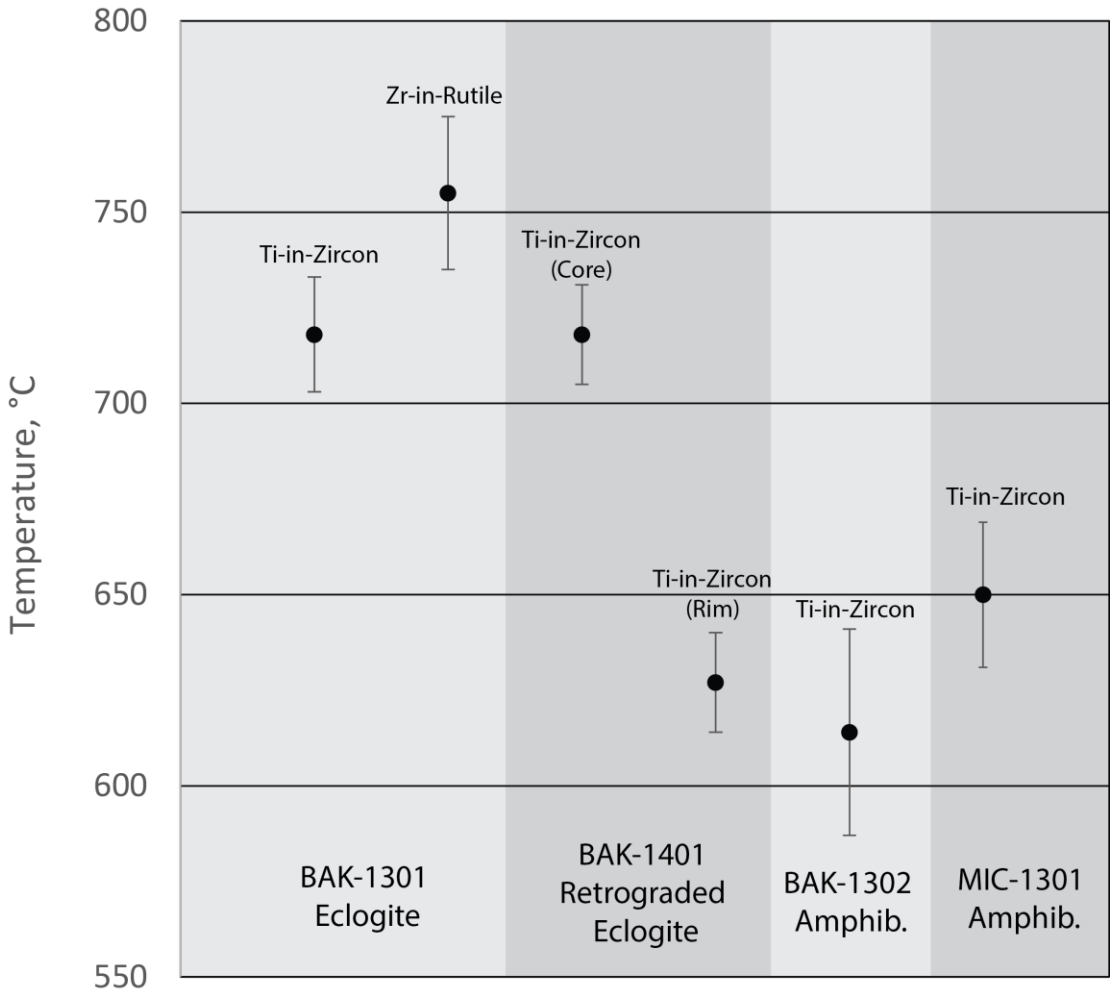

Figure 8. Average temperature ranges for the amphibolite and eclogite samples. Error bars show standard deviations calculated from Monte Carlo simulations.

region of Norway (Kylander-Clark et al., 2013), and the Sesia–Lanzo Zone of the Western Alps (Rubatto, 2002). The flat-to-negative HREE slopes indicate that the zircons grew in the presence of garnet, because the HREEs are incorporated preferentially into garnet during crystallization (Rubatto, 2002; Hoskin and Schaltegger, 2003; Kylander-Clark et al., 2013). Garnet is a primary eclogite mineral, suggesting that the zircons grew during eclogite-facies conditions.

The amphibolite zircons have depleted LREE and MREE, a small Eu anomaly, and enriched HREE with a steep, positive slope (Figures 8C and 8D). In these samples, a positive HREE slope indicates garnet was not growing concurrently with the zircons. The negative Eu anomaly suggests that the zircons crystallized with plagioclase present because the Eu will incorporate preferentially into the plagioclase, reducing its availability for the zircon crystals (Hoskin and Ireland, 2000; Rubatto, 2002; Kylander-Clark et al., 2013). Plagioclase is not stable at eclogite facies, and only occurs in the eclogite as a breakdown product of omphacite at lower pressures (Mysen and Griffen, 1973; Anderson and Moecher, 2007). The amphibolite REE patterns indicate that the zircons grew in the presence of plagioclase and not in the presence of garnet. Therefore, the amphibolites did not experience eclogite-facies conditions and cannot be retrograded eclogite.

Thermometry

Ti-in-zircon thermometry uses the Ti-concentration in zircon to estimate a temperature of crystallization (Watson et al., 2006). The thermometer was calibrated at experimental conditions of 1 GPa, with an estimated pressure correction of 50°C/GPa required for higher-pressure rocks (Ferry and Watson, 2007). Ferriss et al. (2008) found that this pressure correction was insufficient due to the underestimated the effect of pressure on reducing the molar volume of the zircon which limits ion substitution. If less Ti can substitute at higher pressures, then the

thermometer will underestimate temperatures at higher-pressure conditions. Their study found that a pressure correction of 100°C/GPa is required to account for the lower-than-expected Ti-substitution at higher pressures.

The pressure estimate for peak conditions of the eclogite is 1.7 GPa (Willard and Adams, 1994; Page et al., 2003; Anderson and Moecher, 2007), which is 0.7 GPa higher than the conditions used to calibrate the thermometer. Therefore, a pressure correction of 70°C was applied to the results based on the Ferriss et al. (2008) calculations. We analyzed 100 spots on 75 eclogite zircons with Ti concentrations ranging from 1.67-22.3 ppm. The Ti-in-zircon thermometry results for the eclogite BAK-1301 yielded an average crystallization temperature of 718 ± 15°C. The retrograded eclogite BAK-1401 had 70 analyses on 46 zircons with Ti concentration ranging from 1.1-9.6 ppm. The retrograded eclogite yielded an average uncorrected temperature of 639 ± 13°C, but had distinct values for core and rim. The rim average was 627 ± 14°C and the core average was 648 ± 14°C. The core average requires a pressure correction of 70°C, bringing it up to 718 ± 14°C because the core crystallized at depth while the rim retrograded at lower pressure conditions (Figure 9).

The amphibolite MIC-1301 had Ti concentrations of 1.26-10.7 ppm from 72 analyses on 32 zircons. This amphibolite yielded an average Ti-in-zircon temperature of 650 ± 19°C. A pressure correction was not applied because the amphibolites are estimated to have formed at 0.7-1 GPa (Adams and Trupe, 1997), which is close to the 1 GPa calibration of the thermometer. Amphibolite BAK-1302 had an average temperature of 614 ± 27°C, but only had three zircons analyzed

Zr-in-rutile thermometry was only applied to the eclogite BAK-1301. 34 analyses yielded Zr concentrations were between 504-1027 ppm. Zr-in-rutile thermometry using the Tomkins et al. (2007) pressure calibrated equation yielded temperatures of 753 ± 20 °C for the α-quartz (Eq.

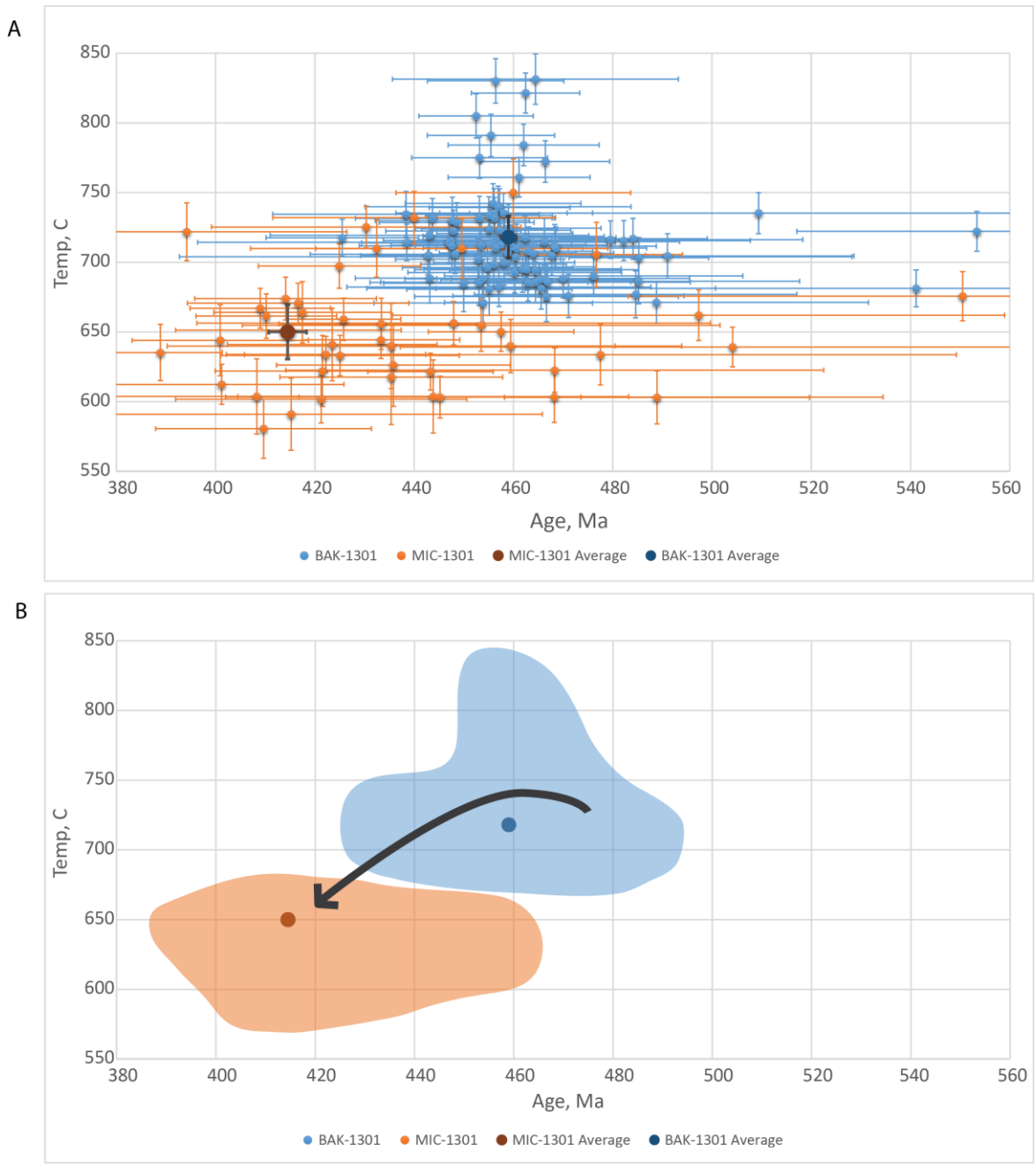

Figure 9. A) Temperature-time plot for amphibolite MIC-1301 and eclogite BAK-1301. Data points are for LASS-ICPMS U-Pb age and Ti-in-zircon thermometry. Larger, darker points are the average temperature values and with ID-TIMS dates. Horizontal error bars represent 2σ uncertainties in age and vertical error bars show Monte Carlo derived standard deviations of the temperatures. B) Temperature-time path of the Ashe Metamorphic Suite interpreted from the data points above.

4) and 757 ± 20 °C for the β-quartz stability fields (Eq. 5). The pressure variable was set at 1.7 GPa after estimates from Willard and Adams (1994) and Anderson and Moecher (2007). The high pressures make it ambiguous whether the eclogite would host α- or β-quartz, but the difference in the results is negligible at only four degrees. Rutile is a primary eclogite mineral, crystallizing during peak metamorphic conditions. The Zr-in-rutile temperatures are about 50°C hotter than the Ti-in-zircon thermometer, indicating that the zircons likely crystallized during cooling shortly after peak conditions. Because of this temperature difference, the 459 Ma zircon age of the eclogite that was thought to represent the timing of peak metamorphic conditions of the eclogite (Miller et al., 2010) may actually record zircon crystallization after the eclogite began to cool. Unfortunately, U-Pb ages on rutile (Miller et al., 2010) record Alleghanian cooling and not eclogite-facies conditions.

These findings are consistent with other studies where Zr-in-rutile thermometry recorded peak temperatures, while Ti-in-zircon thermometry recorded lower cooling temperatures (e.g. Baldwin et al., 2007; Liu et al., 2010; Ewing et al., 2013). The Ewing et al. (2013) investigation of granulite-facies metapelites from the Ivrea-Verbano Zone of northern Italy found that the Zr-in-rutile thermometry recorded temperatures 100-200°C higher than the Ti-in-zircon. They attributed this temperature difference to a delay in metamorphic zircon crystallization until Zr became saturated in the anatectic melt fraction of the granulite.

The split-stream analysis performed at UCSB allowed us to get a simultaneous U-Pb date and a Ti-concentration measurement (Figure 6), which can be plotted together to get the temperature-time (T-t) path for the rocks in the area (Figure 10). While the individual data points have a wide scatter and large error bars, the cumulative pattern in the data is clear. Around 470-450 Ma, temperatures recorded in the eclogite range from about 675-750°C, which cool down to the 600-675°C temperatures recorded in the amphibolite MIC-1301 between 440-400 Ma.

DISCUSSION

The zircon and rutile thermometry results are consistent with previous estimates of peak conditions for the area. Pressure-temperature estimates from the Bakersville eclogite body range from 1.3-1.7 GPa and 625-800ºC (Willard and Adams, 1994; Page et al., 2003; Anderson and Moecher, 2007). The schists and amphibolites of the Ashe Metamorphic Suite record upper-amphibolite conditions of around 0.6–1.2 GPa and 580–750 °C (Abbott and Raymond, 1984; McSween et al., 1989; Willard and Adams, 1994; Adams et al., 1995; Trupe et al., 2004). Our zircon and rutile thermometry results range from 703-775 °C for the eclogite and 614-669 °C for the amphibolites, which fall within the range of previous estimates.

The eclogite records temperatures that are about 100°C hotter than the amphibolites and the zircon crystallization ages are 40-45 Ma older. The amphibolite zircon REE patterns indicate that the zircons grew in the presence of plagioclase and not in the presence of garnet, and therefore did not grow at eclogite conditions. These crucial differences between the eclogite and amphibolite suggest that the amphibolites are not retrograded eclogite. Also, the zircons from the retrograded eclogite (now amphibolite) BAK-1401 show the same characteristics as the eclogite, such as flat HREE patterns and no Eu anomaly, which further suggests that this retrograded-eclogite amphibolite is different from the other amphibolites that we sampled. These results suggest that the eclogite was emplaced into the lower-grade rocks. If regional eclogite-facies conditions were present in the Taconic orogeny, we would expect to see evidence in the amphibolites such as flat HREE patterns and similar U-Pb ages and temperatures in the amphibolite zircons.

By limiting the extent of eclogite-facies conditions, we limit the viability of the extrusion and eduction models for eclogite exhumation (Figures 1D and 1E). These models call for the subduction and exhumation of regional-scale blocks, which would cause the amphibolite bodies that we sampled to experience eclogite-facies conditions. Transpression is also not a likely driver of exhumation. Transpression along the Devonian Burnsville fault has been documented in the vicinity of the Bakersville eclogite (Waters-Tormey and Stewart, 2010), resulting in kilometer-scale synformal folding, however, the timing is different and there is no evidence of uplift associated with the Burnsville fault.

Corner-flow, driven cavity, and plunger-driven models are consistent with the accretionary wedge origin of the Ashe Metamorphic Suite. These accretionary-wedge circulation models result in isolated blocks of eclogite surrounded by lower-grade material. The corner-flow model of Cloos (1982) was developed to explain exhumation of eclogite bodies in the Franciscan complex of California, which are low temperature eclogites (450-590°C, Krogh, 1988) exhumed as meter- and decimeter-scale blocks in a serpentinite and shale matrix (e.g., Coleman et al., 1965; Coleman and Lanphere, 1971; Ernst and Liou, 1995). Corner-flow is generally limited to eclogite blocks < 50 m in size. This size limitation is governed by Stokes Law, which gives the settling velocity of dense objects within a less-dense viscous fluid. The settling velocity, V_s, is given as (Turcotte and Schubert, 1982):

$$V_s = \frac{2(\Delta\rho)\, g\, r^2}{9\, \mu} \quad (6)$$

where $\Delta\rho$ is the density contrast between the eclogite and the matrix, g is 9.8 m/s, r is the radius of the eclogite block, and μ is the viscosity of the matrix. Cloos (1982) estimated a density contrast ($\Delta\rho$) of 0.3 g/cm^3, and a matrix viscosity of 10^{17} poise and found blocks with a radius greater than 25 m would sink faster than they are carried to the surface. Corner flow simply

cannot account for exhumation of blocks as large as the 100x1000x300 m body of Bakersville eclogite, which has a volume equivalent to a sphere with a ~200 m radius.

The driven cavity model circulates material up from depths where sediments from the accretionary wedge pinch out and temperatures are hotter. Circulation from depths of 30-70 km is achieved by hydration of the mantle wedge into serpentinite, which can be driven into cyclic flow as well as lubricate the exhumation of the eclogite (Burov et al., 2001; Guillot et al., 2001). This depth of circulation yields eclogites with temperatures of up to 700°C, which is similar to our results of 703-775 °C (Burov et al., 2001). A matrix composed of serpentinite rather than accretionary-wedge sediments will change the properties of Stokes Law that limits the size of blocks that can be exhumed. A serpentinite matrix viscosity of 10^{19} poise and a density contrast of 0.8 g/cm^3 will allow the maximum radius of an exhumed block to rise as high as 700 m, well over the size of the largest Bakersville eclogite block (Schwartz et al. 2001).

Plunger-driven expulsion works in a similar way to the driven cavity model, but rather than traction along the subducting plate driving the eddy flow, thick and cold continental crust enters the subduction channel and forces downward flow of the hotter, weaker channel material which then hits a 'control point' (Figure 1C). This control point limits the amount of material that can be pushed downward and forces return flow back up in the subduction channel, carrying blocks of eclogite with it (Warren et al., 2008). Plunger-driven expulsion can be difficult to prove in ancient collisional settings because of the deformation associate with continued collision (Warren, 2013), but at least one pulse can expected with the subduction of a continental margin (Warren et al., 2008).

It may be possible to identify which of these models is more likely if more eclogite is identified in the region with different ages. Driven cavity flow can continually exhume eclogite for a period of time, while the plunger-driven flow will typically produce pulses as new plungers

are brought into the channel (Warren et al., 2008; Warren, 2013). Also, eclogites exhumed through this driven cavity serpentinite channel, like the Tso Morari eclogitic unit in the Himalayas (Guillot et al., 2001), or the Monviso eclogite of the western Alps (Schwartz et al., 2001), are still contained in serpentinite units. The Bakersville eclogite bodies are not encased in a serpentinite or peridotite matrix and the Ashe Metamorphic Suite only contains small scattered pods of ultramafic bodies, however, the serpentinite-eclogite unit could have been dismembered later though faulting or mélange mixing.

Silurian-Devonian metamorphic event

The MIC-1301 amphibolite body records an amphibolite-facies event at 414.5 ± 3.8 Ma with temperatures up to 650 ± 19°C. A Silurian-Devonian metamorphic event has not been previously recognized for this part of the southern Appalachians, yet several rocks dated from around the Bakersville area record ages circa 420-415 Ma. Miller et al. (2000a) reported a 420 ± 15 Ma age on zircon rims from retrograded eclogite, however large errors and irreproducibility make this value suspect. Goldberg and Dallmeyer (1997) reported a hornblende Sm-Nd isochron age of 423 ± 14 Ma for a mylonitic garnet amphibolite in the vicinity of Bakersville, NC and a 394 ± 2 Ma Rb-Sr isochron age for another amphibolite body. In partially retrograded Bakersville eclogite, Miller et al. (2010) found titanite ages of 393.5 ± 3.5 Ma, which could record cooling ages from the 415 Ma event recorded in the amphibolite body MIC-1301.

Outside of the Bakersville area, there is little evidence for a Silurian-Devonian metamorphic event in the Blue Ridge apart from a handful of dates with uncertain reliability. A metadiabase from the Grandfather Mountain window is reported as 422 ± 2 Ma and 415 ± 3 Ma (Fetter and Goldberg, 1993). However, this metadiabase in a structurally lower Alleghanian thrust sheet and would have been over 100 km farther west from the Bakersville area before the

thrust sheets were stacked (Trupe et al., 2004), and might not be related. Miller et al. (2000b) dated zircon rims from a trondhjemite dike 10 km north of Asheville which yielded ages of 417 ± 9 Ma and 414 ± 17 Ma. Confidence in these dates is questionable because they come from thin rims on zircons that have large cores that date to 1.0-1.15 Ga, preserved by rapid heating that caused growth of the rims but did not reset the cores of the zircons (Miller et al., 2000b). The Spruce Pine Intrusive Suite is often cited as being circa 377 Ma based on a U-Pb ages from Chalk Mountain and other pegmatites (Johnson et al., 2001; Trupe et al., 2003), but several samples yield Silurian-Devonian ages. Uraninite ages from three pegmatite mines in Spruce Pine record ages of 378-411 Ma, 389-432 Ma, and 418-460 Ma (Warner et al., 2008). Kish (1983) measured whole rock Rb-Sr ages of 435 ± 14 Ma, 404 ± 14 Ma, and 392 ± 15 Ma on three Spruce Pine pegmatites. Moecher et al. (2011) dated detrital zircons and monazite from tributary streams draining the Ashe Metamorphic Suite in the Canton, NC quadrangle. They dated several zircons with a metamorphic rims of 417-425 ± 12 Ma. Unfortunately, the detrital nature of the zircons makes it difficult to identify their source. Based on the current sampling and dating of the Ashe Metamorphic Suite, we cannot say how widespread this Silurian-Devonian metamorphic might be.

One area of the Appalachians active during the late Silurian- Early Devonian is the northern Appalachians. The northern Appalachians have evidence of the Salinic orogeny, recognized as 430-415 Ma regional deformation, plutonism, and uplift (Dunning et al., 1990; Tremblay and Castonguay, 2002; Wilson and Kamo, 2012). The Salinic orogeny in New Brunswick is identified through several unconformities between 440-416 Ma that are attributed to convergence and oblique collision between Laurentia and Ganderia (Wilson and Kamo, 2012). At the same time as Salinic collision was occurring in New Brunswick and Newfoundland, New England was experiencing extension (Rankin et al., 2007). Rankin et al. (2007) hypothesize that

either the promontory-embayment geometry allowed for simultaneous collision and extension, or that sinistral strike-slip motion from deflecting collision off the promontories created pull-apart basins.

The Silurian-Devonian event in the southern Appalachians could be related to the Cherokee orogeny, which is the tectonic equivalent to the Salinic Orogeny (Hibbard et al., 2010). The Cherokee orogeny started around 450 Ma and records the docking of the Carolina terrane with the Laurentian margin (Hibbard et al., 2010). The cessation of Ordovician-Silurian magmatism in the southern Appalachians around 430 Ma suggests that subduction stopped and the Laurentian margin became a transform margin (Hibbard et al., 2010). Silurian clastic wedges in the central Appalachians and the Lay Dam and Cat Square basins in the Piedmont may be evidence of tectonic loading between 440-423 Ma (Hibbard et al., 2010). There is not, however, a major clastic wedge associated with Silurian-Devonian uplift in the southern Appalachians.

The lack of a major clastic wedge in the southern Appalachians suggests that Carolinia collided with Laurentia in the central Appalachians, and then migrated southward (Hibbard and Waldron, 2009). Evidence for this includes the Salinic clastic wedge in the central Appalachians showing a progressive southwestward migration (Ettensohn and Brett, 2002). Dennis (2007) proposes a series of rifting and collisional events between Carolinia and Laurentia, with crustal thickening occurring as Carolinia moves southward down the orogen. Transtensional plutons in the Charlotte terrane of Carolinia have U-Pb ages of 416 ± 5.5 Ma and 415 ± 6 Ma (Hibbard et al., 2012), thought to be formed by extension in response to strike-slip motion as Carolinia was transported southward (Dennis, 2007). One of these collisions between Carolinia and Laurentia could bury this portion of the Blue Ridge sufficiently to create amphibolite-facies conditions.

An alternative hypothesis is that these Silurian-Devonian ages are simply cooling ages from the Taconic orogeny. If the crustal thickening resulting from Taconic collision buried these

rocks to amphibolite-facies depths, then zircons could continue to crystallize until uplift and erosion caused the temperatures to fall below the zircon closure temperatures. Movement along the Burnsville fault may have driven the uplift or maybe erosion alone was sufficient. This alternative hypothesis may explain some of the scatter that we see in the ages of the zircons as they could have crystallized over a longer period of time. However, it is not clear how the eclogite did not retrograde during 45 Ma of amphibolite-facies conditions.

Tectonic Model

Convergence began in the Early Ordovician as the ocean basin separating Laurentia and the Piedmont terrane started subducting into an east-dipping subduction zone (Stewart et al., 1997; Miller et al., 2006; Hibbard et al., 2007). The Ashe Metamorphic Suite took shape as sediments were scraped from the subducting plate to form an accretionary wedge. The Bakersville eclogite was likely formed from this subducting oceanic crust at depths of 50-70km (Figure 11A). Rutile recorded peak temperatures of up to 775° C, while the zircons, which were dated to 460 Ma, recorded temperatures as high as 718° C.

The Laurentian margin entered into the subduction channel in the late Middle to early Late Ordovician (Ettensohn, 2004). This earliest phase of collision is recorded by the Blountian clastic wedge between the Virginia and Alabama Promontories (Ettensohn, 2004). The Blountian clastic wedge consists primarily of turbidites that were deposited on a Cambrian-Ordovician carbonate shelf (Anderson, 1994). The basin shows a significant influx of volcanic sediments, interpreted to result from colliding terranes (Anderson, 1994). We propose driven cavity or plunger-driven circulation exhumed the eclogite to mid-upper crustal levels and into the accretionary mélange (Figure 11B). We speculate that the eclogite was surrounded by serpentinite, and brought into the accretionary mélange of marine sediments, mudstones, and

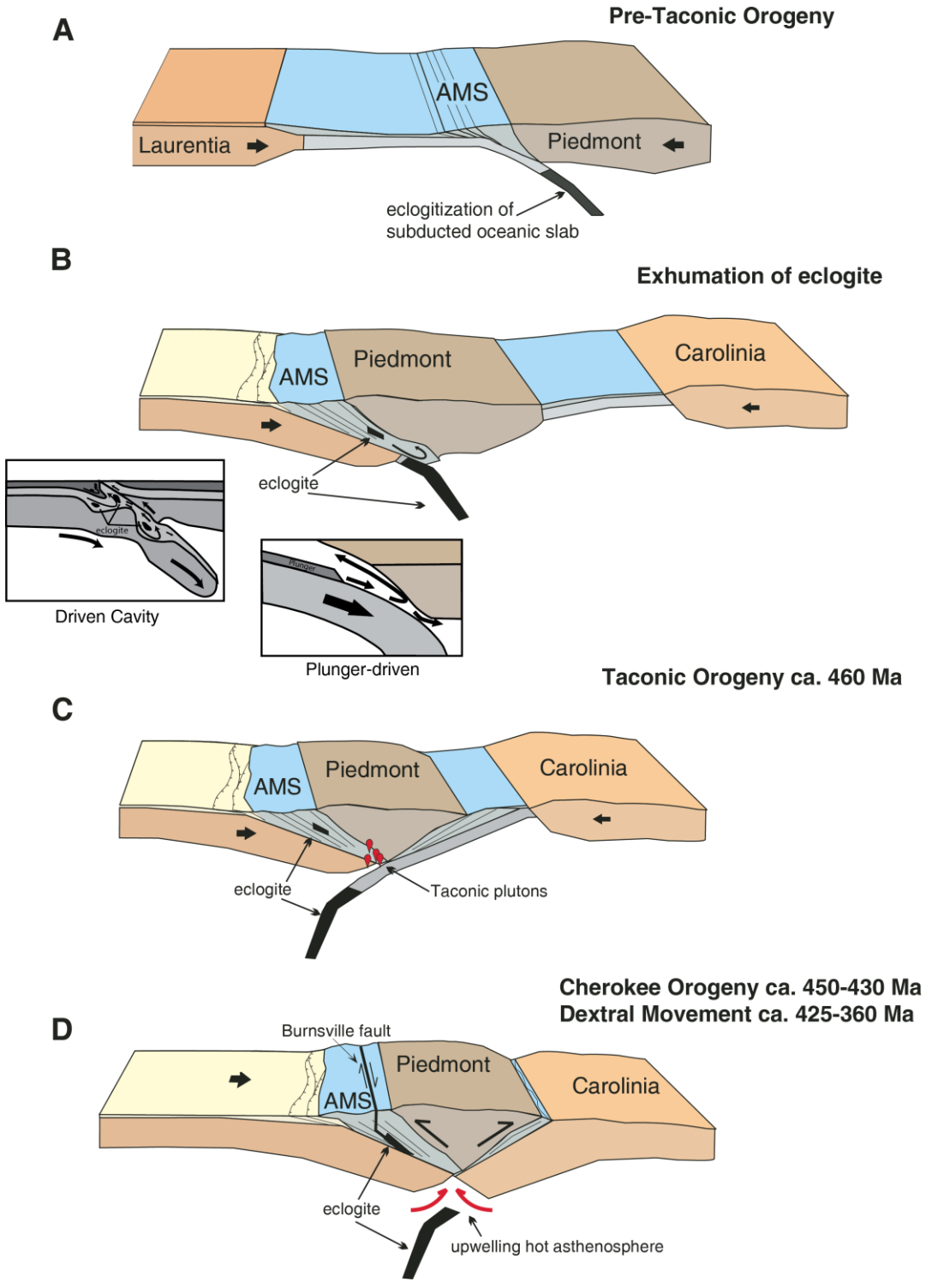

Figure 10. Tectonic model for formation, exhumation, and emplacement of the eclogite. AMS- Ashe Metamorphic Suite. Modified from Miller et al. (2006).

brought into the accretionary mélange of marine sediments, mudstones, and blocks of oceanic crust. Mixing within the mélange could have separated the eclogite from its serpentinite "capsule", resulting in the scattered blocks of ultramafic bodies throughout the Ashe Metamorphic Suite. Swanson and Raymond (2010) demonstrate that the ultramafic bodies of the Spruce Pine area show evidence of being dehydrated from serpentinite. The Taconic orogeny occurred as the collision between the Piedmont and Laurentia continued (Figure 11C). Amphibolite MIC-1301 does not record Taconic metamorphism, and may not have been at amphibolite-facies depths during the Taconic orogeny.

Simultaneous with the peak of the Taconic orogeny at around 460 Ma, subduction switched to west-dipping after accretion of the Piedmont, and the Iapetus Ocean began to be consumed followed by collision between Carolinia and Laurentia (Hibbard, 2000). Around 430 Ma, collision ended between Carolinia and Laurentia in the central Appalachians, followed by dextral strike-slip translation of Carolinia (Hibbard et al., 2010; Dennis, 2007; Figure 11D). Collision and extension with the promontory-embayment geometry of Laurentia created crustal thickening and pull-apart basins as it migrated down the orogen. The Ashe Metamorphic Suite locally reached amphibolite-facies conditions of up to 669°C as recorded in the amphibolites. The proto-Ashe Metamorphic Suite accretionary mélange may have been further mixed as it was compressed and metamorphosed, allowing some deeper rocks that recorded Taconic conditions to be incorporated with the rocks that do not. The translation of eastern Blue Ridge, the Piedmont, and Carolinia southward was accommodated along the Brevard zone, and other shear zones, including the Burnsville Fault, to their current orogenic position (Hatcher, 2002; Hibbard et al., 2012; Adams et al., 1995). Last motion on the Burnsville fault was between 377-360 Ma (Trupe et al., 2003).

CONCLUSIONS

The amphibolite bodies sampled from around the Bakersville eclogite do not record the signatures of previous eclogite-facies conditions and therefore do not represent retrograded eclogite. This suggests that the eclogite was emplaced into lower-grade rocks during its exhumation, consistent with the driven cavity flow or plunger-driven exhumation models. The eclogite reached temperatures of 703-775°C, which suggests it was brought up from depths of 50-70 km. The amphibolite MIC-1301 records a 415 Ma metamorphic event that we propose represents burial associated with crustal thickening from the migration of Carolinia, the Piedmont terrane, and the eastern Blue Ridge southward to their current orogenic position.

APPENDIX A: HAND SAMPLE DESCRIPTIONS AND LOCATIONS

Sample: BAK-1301
Rock Type: Eclogite
Location: Redwood Road, Bakersville, NC
UTM 17S 0396695E/3987059N
Elevation: 769m
Distance From Eclogite: 0 km
Hand Sample Description:

Omphacite and garnet rich Eclogite, some retrogression to pyroxene/amphibole. Not pervasively foliated, moderate weathering rind, dusky orange, fresh rock in center, red and green with some black. Grain size is roughly 0.5-1mm. Very dense.

Sample: BAK-1302
Rock Type: Amphibolite
Location: Dallas Young Rd, Bakersville, NC
UTM 17S 0398199E/3987871N
Elevation: 840m
Distance From Eclogite: 1.7 km
Hand Sample Description:

Well foliated, nematoblastic amphibolite. Some isoclinal folding of the felsic layers. Grain size is fine-medium grained (0.5-2mm). Overall low-mod felsic content, ~10-15%. Hard and fresh sample, no weathering. Quartz, plag and amphibole. Garnets observed in one sample when cutting thin sections.

Sample: MIC-1301
Rock Type: Amphibolite
Location: Railroad cut by the Toe Cane River, south of intersection with Roses Branch Rd
UTM 17S 0392641E/ 3983299N
Elevation: 714m
Distance From Eclogite: 5.5 km
Hand Sample Description:

Well foliated, nematoblastic amphibolite. Grain size .5-3 mm with layers of larger amphibolite crystals up to 20 mm. Overall low felsic content, ~7%. Very fresh outcrop, hard and unweathered. Quartz, plag and amphibole, no garnet observed.

Sample: MIC-1302
Rock Type: Amphibolite
Location: Conley Ridge Road near Wing, NC
UTM 17S 0398002E/3977697N
Elevation: 785m
Distance From Eclogite: 9.5 km

Hand Sample Description:

Well foliated, nematoblastic amphibolite. Grain size is fine-medium grained (0.5-1mm). Hard and fresh sample, no weathering. Overall low felsic content, ~7%. Quartz, plag and amphibole, no garnet observed. Some fracturing with epidote, limonite and MnO staining.

Sample: BUR-1301
Rock Type: Amphibolite
Location: Green Mountain Drive, Burnsville, NC
UTM 17S 0383847E/3976686N
Elevation: 860m
Distance From Eclogite: 16.4 km
Hand Sample Description:

Well foliated, nematoblastic amphibolite. Moderately weathered, plag-> kaolinite. Fairly soft and crumbles under hammer. Higher felsic content, ~20%. Medium grained, 1-3mm. Quartz, plag, kaolinite, and amphibole, no garnet observed.

Sample: BAK-1401
Rock Type: Retrograded Eclogite
Location: 572 Redwood Road, Bakersville, NC
UTM 17S 0396544E/3986933N
Elevation: 784m
Distance From Eclogite: 0 km
Hand Sample Description:

Retrograded eclogite with large amphibole crystals. Collected near a pegmatite vein.

APPENDIX B: LASER-ABLATION TI-IN-ZIRCON THERMOMETRY AND U-PB AGES

Sample, zircon #	Zircon Mount number	Ti ppm	Ti 2σ error	Ti-in-Zircon Temp °C	Monte Carlo Temp, °C	Std Dev	Pressure Correction	U-Pb Age	2σ error
MIC1301 z01	Mount1 run3.d	2.27	0.57	623.38	622.62	15.91		468	54
MIC1301 z01	Mount1 run3.d	2.82	0.49	639.44	639.18	14.18		504	67
MIC1301 z02	Mount1 run3.d	1.97	0.41	613.19	612.44	14.38		401	25
MIC1301 z02	Mount1 run3.d	3.5	0.76	656.01	656.33	15.57		448	52
MIC1301 z02	Mount1 run3.d	1.51	0.46	594.68	593.28	16.68		110	158
MIC1301 z03	Mount1 run3.d	1.72	0.63	603.65	603.05	19.04		489	31
MIC1301 z03	Mount1 run3.d	3.62	0.68	658.66	659.13	15.20		426	11
MIC1301 z03	Mount1 run3.d	10.7	3.6	752.36	749.88	24.23		460	24
MIC1301 z08	Mount1 run3.d	4	0.64	666.56	667.01	14.24		409	14
MIC1301 z09	Mount1 run3.d	2.2	0.39	621.11	621.52	13.21		443	13
MIC1301 z09	Mount1 run3.d	3.02	0.45	644.63	644.39	13.48		433	16
MIC1301 z03	mount3 run 1.d	0.93	0.91	562.87	548.75	51.13		301	191
MIC1301 z03	mount3 run 1.d	3.1	1.5	646.63	644.01	25.43		401	18
MIC1301 z03	mount3 run 1.d	0.98	0.95	566.19				6	112
MIC1301 z04	mount3 run 1.d	2.17	0.79	620.12	618.72	19.59		425	196
MIC1301 z04	mount3 run 1.d	3.75	0.82	661.44	661.39	15.93		410	14
MIC1301 z04	mount3 run 1.d	1.52	0.84	595.13	591.02	25.79		415	51
MIC1301 z06	mount3 run 1.d	1	1.6	567.48				-18	65
MIC1301 z06	mount3 run 1.d	2.87	0.97	640.77	639.90	19.09		459	34
MIC1301 z09	mount3 run 1.d	2.7	1	636.18	634.61	20.60		135	213
MIC1301 z09	mount3 run 1.d	11	1.4	754.99	754.92	15.90		99	175
MIC1301 z10	mount3 run 1.d	1.88	0.96	609.88	607.55	24.32		177	263
MIC1301	mount3 run	0.42	0.95	515.45				166	129

Sample, zircon #	Zircon Mount number	Ti ppm	Ti 2σ error	Ti-in-Zircon Temp °C	Monte Carlo Temp, °C	Std Dev	Pressure Correction	U-Pb Age	2σ error
z11	1.d								
MIC1301 z11	mount3 run 1.d	1.7	1.2	602.83	596.73	32.81		69	157
MIC1301 z12	mount3 run 1.d	0.2	1.7	475.80				437	268
MIC1301 z12	mount3 run 1.d	2.7	1	636.18	635.26	20.18		389	12
MIC1301 z13	mount3 run 1.d	4.1	1.9	668.54	666.41	25.70		-28	67
MIC1301 z14	mount3 run 1.d	3.8	1.1	662.48	662.02	18.15		497	62
MIC1301 z15	mount3 run 1.d	7.7	2.3	721.98	721.87	20.76		394	32
MIC1301 z15	mount3 run 1.d	2.7	1.1	636.18	633.73	21.71		478	72
MIC1301 z17	mount3 run 1.d	1.8	1.2	606.82	601.78	31.34		245	303
MIC1301 z17	mount3 run 1.d	1.8	1	606.82	603.65	26.25		444	39
MIC1301 z17	mount3 run 1.d	1.21	0.65	579.85	576.54	23.95		-281	360
MIC1301 z18	mount3 run 1.d	1.7	1.2	602.83	598.19	33.27		562	129
MIC1301 z18	mount3 run 1.d	8.1	1	726.53	725.33	14.99		430	31
MIC1301 z18	mount3 run 1.d	1.07	0.78	571.83	566.00	31.66		546	156
MIC1301 z19	mount3 run 1.d	3.9	1.5	664.54	664.12	22.06		417	18
MIC1301 z19	mount3 run 1.d	2	1.9	614.26	599.73	53.47		473	67
MIC1301 z26	mount3 run 1.d	2.05	0.89	616.03	613.18	21.10		483	219
MIC1301 z26	mount3 run 1.d	2.3	1.6	624.34	617.61	34.10		435	22
MIC1301 z27	mount3 run 1.d	4.5	1.2	676.07	675.68	17.59		550	67
MIC1301 z28	mount3 run 1.d	3.5	1.1	656.01	654.80	18.65		453	48
MIC1301 z28	mount3 run 1.d	1.3	1.2	584.60	574.15	47.72		425	133
MIC1301 z30	mount3 run 1.d	6.6	2.5	708.35	705.52	23.18		477	17
MIC1301 z30	mount3 run 1.d	4.2	1.6	670.48	668.70	22.56		1	7
MIC1301 z31	mount3 run 1.d	5.8	1.2	697.22	697.32	15.92		425	16
MIC1301 z31	mount3 run 1.d	2.3	1.2	624.34	622.01	25.44		422	22
MIC1301 z32	mount3 run 1.d	8.7	2.1	733.04	732.04	18.72		440	28

Sample, zircon #	Zircon Mount number	Ti ppm	Ti 2σ error	Ti-in-Zircon Temp °C	Monte Carlo Temp, °C	Std Dev	Pressure Correction	U-Pb Age	2σ error
MIC1301 z32	mount3 run 1.d	3.5	1.1	656.01	655.78	18.37		433	21
MIC1301 z33	mount3 run 1.d	3.4	1.1	653.76	651.33	18.73		415	23
MIC1301 z33	mount3 run 1.d	1.8	1	606.82	603.72	26.98		408	37
MIC1301 z35	mount3 run 1.d	6.8	2.2	710.96	709.90	21.26		450	29
MIC1301 z35	mount3 run 1.d	1.5	1.1	594.23	589.26	35.02		-60	1269
MIC1301 z35	mount3 run 1.d	4.3	1.4	672.38	669.90	19.99		523	189
MIC1301 z36	mount3 run 1.d	3.4	1.2	653.76	652.95	20.01		735	148
MIC1301 z36	mount3 run 1.d	2.5	1.5	630.45	626.22	29.56		436	24
MIC1301 z36	mount3 run 1.d	3	1.5	644.13	641.03	26.13		423	21
MIC1301 z36	mount3 run 1.d	2.3	1.8	624.34	615.31	40.00		492	34
MIC1301 z37	mount3 run 1.d	0.03	0.84	390.49				0	#VALUE!
MIC1301 z37	mount3 run 1.d	3	1.7	644.13	639.92	30.46		435	45
MIC1301 z37	mount3 run 1.d	6.8	2.1	710.96	709.91	20.55		432	25
MIC1301 z37	mount3 run 1.d	1.2	1.4	579.30				281	169
MIC1301 z01	Mount3 run2.d	1.75	0.64	604.85	603.29	18.18		468	66
MIC1301 z01	Mount3 run2.d	3.26	0.45	650.50	650.22	14.14		458	15
MIC1301 z01	Mount3 run2.d	4.23	0.66	671.05	670.70	14.33		417	22
MIC1301 z01	Mount3 run2.d	2.61	0.54	633.65	633.16	14.47		425	24
MIC1301 z01	Mount3 run2.d	1.71	0.44	603.24	603.24	15.05		445	28
MIC1301 z05	Mount3 run2.d	1.26	0.56	582.52	580.59	21.16		410	22
MIC1301 z05	Mount3 run2.d	4.39	0.74	674.06	673.97	15.31		414	18
MIC1301 z05	Mount3 run2.d	1.68	0.53	602.01	601.76	17.04		421	29
MIC1301 z05	Mount3 run2.d	2.63	0.4	634.21	633.93	12.82		422	20
MIC1301 z05	Mount3 run2.d	1.57	0.32	597.35	597.36	13.83		~~431~~	~~220~~

Sample, zircon #	Zircon Mount number	Ti ppm	Ti 2σ error	Ti-in-Zircon Temp °C	Monte Carlo Temp, °C	Std Dev	Pressure Correction	U-Pb Age	2σ error
Sample, zircon #	Zircon Mount number	Ti ppm	Ti 2σ error	Ti-in-Zircon Temp °C	Monte Carlo Temp, °C	Std Dev	Pressure Correction	Age	2σ error
BAK1301 z03	Mount1 run4.d	2.11	0.36	618.10	618.39	13.98	688.10	470	25
BAK1301 z03	Mount1 run4.d	2.98	0.77	643.62	642.29	16.30	713.62	454	18
BAK1301 z03	Mount1 run4.d	2.58	0.48	632.79	633.29	14.42	702.79	485	14
BAK1301 z04	Mount1 run4.d	2.80	0.80	638.90	638.01	17.43	708.90	463	13
BAK1301 z05	Mount1 run4.d	3.00	0.82	644.13	643.91	16.66	714.13	555	344
BAK1301 z05	Mount1 run4.d	3.30	0.55	651.44	652.24	14.25	721.44	553	36
BAK1301 z06	Mount1 run4.d	2.05	0.54	616.03	615.54	16.47	686.03	453	22
BAK1301 z06	Mount1 run4.d	4.00	1.10	666.56	665.41	17.45	736.56	456	20
BAK1301 z06	Mount1 run4.d	4.17	0.71	669.90	669.90	14.68	739.90	457	27
BAK1301 z07	Mount1 run4.d	3.24	0.49	650.02	649.28	13.82	720.02	443	32
BAK1301 z07	Mount1 run4.d	3.96	0.73	665.76	665.23	14.74	735.76	509	58
							70.00		
BAK1301 z08	Mount1 run4.d	2.73	0.61	637.00	636.68	15.18	707.00	459	14
BAK1301 z08	Mount1 run4.d	2.14	0.71	619.11	616.61	18.11	689.11	455	115
BAK1301 z10	Mount1 run4.d	11.80	2.40	761.75	761.45	18.11	831.75	464	29
BAK1301 z10	Mount1 run4.d	3.81	0.72	662.69	661.63	14.92	732.69	456	12
BAK1301 z11	Mount1 run4.d	2.24	0.59	622.41	621.83	15.83	692.41	522	330
BAK1301 z13	Mount1 run4.d	3.15	0.34	647.86	647.66	13.22	717.86	426	15
BAK1301 z14	Mount1 run4.d	7.07	0.96	714.39	714.19	14.80	784.39	462	15
BAK1301 z14	Mount1 run4.d	7.70	1.10	721.98	721.03	15.25	791.98	455	13
BAK1301 z14	Mount1 run4.d	3.81	0.87	662.69	661.69	15.76	732.69	453	15
BAK1301 z15	Mount1 run4.d	3.00	0.36	644.13	644.30	13.13	714.13	438	42
BAK1301 z15	Mount1 run4.d	2.64	0.43	634.50	634.01	13.48	704.50	460	68
BAK1301 z16	Mount1 run4.d	2.39	0.58	627.14	626.70	15.25	697.14	462	14

Sample, zircon #	Zircon Mount number	Ti ppm	Ti 2σ error	Ti-in-Zircon Temp °C	Monte Carlo Temp, °C	Std Dev	Pressure Correction	U-Pb Age	2σ error
BAK1301 z16	Mount1 run4.d	3.74	0.57	661.22	661.55	14.27	731.22	444	16
BAK1301 z16	Mount1 run4.d	2.16	0.69	619.78	618.68	17.99	689.78	443	15
							70.00		
BAK1301 z18	Mount1 run3.d	1.80	0.49	606.82	606.41	15.61	676.82	378	222
BAK1301 z18	Mount1 run3.d	1.99	0.41	613.91	613.72	14.28	683.91	520	150
BAK1301 z18	Mount1 run3.d	2.13	0.64	618.77	617.42	17.10	688.77	422	300
BAK1301 z18	Mount1 run3.d	1.92	0.30	611.37	611.28	13.23	681.37	541	97
BAK1301 z19	Mount1 run3.d	2.91	0.68	641.81	641.76	16.10	711.81	448	19
BAK1301 z19	Mount1 run3.d	2.33	0.50	625.28	624.75	14.88	695.28	463	23
BAK1301 z19	Mount1 run3.d	2.45	0.58	628.96	628.55	15.48	698.96	456	15
BAK1301 z22	Mount1 run3.d	22.30	2.10	827.34	826.98	16.29	897.34	462	11
BAK1301 z22	Mount1 run3.d	10.66	0.62	752.00	751.48	14.34	822.00	462	11
BAK1301 z24	Mount1 run3.d	2.07	0.84	616.72	614.98	20.48	686.72	450	16
BAK1301 z24	Mount1 run3.d	1.96	0.69	612.83	610.64	18.66	682.83	455	17
BAK1301 z24	Mount1 run3.d	2.38	0.48	626.83	626.23	14.28	696.83	455	17
~~**BAK1301 z24**~~	~~Mount1 run3.d~~	~~3510.00~~	~~510.00~~	~~1944.25~~	~~1941.14~~	~~60.91~~	2014.25	~~582~~	~~216~~
BAK1301 z26	Mount1 run3.d	6.36	0.88	705.14	705.00	14.85	775.14	453	14
BAK1301 z26	Mount1 run3.d	3.98	0.96	666.16	664.47	16.37	736.16	438	27
BAK1301 z30	Mount1 run3.d	2.48	0.64	629.86	629.82	16.28	699.86	458	14
BAK1301 z31	Mount1 run3.d	3.36	0.65	652.84	652.48	14.84	722.84	448	14
BAK1301 z31	Mount1 run3.d	2.65	0.43	634.78	634.80	13.65	704.78	443	14
BAK1301 z31	Mount1 run3.d	2.86	0.82	640.50	639.88	17.44	710.50	461	16
BAK1301 z32	Mount1 run3.d	3.08	0.46	646.13	645.68	13.47	716.13	447	14
BAK1301 z32	Mount1 run3.d	2.86	0.44	640.50	640.49	13.76	710.50	456	15
BAK1301 z33	Mount1 run3.d	1.67	0.44	601.60	601.16	14.87	671.60	489	43
BAK1301	Mount1	3.67	0.87	659.73	659.99	16.74	729.73	448	16

Sample, zircon #	Zircon Mount number	Ti ppm	Ti 2σ error	Ti-in-Zircon Temp °C	Monte Carlo Temp, °C	Std Dev	Pressure Correction	U-Pb Age	2σ error
z33	run3.d								
BAK1301 z34	Mount1 run3.d	1.64	0.32	600.35	600.60	13.39	670.35	160	196
BAK1301 z35	Mount1 run3.d	4.29	0.56	672.19	672.28	14.07	742.19	456	18
BAK1301 z35	Mount1 run3.d	3.45	0.91	654.89	654.46	17.04	724.89	459	19
							70.00		
BAK1301 z39	Mount3 run2.d	5.39	0.73	691.01	690.98	14.19	761.01	461	14
BAK1301 z38	Mount3 run2.d	3.04	0.56	645.14	644.49	14.03	715.14	~~603~~	~~240~~
BAK1301 z37	Mount3 run2.d	2.06	0.33	616.38	615.47	13.22	686.38	463	13
BAK1301 z37	Mount3 run2.d	3.87	0.47	663.93	663.67	13.39	733.93	455	13
BAK1301 z36	Mount3 run2.d	2.98	0.63	643.62	643.98	14.83	713.62	447	18
BAK1301 z35	Mount3 run2.d	9.00	1.20	736.15	734.97	15.85	806.15	452	12
BAK1301 z34	Mount3 run2.d	2.08	0.54	617.07	616.37	16.21	687.07	485	32
BAK1301 z34	Mount3 run2.d	2.22	0.54	621.76	620.78	15.39	691.76	599	114
BAK1301 z33	Mount3 run2.d	2.20	0.36	621.11	620.22	13.15	691.11	476	30
BAK1301 z33	Mount3 run2.d	1.82	0.53	607.60	607.02	16.86	677.60	485	32
BAK1301 z32	Mount3 run2.d	2.71	0.38	636.45	636.36	12.92	706.45	464	16
BAK1301 z31	Mount3 run2.d	3.62	0.55	658.66	658.60	14.18	728.66	449	16
BAK1301 z30	Mount3 run2.d	2.65	0.64	634.78	634.56	15.98	704.78	491	38
BAK1301 z29	Mount3 run2.d	3.36	0.49	652.84	652.98	13.64	722.84	457	14
BAK1301 z28	Mount3 run2.d	1.95	0.43	612.46	611.33	14.89	682.46	466	35
BAK1301 z28	Mount3 run2.d	2.50	0.56	630.45	629.89	15.42	700.45	~~306~~	~~142~~
BAK1301 z26	Mount3 run2.d	2.57	0.49	632.50	632.23	14.50	702.50	453	17
BAK1301 z26	Mount3 run2.d	3.96	0.54	665.76	665.39	14.01	735.76	458	13
BAK1301 z25	Mount3 run2.d	2.31	0.35	624.65	624.01	12.56	694.65	464	17
BAK1301 z24	Mount3 run2.d	11.60	1.50	760.10	760.22	15.91	830.10	456	14
BAK1301 z23	Mount3 run2.d	3.20	0.66	649.07	648.61	15.04	719.07	460	18

Sample, zircon #	Zircon Mount number	Ti ppm	Ti 2σ error	Ti-in-Zircon Temp °C	Monte Carlo Temp, °C	Std Dev	Pressure Correction	U-Pb Age	2σ error
BAK1301 z23	Mount3 run2.d	2.11	0.58	618.10	617.92	16.44	688.10	466	19
BAK1301 z22	Mount3 run2.d	2.67	0.45	635.34	634.97	14.37	705.34	468	19
BAK1301 z22	Mount3 run2.d	2.86	0.57	640.50	640.30	15.11	710.50	469	18
BAK1301 z21	Mount3 run2.d	6.19	0.82	702.80	702.31	14.86	772.80	466	13
BAK1301 z20	Mount3 run2.d	2.07	0.45	616.72	615.76	14.50	686.72	464	31
BAK1301 z20	Mount3 run2.d	1.97	0.42	613.19	612.27	13.99	683.19	457	31
BAK1301 z19	Mount3 run2.d	2.88	0.57	641.03	640.49	14.90	711.03	459	15
BAK1301 z19	Mount3 run2.d	2.98	0.68	643.62	642.77	15.43	713.62	457	17
BAK1301 z17	Mount3 run2.d	3.44	0.53	654.67	653.99	13.96	724.67	455	14
BAK1301 z16	Mount3 run2.d	1.80	0.59	606.82	605.44	18.00	676.82	467	27
BAK1301 z15	Mount3 run2.d	2.11	0.36	618.10	618.09	13.45	688.10	454	16
BAK1301 z15	Mount3 run2.d	4.12	0.53	668.93	669.21	13.59	738.93	457	14
BAK1301 z13	Mount3 run2.d	1.65	0.41	600.77	599.50	14.99	670.77	496	104
BAK1301 z12	Mount3 run2.d	2.39	0.70	627.14	625.28	16.84	697.14	462	20
BAK1301 z11	Mount3 run2.d	3.16	0.73	648.10	647.66	15.58	718.10	462	18
BAK1301 z09	Mount3 run2.d	2.10	0.23	617.75	617.31	12.32	687.75	465	20
BAK1301 z09	Mount3 run2.d	3.29	0.73	651.21	650.63	15.83	721.21	458	14
BAK1301 z08	Mount3 run2.d	3.12	0.64	647.12	646.89	14.68	717.12	484	15
BAK1301 z08	Mount3 run2.d	2.92	0.55	642.07	642.44	14.28	712.07	460	19
BAK1301 z07	Mount3 run2.d	3.09	0.44	646.38	646.23	13.43	716.38	480	39
BAK1301 z07	Mount3 run2.d	1.96	0.50	612.83	612.00	14.98	682.83	~~87~~	~~266~~
BAK1301 z06	Mount3 run2.d	3.04	0.55	645.14	645.56	14.41	715.14	482	25
BAK1301 z06	Mount3 run2.d	2.04	0.36	615.68	615.91	13.67	685.68	467	17
BAK1301 z05	Mount3 run2.d	1.79	0.46	606.43	605.92	15.55	676.43	471	23
BAK1301 z05	Mount3 run2.d	2.93	0.66	642.33	641.59	15.52	712.33	468	20
BAK1301	Mount3	1.68	0.53	602.01	600.79	17.22	672.01	454	22

Sample, zircon #	Zircon Mount number	Ti ppm	Ti 2σ error	Ti-in-Zircon Temp °C	Monte Carlo Temp, °C	Std Dev	Pressure Correction	U-Pb Age	2σ error
z05	run2.d								
BAK1301 z04	Mount3 run2.d	2.27	0.48	623.38	622.75	14.64	693.38	460	22
BAK1301 z04	Mount3 run2.d	3.03	0.85	644.89	644.80	16.89	714.89	466	27
BAK1301 z04	Mount3 run2.d	2.70	0.39	636.18	635.73	13.84	706.18	448	29
Sample, zircon #	**Zircon Mount number**	**Ti ppm**	**Ti 2σ error**	**Ti-in-Zircon Temp °C**	**Monte Carlo Temp, °C**	**Std Dev**	**Pressure Correction**	**Age**	**2σ error**
BAK1302 z27	mount3 run 1.d	1.21	0.91	579.85	573.06	33.97		68	90
BAK1302 z27	mount3 run 1.d	-0.03	0.97	#NUM!				-37	206
BAK1302 z27	mount3 run 1.d	2.2	1.3	621.11	616.45	28.75		-117	431
BAK1302 z27	mount3 run 1.d	1.1	1.7	573.62				-25	178
BAK1302 z26	mount3 run 1.d	3.5	1.6	656.01	653.06	23.60		416	240
BAK1302 z26	mount3 run 1.d	1.9	1.1	610.63	605.30	27.96		1	46
BAK1302 z26	mount3 run 1.d	1.8	1.2	606.82	601.97	31.86		100	192
BAK1302 z18	mount3 run 1.d	2.2	1.4	621.11	615.98	31.69		44	137
BAK1302 z18	mount3 run 1.d	2.08	0.76	617.07	616.58	19.89		542	159
BAK1302 z18	mount3 run 1.d	2.57	0.89	632.50	630.82	18.95		49	43
Sample, zircon #	**Core/Rim**	**Ti ppm**	**Ti error**	**Ti-in-Zircon Temp °C**	**Monte Carlo Temp, °C**	**Std Dev**	**Pressure Correction**	**Age**	**2σ error**
BAK-1401 z1	C	2.151180319	0.714		618.91	17.37	688.91		
BAK-1401 z3	C	2.368208099	0.223		627.12	12.02	697.12		
BAK-1401 z5	C	2.502508659	0.266		630.65	12.73	700.65		
BAK-1401 z6	C	3.415256528	0.209		654.17	12.54	724.17		
BAK-1401 z7	C	3.259895363	0.43		650.29	13.35	720.29		
BAK-1401 z9	C	1.83794299	0.434		608.08	14.55	678.08		

Sample, zircon #	Zircon Mount number	Ti ppm	Ti 2σ error	Ti-in-Zircon Temp °C	Monte Carlo Temp, °C	Std Dev	Pressure Correction	U-Pb Age	2σ error
BAK-1401 z10	C	2.421466922	0.385		628.38	13.52	698.38		
BAK-1401 z11	C	3.665985418	0.375		659.44	12.76	729.44		
BAK-1401 z11	C	2.94323697	0.384		643.19	13.27	713.19		
BAK-1401 z12	C	3.557589414	0.223		657.25	12.63	727.25		
BAK-1401 z13	C	5.1568	0.209		687.00	12.58	757.00		
BAK-1401 z14	C	2.534315056	0.442		631.00	13.77	701.00		
BAK-1401 z15	C	3.067120173	0.365		646.00	12.83	716.00		
BAK-1401 z16	C	1.944622469	0.223		611.97	12.45	681.97		
BAK-1401 z17	C	1.935735475	0.365		611.66	13.88	681.66		
BAK-1401 z19	C	9.5763	0.203		742.09	13.98	812.09		
BAK-1401 z20	C	3.716506033	0.219		661.67	12.60	731.67		
BAK-1401 z23	C	2.5589	0.29		632.56	12.96	702.56		
BAK-1401 z24	C	1.984879979	0.288		613.65	12.80	683.65		
BAK-1401 z26	C	2.168993072	0.218		620.29	11.91	690.29		
BAK-1401 z27	C	2.060844977	0.246		616.81	12.59	686.81		
BAK-1401 z28	C	3.3573	0.259		652.79	12.80	722.79		
BAK-1401 z29	C	3.076768711	0.219		646.07	11.91	716.07		
BAK-1401 z30	C	8.382803523	0.198		728.69	13.46	798.69		
BAK-1401 z30	C	2.928468551	0.194		642.57	11.87	712.57		
BAK-1401 z32	C	2.7085	0.185		636.09	12.53	706.09		
BAK-1401 z33	C	4.3459	0.235		673.11	12.89	743.11		
BAK-1401 z34	C	3.182968215	0.203		648.88	12.41	718.88		

Sample, zircon #	Zircon Mount number	Ti ppm	Ti 2σ error	Ti-in-Zircon Temp °C	Monte Carlo Temp, °C	Std Dev	Pressure Correction	U-Pb Age	2σ error
BAK-1401 z36	C	3.4683	0.184		654.65	12.33	724.65		
BAK-1401 z37	C	2.5265 59649	0.241		630.99	12.76	700.99		
BAK-1401 z38	C	6.3552 33326	0.786		704.62	14.14	774.62		
BAK-1401 z39	C	2.2281 21288	0.085		622.06	11.86	692.06		
BAK-1401 z40	C	3.8626 35956	0.456		663.83	13.65	733.83		
BAK-1401 z41	C	3.293	0.227		651.31	12.52	721.31		
BAK-1401 z43	C	9.4928 66739	0.588		740.90	14.86	810.90		
BAK-1401 z43	C	5.4889 10624	0.598		692.09	13.77	762.09		
BAK-1401 z44	C	1.8654	0.235		609.80	12.39	679.80		
BAK-1401 z45	C	2.8458 56997	0.116		640.65	12.48	710.65		
BAK-1401 z45	C	2.0803 35828	0.111		617.16	11.71	687.16		
BAK-1401 z46	C	2.2002 12046	0.199		621.39	12.00	691.39		
BAK-1401 z1	R	3.9472 62031	0.746		664.40	15.21			
BAK-1401 z3	R	1.7422 82631	0.285		604.77	12.66			
BAK-1401 z5	R	1.4109 9479	0.271		589.82	13.44			
BAK-1401 z6	R	2.5989 79996	0.221		632.68	12.19			
BAK-1401 z7	R	1.5266 02212	0.446		594.96	16.01			
BAK-1401 z9	R	2.3970 98655	0.418		627.52	13.32			
BAK-1401 z10	R	2.6211 30482	0.398		633.97	13.40			
BAK-1401 z10	R	2.1049 71297	0.377		617.12	13.37			
BAK-1401 z11	R	5.2649 14969	0.382		688.58	12.95			
BAK-1401 z12	R	1.7317 55876	0.226		603.22	12.43			

Sample, zircon #	Zircon Mount number	Ti ppm	Ti 2σ error	Ti-in-Zircon Temp °C	Monte Carlo Temp, °C	Std Dev	Pressure Correction	U-Pb Age	2σ error
BAK-1401 z14	R	1.753508728	0.451		604.26	15.57			
BAK-1401 z15	R	1.998144074	0.389		613.83	13.46			
BAK-1401 z16	R	1.897760128	0.218		611.39	11.89			
BAK-1401 z16	R	1.579186294	0.214		597.31	12.28			
BAK-1401 z17	R	1.65033264	0.377		600.02	14.08			
BAK-1401 z20	R	1.894870784	0.217		610.49	12.71			
BAK-1401 z24	R	2.846270933	0.761		639.47	17.78			
BAK-1401 z26	R	1.579788521	0.225		597.70	12.47			
BAK-1401 z27	R	2.500878255	0.238		630.16	12.63			
BAK-1401 z29	R	1.125304562	0.217		575.66	13.41			
BAK-1401 z30	R	4.876555707	0.196		682.71	12.98			
BAK-1401 z30	R	3.394076693	0.217		653.72	12.63			
BAK-1401 z34	R	1.787641128	0.198		606.66	12.46			
BAK-1401 z37	R	1.679186928	0.239		601.55	12.80			
BAK-1401 z38	R	5.507343455	0.774		692.52	14.84			
BAK-1401 z38	R	4.849374153	0.81		682.31	15.11			
BAK-1401 z39	R	1.97409243	0.086		613.31	11.33			
BAK-1401 z40	R	1.983480584	0.456		614.09	15.20			
BAK-1401 z43	R	3.857238821	0.565		663.91	13.77			
BAK-1401 z43	R	2.71379695	0.572		636.26	15.28			
BAK-1401 z46	R	3.557921674	0.195		657.14	12.56			

APPENDIX C: RARE EARTH ELEMENT ABUNDANCE (NORMALIZED TO CHONDRITE)

	Chondrite	0.24	0.613	0.093	0.457	0.148	0.056	0.199	0.036	0.246	0.055	0.16	0.025	0.161	0.025	0.103	
Sample, zircon #	Zircon Mount	La	Ce	Pr	Nd	Sm	Eu	Gd	Tb	Dy	Ho	Er	Tm	Yb	Lu	Hf	Th/U
BAK1301 z03	Mnt1run4	-0.01	0.38	0.04	0.05	1.55	4.66	17.79	26.94	28.62	27.45	20.31	16.68	15.96	15.72	107766.99	0.05
BAK1301 z03	Mnt1run4	0.00	0.22	0.08	0.06	0.99	2.36	8.59	20.83	30.49	34.73	24.06	20.40	21.43	19.04	114757.28	0.14
BAK1301 z03	Mnt1run4	0.01	0.82	0.01	0.17	3.62	7.04	21.76	34.72	33.33	27.64	22.31	17.68	21.37	24.44	103786.41	0.05
BAK1301 z04	Mnt1run4	0.00	0.14	0.06	0.10	1.10	4.43	20.75	49.44	64.63	55.09	37.69	24.00	21.55	17.56	119417.48	0.01
BAK1301 z05	Mnt1run4	0.04	0.04	0.01	0.04	0.23	1.05	2.21	8.03	21.06	35.09	40.06	37.60	31.43	30.36	102330.10	0.07
BAK1301 z05	Mnt1run4	0.46	0.18	0.76	0.52	1.29	3.02	8.49	17.97	30.28	40.55	36.94	27.20	27.89	29.60	97378.64	0.08
BAK1301 z06	Mnt1run4	0.03	0.07	0.06	0.11	0.26	1.43	4.92	14.97	23.58	26.00	17.31	12.00	12.48	11.48	109320.39	0.04
BAK1301 z06	Mnt1run4	0.02	0.18	0.06	0.02	0.74	2.54	9.15	27.69	57.32	81.82	79.75	72.80	73.29	65.20	106796.12	0.05
BAK1301 z06	Mnt1run4	0.14	0.23	0.25	0.22	0.53	1.14	3.07	10.97	17.40	18.91	14.88	12.64	14.04	11.04	115339.81	0.10
BAK1301 z07	Mnt1run4	0.04	0.02	0.08	0.06	0.87	0.75	1.86	6.19	14.47	25.09	27.88	24.40	28.94	27.20	108737.86	0.18
BAK1301 z07	Mnt1run4	0.02	0.06	0.04	0.07	0.54	0.48	2.51	8.75	14.55	25.45	30.00	28.40	34.91	30.40	106407.77	0.01
BAK1301 z08	Mnt1run4	0.04	0.97	0.09	0.21	5.14	9.25	28.24	44.17	44.72	35.09	30.69	28.00	29.57	32.44	112233.01	0.04
BAK1301 z08	Mnt1run4	0.04	0.09	0.04	0.17	0.33	0.63	1.91	5.72	9.35	17.22	20.81	22.28	25.59	28.80	111262.14	-0.23
BAK1301 z10	Mnt1run4	0.46	0.53	0.63	0.55	0.61	2.39	6.88	27.50	63.41	100.18	106.25	87.60	87.58	80.00	104368.93	0.08
BAK1301 z10	Mnt1run4	0.27	0.88	0.74	0.40	2.64	7.18	18.79	30.36	34.43	33.64	25.75	19.08	20.37	20.80	81844.66	0.01
BAK1301 z11	Mnt1run4	0.01	0.03	-0.02	0.15	0.45	0.96	3.32	9.69	23.50	37.82	37.38	31.88	29.32	29.08	107669.90	-0.06
BAK1301 z13	Mnt1run4	0.01	0.39	0.08	0.12	2.36	5.63	27.09	48.89	52.44	52.73	38.63	33.20	40.75	39.20	101553.40	0.09
BAK1301 z14	Mnt1run4	0.01	0.86	0.23	0.54	3.85	6.20	15.03	30.00	34.72	38.18	29.81	19.20	22.42	27.60	99126.21	0.06
BAK1301 z14	Mnt1run4	0.02	0.77	0.09	0.55	3.68	9.54	29.20	53.33	68.70	60.91	48.56	30.64	30.43	31.60	101844.66	0.04
BAK1301 z14	Mnt1run4	0.01	0.42	0.01	0.21	2.97	5.20	13.52	26.39	32.72	30.55	22.31	18.40	17.20	16.68	101650.49	0.01
BAK1301 z15	Mnt1run4	0.01	0.08	0.03	0.04	0.27	0.98	2.81	10.81	30.00	54.73	65.00	59.20	53.42	52.00	98058.25	0.10
BAK1301 z15	Mnt1run4	0.02	0.03	-0.01	0.09	0.09	0.70	2.11	9.17	19.92	33.27	32.56	21.32	22.98	18.00	92330.10	-0.15
BAK1301 z16	Mnt1run4	0.00	0.26	0.02	0.09	1.24	3.45	12.11	31.11	35.77	35.27	24.75	20.88	20.56	18.00	105533.98	-0.02
BAK1301 z16	Mnt1run4	0.03	0.19	0.01	0.12	0.82	2.82	12.01	32.22	48.90	56.91	47.81	39.36	34.29	34.00	105825.24	0.04
BAK1301 z16	Mnt1run4	0.05	0.11	0.00	0.13	0.94	2.29	8.94	23.89	33.90	31.82	26.38	20.28	21.24	15.40	109417.48	-0.04
BAK1301 z18	Mnt1run3	0.03	0.02	0.04	0.08	0.65	0.46	0.46	2.11	6.22	9.75	12.00	15.32	11.24	10.68	107766.99	0.06
BAK1301 z18	Mnt1run3	0.92	0.13	1.89	1.68	1.28	1.50	2.15	6.44	12.93	22.85	31.44	26.92	23.42	23.60	98446.60	-0.12
BAK1301 z18	Mnt1run3	0.03	0.02	0.05	0.12	0.27	0.30	1.21	3.22	8.50	15.67	21.19	22.12	19.07	21.00	108155.34	0.21
BAK1301 z18	Mnt1run3	0.00	0.01	0.07	0.09	0.24	0.41	1.24	2.72	6.71	13.07	16.00	14.84	15.84	12.52	110582.52	0.07
BAK1301 z19	Mnt1run3	0.01	0.13	0.05	0.16	1.55	7.04	25.48	67.78	104.47	93.82	67.63	62.80	62.73	60.40	110291.26	0.01
BAK1301 z19	Mnt1run3	0.01	0.11	0.08	0.06	0.89	3.48	11.81	33.33	48.09	42.91	31.50	29.12	28.45	32.80	119417.48	-0.03
BAK1301 z19	Mnt1run3	0.04	0.15	0.05	0.15	0.99	3.59	13.52	31.11	40.28	34.73	33.25	25.20	28.82	29.00	108737.86	-0.03
BAK1301 z22	Mnt1run3	0.04	4.29	0.32	1.18	12.23	23.93	35.33	40.00	40.24	31.45	25.00	19.60	19.01	19.20	113592.23	0.06
BAK1301 z22	Mnt1run3	0.14	3.47	0.27	1.01	8.58	20.23	42.66	50.28	47.64	39.64	27.31	22.72	21.86	18.44	107281.55	0.07
BAK1301 z24	Mnt1run3	0.02	0.21	0.04	0.27	1.06	2.84	10.95	22.86	30.93	33.09	22.25	14.00	17.83	17.48	98932.04	-0.06
BAK1301 z24	Mnt1run3	0.04	0.16	0.01	0.10	0.75	2.02	8.49	23.89	34.31	31.82	20.88	18.64	16.89	13.64	109514.56	-0.02
BAK1301 z24	Mnt1run3	0.00	0.17	0.02	0.04	0.74	2.59	8.44	23.58	42.24	41.64	31.13	23.60	19.50	19.24	104854.37	0.04
BAK1301 z24	Mnt1run3	1.28	5.63	9.03	14.44	27.23	40.36	49.75	64.72	58.13	36.55	28.75	17.60	15.40	23.20	98058.25	0.18
BAK1301 z26	Mnt1run3	0.03	1.28	0.09	0.28	2.30	5.71	10.60	10.61	10.98	14.25	14.38	11.44	12.61	10.56	106893.20	0.10
BAK1301 z26	Mnt1run3	0.02	0.24	0.06	0.14	0.35	1.05	2.36	8.25	12.85	23.09	26.69	19.68	21.12	16.12	107281.55	0.21
~~BAK1301 z28~~	~~Mnt1run3~~	~~0.04~~	~~19.74~~	~~0.39~~	~~1.12~~	~~9.66~~	~~6.89~~	~~38.69~~	~~75.83~~	~~153.25~~	~~300.00~~	~~536.88~~	~~844.00~~	~~1378.88~~	~~2152.00~~	~~106116.50~~	~~0.44~~
~~BAK1301 z28~~	~~Mnt1run3~~	~~0.05~~	~~19.64~~	~~1.30~~	~~4.49~~	~~24.59~~	~~15.88~~	~~104.52~~	~~200.56~~	~~343.50~~	~~636.36~~	~~1006.25~~	~~1532.00~~	~~2291.93~~	~~3380.00~~	~~97475.73~~	~~0.51~~
BAK1301 z30	Mnt1run3	0.03	0.88	0.02	0.15	2.77	6.36	19.65	28.89	28.58	25.64	21.69	19.24	22.67	24.40	101941.75	0.05
BAK1301 z31	Mnt1run3	0.02	0.37	0.03	0.16	2.20	8.80	34.17	84.72	125.20	127.09	92.50	80.40	67.70	71.20	96699.03	0.01
BAK1301 z31	Mnt1run3	0.03	0.38	0.00	0.13	1.96	6.23	19.85	44.44	68.29	58.91	45.13	36.40	30.75	30.96	100000.00	0.03
BAK1301 z31	Mnt1run3	0.02	0.57	0.04	0.13	1.12	4.86	14.17	21.39	27.76	27.09	23.19	16.28	18.70	22.24	100776.70	0.03
BAK1301 z32	Mnt1run3	0.05	0.30	0.05	0.17	2.50	9.71	38.39	91.11	100.00	80.91	56.25	33.08	30.50	31.20	121553.40	-0.01
BAK1301 z32	Mnt1run3	0.01	0.32	0.00	0.27	3.31	11.50	44.72	81.39	87.80	57.09	37.06	23.72	20.25	19.20	116893.20	0.03
BAK1301 z33	Mnt1run3	0.01	0.06	0.02	0.12	0.37	1.23	5.18	12.53	16.26	17.16	11.88	9.20	7.76	9.80	99902.91	-0.01
BAK1301 z33	Mnt1run3	0.00	0.20	0.01	0.14	1.03	4.84	21.21	57.78	84.55	83.64	58.56	47.20	41.12	44.00	112621.36	0.04
BAK1301 z34	Mnt1run3	0.02	0.01	0.02	0.08	0.48	0.41	0.79	2.75	8.21	13.51	18.69	15.08	13.79	13.88	108349.51	-0.26
BAK1301 z35	Mnt1run3	0.02	0.45	-0.01	0.11	0.95	4.73	17.49	52.50	84.15	76.91	57.19	34.44	30.87	26.80	116796.12	0.04
BAK1301 z35	Mnt1run3	0.02	0.33	0.03	0.14	1.14	3.71	11.21	24.08	36.10	40.36	30.44	21.84	22.24	20.44	116796.12	0.00

	Chondrite	0.24	0.613	0.093	0.457	0.148	0.056	0.199	0.036	0.246	0.055	0.16	0.025	0.161	0.025	0.103	
Sample, zircon #	Zircon Mount	La	Ce	Pr	Nd	Sm	Eu	Gd	Tb	Dy	Ho	Er	Tm	Yb	Lu	Hf	Th/U
BAK1301 z08	Mnt3run2	0.03	1.52	0.06	0.27	4.05	6.82	20.85	32.50	36.18	32.18	32.13	25.72	28.26	30.80	90388.35	0.01
BAK1301 z35	Mnt3run2	0.03	1.66	0.13	0.32	3.80	7.27	18.54	27.78	36.59	38.55	32.00	24.80	21.68	20.80	93786.41	0.09
BAK1301 z37	Mnt3run2	0.02	0.27	0.02	0.12	1.53	5.80	23.72	62.50	80.89	66.18	49.13	31.88	26.83	21.84	105145.63	0.00
BAK1301 z17	Mnt3run2	0.02	0.30	0.05	0.16	1.36	4.54	14.87	35.00	60.98	61.45	49.56	39.60	33.66	29.60	107766.99	0.06
BAK1301 z21	Mnt3run2	0.04	0.59	0.08	0.32	2.29	5.05	16.63	36.11	53.25	57.64	44.00	33.20	28.45	27.60	99902.91	-0.01
BAK1301 z37	Mnt3run2	0.02	0.27	0.09	0.12	0.86	5.43	23.82	62.78	100.81	79.09	58.19	38.80	31.99	25.20	112621.36	0.00
BAK1301 z24	Mnt3run2	0.03	1.67	0.31	0.79	6.69	9.77	23.82	40.00	45.93	45.27	36.50	31.20	35.90	36.68	97475.73	0.02
BAK1301 z26	Mnt3run2	0.02	0.66	0.07	0.22	3.85	8.38	30.60	50.28	52.44	42.00	33.00	27.04	29.63	28.28	105533.98	0.03
BAK1301 z09	Mnt3run2	1.22	1.60	1.25	1.73	2.91	5.70	17.79	48.33	72.36	56.00	38.63	26.00	20.25	18.76	105922.33	-0.02
BAK1301 z19	Mnt3run2	0.00	0.43	0.06	0.17	3.04	9.48	37.74	62.50	62.52	57.82	49.00	44.80	47.45	48.00	101262.14	0.12
BAK1301 z15	Mnt3run2	0.01	0.17	0.03	0.09	1.85	6.04	23.92	49.17	67.89	78.00	65.63	47.20	49.07	45.20	104271.84	0.00
BAK1301 z06	Mnt3run2	0.01	0.11	0.03	0.05	0.83	2.36	10.70	30.00	47.56	45.82	27.69	19.92	14.72	13.24	101067.96	-0.02
BAK1301 z19	Mnt3run2	0.03	0.62	0.03	0.26	3.31	13.02	43.07	58.06	60.57	54.18	41.06	37.84	43.35	38.40	105825.24	0.08
BAK1301 z39	Mnt3run2	0.03	0.54	0.12	0.27	2.41	6.29	14.47	35.83	56.10	56.91	50.56	37.20	44.97	36.40	106796.12	-0.03
BAK1301 z15	Mnt3run2	0.03	0.27	0.02	0.09	1.23	4.29	13.27	34.86	43.70	48.91	40.00	30.64	29.38	29.44	94174.76	-0.02
BAK1301 z29	Mnt3run2	0.01	0.13	0.02	0.05	0.80	2.32	6.88	23.44	39.23	40.73	34.38	22.80	24.16	21.48	112135.92	0.03
BAK1301 z26	Mnt3run2	0.02	0.48	0.05	0.24	5.88	15.18	47.19	78.06	75.61	64.73	47.19	36.80	42.05	43.84	103592.23	0.05
BAK1301 z32	Mnt3run2	0.01	0.21	0.07	0.13	0.68	4.18	11.16	36.39	50.41	50.36	45.13	29.84	27.33	24.52	88640.78	0.05
BAK1301 z25	Mnt3run2	0.00	0.45	0.07	0.17	4.05	11.25	38.14	58.61	60.98	52.00	45.75	37.68	42.67	42.80	104660.19	0.03
BAK1301 z22	Mnt3run2	0.02	0.82	0.03	0.19	2.36	6.20	21.21	30.83	30.89	30.55	26.25	26.80	26.58	24.76	99126.21	0.02
BAK1301 z23	Mnt3run2	0.02	0.09	0.07	0.04	1.03	4.21	14.72	51.67	82.93	95.82	70.63	44.00	44.72	38.40	113300.97	0.05
BAK1301 z23	Mnt3run2	0.01	0.15	0.11	0.11	0.70	2.71	10.70	26.39	40.12	39.27	27.13	18.96	18.01	16.08	105145.63	0.03
BAK1301 z36	Mnt3run2	0.03	0.40	0.06	0.17	0.95	2.89	9.10	19.50	32.36	32.00	26.94	17.76	18.32	24.00	102912.62	0.08
BAK1301 z05	Mnt3run2	0.02	0.13	0.02	0.07	1.53	3.98	19.30	46.67	73.58	59.64	46.81	39.20	36.02	33.20	103398.06	-0.08
BAK1301 z11	Mnt3run2	0.01	0.17	0.02	0.08	1.03	2.09	9.40	21.08	30.57	33.27	30.19	22.40	24.16	20.76	111553.40	0.12
BAK1301 z31	Mnt3run2	0.03	0.13	0.05	0.08	1.12	2.91	15.58	36.03	54.07	47.27	40.00	31.64	32.73	29.60	110485.44	0.02
BAK1301 z22	Mnt3run2	0.01	0.31	0.02	0.16	2.41	6.70	22.71	42.22	45.93	41.09	33.50	25.64	32.11	30.40	105825.24	-0.01
BAK1301 z09	Mnt3run2	0.01	0.11	0.04	0.06	0.47	1.34	6.28	19.25	35.00	39.82	33.69	26.08	19.07	13.04	109902.91	0.05
BAK1301 z05	Mnt3run2	0.01	0.12	0.00	0.09	0.83	1.98	5.83	19.61	25.45	21.64	15.75	16.28	13.17	14.32	110582.52	0.04
BAK1301 z12	Mnt3run2	0.03	0.12	0.06	0.08	1.11	2.82	11.76	26.19	29.43	25.82	18.13	17.64	17.95	18.52	111553.40	0.03
BAK1301 z04	Mnt3run2	0.02	0.09	0.04	0.16	0.24	1.84	5.98	18.33	25.53	18.91	13.56	11.76	11.49	12.32	95728.16	0.01
BAK1301 z06	Mnt3run2	0.02	0.12	0.02	0.10	0.89	2.00	10.65	37.78	73.98	79.64	53.75	38.80	29.38	28.00	112621.36	-0.01
BAK1301 z08	Mnt3run2	0.02	0.27	0.02	0.15	2.26	5.38	22.06	43.06	59.76	60.73	53.31	48.80	47.27	47.44	102912.62	0.00
BAK1301 z05	Mnt3run2	0.03	0.09	0.00	0.09	0.64	1.46	6.83	17.00	27.07	22.73	19.38	16.36	16.34	13.60	105339.81	-0.02
BAK1301 z04	Mnt3run2	0.04	0.12	0.02	0.06	1.22	3.75	15.88	41.94	67.48	60.00	46.06	34.16	34.53	29.20	96699.03	-0.02
BAK1301 z04	Mnt3run2	0.03	0.06	0.02	0.14	1.14	2.86	9.85	31.11	47.03	38.36	29.38	22.00	22.17	22.12	92621.36	0.05
BAK1301 z34	Mnt3run2	0.02	0.09	0.06	0.08	0.33	0.88	3.37	9.81	18.09	26.18	20.63	15.72	15.28	14.48	112815.53	0.14
BAK1301 z33	Mnt3run2	0.04	0.08	0.21	0.11	0.35	1.46	6.08	19.58	35.37	37.82	33.44	24.08	23.42	20.60	119611.65	0.02
BAK1301 z28	Mnt3run2	0.02	0.03	0.00	0.10	0.18	0.79	2.21	6.67	16.10	18.73	14.38	10.24	12.05	10.76	99514.56	-0.11
BAK1301 z33	Mnt3run2	0.00	0.03	0.04	0.08	0.38	1.63	4.52	16.97	32.28	29.82	23.88	18.04	16.58	17.84	108737.86	-0.10
BAK1301 z20	Mnt3run2	0.01	0.05	0.03	0.09	0.44	1.11	5.33	14.17	24.51	30.91	27.50	20.24	18.14	17.44	108737.86	0.05
BAK1301 z20	Mnt3run2	0.02	0.08	0.05	0.03	0.29	1.14	3.72	9.69	17.11	26.00	19.56	16.00	14.10	13.88	105825.24	0.08
BAK1301 z16	Mnt3run2	0.01	0.07	0.04	0.08	0.80	1.48	9.20	24.81	54.47	69.09	58.88	48.24	36.09	37.60	100873.79	-0.08
BAK1301 z30	Mnt3run2	0.01	0.15	0.06	0.09	0.76	1.48	6.13	18.06	33.86	42.55	41.38	31.20	28.88	28.48	110679.61	0.30
BAK1301 z07	Mnt3run2	0.03	0.06	0.03	0.10	0.39	0.63	1.61	5.61	16.50	32.36	41.88	44.40	43.35	38.00	96699.03	-0.03
BAK1301 z13	Mnt3run2	0.02	0.05	0.03	0.06	0.35	1.18	4.17	14.78	24.51	27.27	24.13	19.92	15.09	18.00	107961.17	-0.28
BAK1301 z34	Mnt3run2	0.00	0.04	0.03	0.11	-0.01	0.46	0.91	3.81	9.80	18.55	24.63	22.72	25.28	20.40	107184.47	-0.12
BAK1301 z38	~~Mnt3run2~~	0.01	0.04	0.09	0.11	0.32	1.38	3.82	13.86	31.30	43.64	35.06	33.20	35.47	29.48	113592.23	0.13
BAK1301 z28	~~Mnt3run2~~	0.02	0.02	0.00	0.04	0.68	0.14	0.55	2.44	7.48	24.18	34.94	36.00	35.84	31.68	116407.77	-0.18
BAK1301 z07	~~Mnt3run2~~	0.01	0.01	0.01	0.12	0.36	0.38	0.86	3.19	9.43	16.51	23.06	19.36	18.51	18.20	98932.04	-0.15
BAK1302 z27	Mnt3run1	0.02	0.02	0.07	0.39	0.46	0.52	2.11	4.89	10.69	24.18	63.75	110.80	254.66	392.00	103883.50	-5.83
BAK1302 z27	Mnt3run1	0.01	0.02	0.06	0.11	1.55	0.39	3.32	6.97	18.90	46.18	101.25	203.20	427.95	792.00	102524.27	-2.25
BAK1302 z27	Mnt3run1	0.02	0.03	0.07	0.06	0.05	0.68	2.26	9.19	21.95	59.82	131.88	238.80	490.68	904.00	93203.88	5.33
BAK1302 z27	Mnt3run1	0.05	0.03	0.07	0.39	0.06	0.39	1.36	4.44	14.07	30.18	84.38	186.40	478.26	812.00	130097.09	6.67
BAK1302 z26	Mnt3run1	0.02	0.03	0.01	0.12	1.08	0.61	0.80	2.83	8.54	20.36	65.63	116.40	229.81	364.00	113592.23	0.86
BAK1302 z26	Mnt3run1	0.05	0.02	0.10	0.24	1.76	0.70	0.45	3.78	6.02	19.27	51.25	89.20	157.76	253.60	110679.61	3.91
BAK1302 z26	Mnt3run1	0.02	0.01	0.18	0.23	0.68	0.32	0.75	1.25	3.25	8.18	16.88	42.80	69.57	118.80	93203.88	-9.00
BAK1302 z18	Mnt3run1	0.01	0.02	0.02	0.06	1.15	0.13	0.75	5.53	9.80	42.55	135.63	360.00	807.45	1376.00	103009.71	0.18
BAK1302 z18	Mnt3run1	0.06	0.05	0.00	0.55	-0.06	0.93	1.06	3.14	8.46	27.82	80.63	188.80	428.57	716.00	102912.62	-0.36
BAK1302 z18	Mnt3run1	0.04	0.01	0.01	0.13	1.01	0.11	0.35	3.00	12.85	38.00	144.38	338.40	838.51	1240.00	117475.73	0.67

	Chondrite	0.24	0.613	0.093	0.457	0.148	0.056	0.199	0.036	0.246	0.055	0.16	0.025	0.161	0.025	0.103	
Sample, zircon #	Zircon Mount	La	Ce	Pr	Nd	Sm	Eu	Gd	Tb	Dy	Ho	Er	Tm	Yb	Lu	Hf	Th/U
MIC1301 z12	Mnt3run1	0.01	0.14	0.02	0.14	0.07	0.18	1.91	6.81	18.46	60.18	227.50	528.00	1627.33	3448.00	97475.73	0.04
MIC1301 z15	Mnt3run1	0.03	0.29	0.20	0.20	0.81	1.71	7.29	16.94	48.37	130.91	336.25	628.00	1242.24	2392.00	86407.77	0.05
MIC1301 z03	Mnt3run1	0.02	0.06	0.12	0.11	0.79	0.36	2.26	5.17	17.89	67.27	181.88	460.00	1012.42	2240.00	100970.87	0.08
MIC1301 z01	Mnt1run3	0.02	0.02	0.06	0.07	0.38	0.34	0.73	2.44	11.34	36.00	156.25	442.80	1385.09	3672.00	85728.16	0.05
MIC1301 z33	Mnt3run1	0.01	0.04	0.08	0.07	1.07	0.98	1.76	4.86	19.47	50.18	130.00	263.20	639.75	1124.00	93203.88	0.11
MIC1301 z08	Mnt1run3	0.01	0.03	0.05	0.14	0.43	0.41	1.91	6.42	27.52	96.18	301.88	664.00	1472.05	3128.00	117766.99	0.08
MIC1301 z05	Mnt3run2	0.01	0.06	0.07	0.03	0.30	0.37	1.31	3.17	9.51	25.45	69.38	146.80	362.11	780.00	99417.48	0.23
MIC1301 z04	Mnt3run1	0.00	0.14	0.02	0.18	1.49	0.86	2.36	6.03	16.99	52.55	185.63	498.00	1354.04	2808.00	87378.64	0.12
MIC1301 z05	Mnt3run2	0.06	0.51	0.24	0.26	0.84	1.13	2.16	8.17	19.67	60.36	180.63	476.00	1242.24	3404.00	95145.63	0.41
MIC1301 z33	Mnt3run1	0.03	0.65	0.11	0.39	1.69	3.75	12.26	35.83	82.11	205.45	431.25	712.00	1397.52	2352.00	82330.10	0.17
MIC1301 z04	Mnt3run1	0.00	0.04	0.06	0.40	0.51	0.38	1.41	2.06	7.93	27.27	66.25	134.00	262.11	560.00	110097.09	0.13
MIC1301 z01	Mnt3run2	0.01	0.07	0.06	0.06	0.30	0.25	0.78	5.67	18.37	60.36	188.75	432.40	1000.00	2152.00	112233.01	-0.03
MIC1301 z19	Mnt3run1	0.04	0.13	0.11	0.57	0.88	0.75	2.51	6.47	19.35	73.45	253.75	660.00	1770.19	4440.00	96699.03	0.09
MIC1301 z05	Mnt3run2	0.04	0.44	0.12	0.23	0.72	1.05	2.06	5.58	13.29	33.82	86.25	198.40	524.22	1160.00	98252.43	0.03
MIC1301 z31	Mnt3run1	0.01	0.04	0.18	0.25	1.42	0.93	1.86	11.31	22.76	72.91	153.13	290.40	596.27	1144.00	94368.93	-0.03
MIC1301 z05	Mnt3run2	0.02	0.09	0.02	0.06	0.29	0.38	1.09	2.97	13.62	31.64	88.13	209.20	560.25	1228.00	92815.53	0.21
MIC1301 z36	Mnt3run1	0.00	0.03	0.01	0.11	0.88	0.82	0.51	5.81	17.80	57.82	151.25	433.60	1192.55	2204.00	99029.13	0.08
MIC1301 z31	Mnt3run1	0.02	0.08	0.12	0.19	1.89	1.14	1.71	8.00	24.27	83.45	258.13	620.00	1633.54	3280.00	96116.50	0.03
MIC1301 z01	Mnt3run2	0.02	0.08	0.11	0.06	0.30	0.23	1.63	9.56	32.68	120.18	395.00	880.00	2329.19	6200.00	100970.87	-0.02
MIC1301 z03	Mnt1run3	0.06	0.14	0.17	0.10	0.51	0.77	1.41	4.11	18.58	65.09	218.75	572.00	1552.80	3356.00	97669.90	0.04
MIC1301 z18	Mnt3run1	0.10	0.45	0.42	0.81	0.49	1.54	5.03	17.22	54.07	131.45	318.75	624.00	1416.15	2856.00	96796.12	0.08
MIC1301 z37	Mnt3run1	0.02	0.23	0.13	0.07	1.42	4.25	16.98	48.61	118.70	252.73	543.75	880.00	1652.17	2696.00	96116.50	0.21
MIC1301 z09	Mnt1run3	0.04	0.10	0.15	0.12	0.53	0.61	2.17	10.22	28.78	93.27	247.50	512.00	993.79	1984.00	106893.20	0.02
MIC1301 z32	Mnt3run1	0.01	0.06	0.08	0.35	0.88	1.21	5.08	21.75	48.37	123.64	304.38	544.00	1093.17	1776.00	110679.61	0.07
MIC1301 z37	Mnt3run1	0.00	0.06	0.07	0.13	0.55	1.52	5.83	18.33	52.44	150.91	376.88	684.00	1378.88	2480.00	99029.13	-0.12
MIC1301 z26	Mnt3run1	0.01	0.05	0.12	0.07	1.76	1.66	7.24	24.44	69.51	152.73	330.63	580.00	1142.86	1880.00	122330.10	-0.03
MIC1301 z36	Mnt3run1	0.02	0.08	0.06	0.57	0.42	0.50	1.81	3.75	16.50	62.18	191.88	384.00	1055.90	2476.00	91262.14	0.03
MIC1301 z32	Mnt3run1	0.02	0.05	0.00	0.46	1.82	6.79	36.18	160.56	495.93	1345.45	3168.75	5680.00	########	######	123300.97	0.09
MIC1301 z09	Mnt1run3	0.02	0.06	0.07	0.07	0.22	0.71	1.91	9.36	31.50	96.00	231.88	450.80	981.37	1688.00	106116.50	0.02
MIC1301 z17	Mnt3run1	0.01	0.14	0.04	0.42	1.89	1.07	6.08	19.17	62.60	138.18	343.75	604.00	1291.93	2056.00	78737.86	0.00
MIC1301 z01	Mnt3run2	0.01	0.02	0.02	0.06	0.07	0.14	0.96	3.69	13.54	48.00	158.13	378.40	1031.06	2440.00	100000.00	0.03
MIC1301 z02	Mnt1run3	0.02	0.02	0.04	0.01	0.19	0.24	0.69	2.28	8.98	28.36	91.88	259.60	644.10	1420.00	102524.27	0.02
MIC1301 z35	Mnt3run1	0.03	0.10	0.08	0.30	1.22	1.41	4.77	16.25	50.00	138.18	378.75	772.00	1993.79	3560.00	107766.99	-0.07
MIC1301 z28	Mnt3run1	0.01	0.73	0.14	0.24	2.23	3.93	10.55	40.00	113.82	249.09	575.00	1144.00	2099.38	4120.00	75728.16	0.32
MIC1301 z01	Mnt3run2	0.01	0.02	0.06	0.07	0.29	0.33	0.65	2.08	5.93	18.55	59.81	150.40	337.27	734.00	106116.50	0.00
MIC1301 z06	Mnt3run1	0.01	0.08	0.08	0.33	0.57	0.59	2.51	6.97	24.07	89.64	274.38	692.40	1937.89	3696.00	87572.82	-0.18
MIC1301 z03	Mnt1run3	0.34	0.42	0.44	0.43	0.32	0.33	0.88	3.64	12.11	33.27	87.50	185.60	446.58	848.00	94563.11	0.01
MIC1301 z01	Mnt3run2	0.01	0.01	0.02	0.08	0.15	0.14	0.52	2.17	9.43	36.18	118.75	257.20	638.51	1400.00	107766.99	0.08
MIC1301 z002	Mnt1run3	0.05	0.02	0.08	0.10	0.12	0.41	0.53	1.33	3.50	10.80	32.69	83.60	203.73	396.00	95922.33	0.17
MIC1301 z19	Mnt3run1	0.04	0.04	0.18	0.09	0.88	0.63	0.95	4.89	12.15	35.64	84.38	151.60	322.98	632.00	88737.86	0.03
MIC1301 z30	Mnt3run1	0.01	0.50	0.12	0.32	3.18	11.79	34.17	99.72	189.02	401.82	603.75	840.00	1111.80	1680.00	73106.80	-0.01
MIC1301 z15	Mnt3run1	0.04	0.06	0.04	0.19	0.21	0.21	1.61	5.64	8.90	32.36	73.13	178.80	397.52	828.00	96699.03	0.19
MIC1301 z03	Mnt1run3	0.03	0.03	0.07	0.05	0.28	0.32	1.51	5.44	20.28	56.91	137.50	269.60	530.43	864.00	111844.66	0.05
MIC1301 z36	Mnt3run1	0.02	0.02	0.16	0.16	0.95	1.46	2.56	6.83	26.02	70.55	166.88	299.60	664.60	1160.00	107766.99	0.02
MIC1301 z14	Mnt3run1	0.00	0.06	0.10	0.13	0.24	0.73	0.90	9.44	29.27	126.73	450.00	1272.00	2683.23	5960.00	101941.75	0.32
MIC1301 z01	Mnt1run3	0.01	0.01	0.07	0.09	0.24	0.15	1.11	3.00	9.63	33.09	111.88	328.00	944.10	2144.00	96699.03	-0.15
MIC1301 z27	Mnt3run1	0.01	0.09	0.05	0.09	1.62	0.43	5.83	28.61	102.03	301.82	700.00	1524.00	3049.69	5160.00	84854.37	0.00
MIC1301 z36	Mnt3run1	0.01	0.02	0.01	0.11	0.41	0.57	3.27	10.00	30.53	81.09	190.00	366.80	683.23	1208.00	109708.74	-0.14
MIC1301 z18	Mnt3run1	0.00	0.03	0.15	0.05	0.74	0.48	3.02	8.11	23.78	62.55	166.25	274.00	602.48	1004.00	109708.74	0.47
MIC1301 z18	Mnt3run1	0.02	0.09	0.10	-0.01	0.88	0.57	1.71	7.92	20.33	59.09	135.00	239.20	577.64	988.00	120388.35	-0.40
MIC1301 z35	Mnt3run1	0.01	0.08	0.05	0.02	0.50	0.98	4.07	10.83	36.18	123.64	342.50	732.00	1776.40	4080.00	109708.74	0.13
MIC1301 z28	Mnt3run1	0.01	0.25	0.12	0.39	1.22	1.27	8.14	22.22	51.22	145.45	295.00	592.00	1173.91	2056.00	68834.95	-0.16
MIC1301 z26	Mnt3run1	0.02	0.01	0.16	0.05	0.41	0.46	0.70	2.14	6.34	17.09	69.38	211.20	542.86	1404.00	90000.00	0.03
MIC1301 z04	Mnt3run1	0.01	0.05	0.14	0.12	0.29	0.38	0.25	4.14	10.28	22.18	66.25	116.40	250.31	492.00	111650.49	0.60
MIC1301 z05	~~Mnt3run2~~	0.01	0.06	0.05	0.12	0.09	0.52	1.04	4.03	12.07	36.00	89.38	199.20	467.70	1104.00	97572.82	-0.04
MIC1301 z12	Mnt3run1	0.00	0.00	0.09	0.06	0.45	0.16	0.30	3.06	6.83	21.45	64.38	138.40	343.48	668.00	103883.50	-0.29
MIC1301 z37	Mnt3run1	0.02	0.04	0.02	0.07	0.08	0.29	0.50	2.61	3.70	18.00	54.38	125.60	314.91	628.00	78640.78	-0.40

	Chondrite	0.24	0.613	0.093	0.457	0.148	0.056	0.199	0.036	0.246	0.055	0.16	0.025	0.161	0.025	0.103	
Sample, zircon #	Zircon Mount	La	Ce	Pr	Nd	Sm	Eu	Gd	Tb	Dy	Ho	Er	Tm	Yb	Lu	Hf	Th/U
MIC1301 z03	Mnt3run1	0.01	0.06	0.04	0.11	0.74	0.27	1.36	4.00	16.67	40.55	133.13	264.80	540.37	1212.00	98058.25	-0.09
MIC1301 z11	Mnt3run1	0.03	0.03	0.24	0.10	0.74	0.46	0.70	0.81	4.92	16.55	50.00	114.80	277.02	556.00	111650.49	-3.85
MIC1301 z17	Mnt3run1	0.02	0.01	0.12	0.24	0.47	0.77	1.26	3.69	7.64	24.91	60.63	124.40	313.66	552.00	108737.86	0.32
MIC1301 z10	Mnt3run1	0.00	0.02	0.13	-0.01	0.61	0.16	0.85	3.67	11.50	30.91	88.13	226.80	540.99	1188.00	100000.00	-0.76
MIC1301 z09	Mnt3run1	0.04	0.05	0.05	0.22	0.27	0.80	2.61	15.56	30.08	80.91	201.88	440.00	1354.04	2172.00	200000.00	-0.39
MIC1301 z09	Mnt3run1	0.04	0.00	0.04	0.30	0.26	0.20	0.11	1.39	13.21	71.27	316.25	1012.00	3645.96	9360.00	104854.37	0.28
MIC1301 z02	Mnt1run3	0.02	0.02	0.03	0.09	0.11	0.06	0.40	1.33	3.62	13.27	40.88	93.60	263.98	584.00	98058.25	0.26
MIC1301 z11	Mnt3run1	0.01	0.03	0.04	0.31	0.88	0.30	2.41	7.53	28.05	86.18	253.75	516.00	1130.43	2052.00	118446.60	-1.54
MIC1301 z30	Mnt3run1	0.00	0.02	0.06	0.06	0.81	0.23	2.01	5.64	15.69	59.64	206.25	500.00	1173.91	2200.00	153398.06	1.67
MIC1301 z03	Mnt3run1	0.01	0.00	0.12	0.20	0.26	0.08	0.55	1.69	7.20	18.00	45.38	105.20	231.68	484.00	109708.74	-1.32
MIC1301 z35	Mnt3run1	0.02	0.05	0.05	0.14	0.88	0.73	1.11	5.33	17.68	57.82	158.13	316.00	701.86	1248.00	104854.37	0.40
MIC1301 z06	Mnt3run1	0.01	0.06	0.00	0.13	-0.05	0.79	0.37	1.17	3.41	13.13	38.00	84.00	202.48	420.00	106796.12	5.83
MIC1301 z13	Mnt3run1	0.01	0.00	-0.02	0.13	0.74	0.57	1.61	13.22	59.76	194.55	596.25	1176.00	2720.50	4880.00	104174.76	-3.57
MIC1301 z17	Mnt3run1	0.01	0.02	0.18	0.33	0.46	0.70	2.06	2.28	11.22	33.09	89.38	186.80	447.20	864.00	96116.50	0.43
MIC1301 z37	Mnt3run1	0.01	0.07	0.07	0.23	0.43	0.36	0.85	1.47	4.15	9.27	32.38	78.40	185.09	380.00	98155.34	1.67
BAK-1401	11	0.02	0.29	0.22	0.22	1.48	3.14	9.96	19.54	24.18	19.83	18.27	18.80	20.52	18.34	103900.91	
BAK-1401	11	0.02	0.13	0.20	0.23	0.44	0.95	2.69	6.69	11.27	15.87	23.62	26.92	32.08	26.54	110074.46	
BAK-1401	10	0.00	0.21	0.20	0.19	1.76	4.51	16.51	32.03	32.75	19.63	13.86	10.22	11.55	11.15	108699.91	
BAK-1401	9	0.00	0.28	0.18	0.23	1.87	5.26	16.22	23.41	17.06	8.79	6.83	5.49	6.65	6.40	107107.47	
BAK-1401	7	0.05	0.27	0.26	0.27	0.67	1.65	4.30	10.51	20.61	24.10	26.68	25.33	28.11	20.79	111284.39	
BAK-1401	6	0.02	0.22	0.20	0.24	0.72	1.43	2.56	4.05	6.15	9.70	14.54	18.13	22.36	16.65	99848.11	
BAK-1401	5	0.00	0.04	0.15	0.13	0.25	0.46	1.39	3.50	8.79	14.32	18.17	17.52	19.32	14.40	105741.66	
BAK-1401	3	0.00	0.02	0.16	0.09	0.19	0.37	1.63	5.46	12.66	17.35	19.03	17.94	20.63	15.34	105939.42	
BAK-1401	1	0.07	0.37	0.29	0.45	1.41	2.69	7.82	17.12	26.58	27.91	28.74	25.17	28.44	28.86	101398.27	
BAK-1401	12	0.01	0.15	0.14	0.17	0.41	1.02	4.17	12.50	24.83	28.70	27.30	24.16	24.97	18.67	107172.38	
BAK-1401	13	0.05	0.47	0.21	0.31	1.06	1.38	3.15	6.63	13.85	16.97	16.58	13.70	12.37	9.05	110565.25	
BAK-1401	14	0.00	0.10	0.12	0.10	1.93	5.99	24.01	52.82	63.38	39.70	25.49	17.51	18.87	12.93	99630.24	
BAK-1401	15	0.00	0.05	0.14	0.11	0.23	0.57	2.35	7.97	18.67	24.27	23.75	19.03	17.68	13.65	107006.42	
BAK-1401	16	0.00	0.03	0.13	0.10	0.16	0.25	0.62	1.69	4.09	5.97	6.60	5.96	5.72	5.00	119935.27	
BAK-1401	17	0.02	0.19	0.13	0.11	0.62	1.28	4.78	14.99	28.47	34.16	37.72	41.89	60.79	76.81	106996.03	
BAK-1401	19	0.07	0.66	0.55	0.99	1.48	1.36	1.80	3.41	6.83	9.97	11.24	9.92	9.94	7.46	114560.91	
BAK-1401	20	0.00	0.06	0.13	0.13	0.27	0.65	2.86	8.81	22.71	30.23	30.69	24.80	24.38	18.30	107172.66	
BAK-1401	23	0.00	0.12	0.14	0.13	1.69	5.66	22.10	49.28	59.29	40.34	25.89	18.34	18.60	14.80	98000.48	
BAK-1401	24	0.02	0.02	0.11	0.08	0.33	0.48	1.78	5.02	9.86	11.66	10.96	9.30	9.96	7.41	107978.24	
BAK-1401	26	0.00	0.09	0.12	0.13	1.12	2.53	10.94	19.55	21.28	14.33	10.50	9.50	11.33	10.20	104113.77	
BAK-1401	27	0.00	0.12	0.10	0.15	1.07	3.19	10.96	27.14	37.67	26.34	14.32	8.84	7.49	4.83	96774.99	
BAK-1401	28	0.03	0.41	0.18	0.24	4.36	12.33	40.37	70.67	68.42	37.40	19.44	11.82	9.77	6.06	99506.06	
BAK-1401	29	0.17	0.50	0.37	0.47	1.00	1.55	3.82	5.67	9.36	11.60	12.55	11.44	11.51	8.50	113310.84	
BAK-1401	30	0.09	2.29	0.42	1.19	4.29	5.95	10.71	18.56	29.17	25.76	17.58	11.51	10.30	8.19	105781.51	
BAK-1401	30	0.00	0.33	0.17	0.25	0.97	1.63	5.46	14.71	21.36	16.75	10.37	6.56	6.28	4.57	108226.24	
BAK-1401	32	0.02	0.19	0.15	0.20	1.71	5.56	18.21	35.84	34.46	19.25	10.93	7.91	8.41	6.28	107618.67	
BAK-1401	33	0.03	0.20	0.14	0.17	1.22	3.98	13.60	31.21	37.99	25.88	18.25	13.99	13.95	10.45	107932.29	
BAK-1401	34	0.02	0.25	0.10	0.11	0.88	2.69	9.50	26.69	41.62	38.64	33.76	30.52	34.39	27.55	102892.12	
BAK-1401	36	0.02	0.55	0.16	0.37	7.33	19.01	54.98	68.47	48.67	27.26	20.32	19.08	23.04	19.14	104605.95	
BAK-1401	37	0.02	0.07	0.14	0.16	0.17	0.28	0.91	3.29	9.61	17.29	22.70	20.93	22.25	16.27	111800.58	
BAK-1401	38	0.00	1.60	0.22	0.90	11.26	24.14	67.54	116.22	164.97	186.47	211.05	231.10	299.18	273.91	93648.76	
BAK-1401	39	0.01	0.22	0.12	0.16	1.10	2.35	6.91	15.19	18.30	11.70	7.27	5.03	5.01	3.70	107351.00	
BAK-1401	40	0.03	0.07	0.12	0.14	0.57	0.90	3.08	11.22	21.19	25.37	24.78	20.99	21.19	14.49	110070.01	
BAK-1401	41	0.02	0.16	0.11	0.10	1.41	5.40	18.51	44.04	52.55	36.83	25.25	19.79	21.56	16.02	101749.78	
BAK-1401	43	0.00	0.35	0.19	0.40	2.75	4.42	7.93	15.52	22.81	18.39	11.31	7.61	6.29	3.54	94716.30	
BAK-1401	43	0.00	0.54	0.17	0.27	1.81	3.15	5.81	10.00	19.33	27.03	27.00	23.08	34.22	37.92	98324.64	
BAK-1401	44	0.00	0.05	0.10	0.09	0.69	1.72	7.22	21.28	35.27	25.80	15.15	10.06	9.07	6.37	98385.88	
BAK-1401	45	0.06	0.39	0.11	0.13	0.74	1.43	3.47	8.05	15.80	20.41	22.54	21.57	22.52	14.90	110097.94	
BAK-1401	45	0.01	0.27	0.13	0.30	1.59	3.40	10.82	25.40	27.27	14.91	8.49	6.16	6.41	4.33	101924.02	
BAK-1401	46	0.00	0.04		0.06	0.35	1.27	5.18	15.46	22.72	15.76	9.54	6.07	6.14	4.27	100504.02	
BAK-1401	11	0.00	2.14	0.25	0.60	6.63	13.28	37.47	67.21	96.25	110.36	128.37	131.63	158.96	150.90	84644.67	
BAK-1401	10	0.04	0.39	0.24	0.40	1.38	3.33	12.97	24.93	27.93	16.85	10.63	7.97	7.82	6.12	102951.83	

	Chondrite	0.24	0.613	0.093	0.457	0.148	0.056	0.199	0.036	0.246	0.055	0.16	0.025	0.161	0.025	0.103
Sample, zircon #	Zircon Mount	La	Ce	Pr	Nd	Sm	Eu	Gd	Tb	Dy	Ho	Er	Tm	Yb	Lu	Hf
BAK-1401	10	0.00	0.22	0.13	0.15	1.23	3.28	11.52	21.48	24.41	16.06	11.98	9.21	9.64	8.19	102514.52
BAK-1401	9	0.00	0.43	0.18	0.25	2.59	6.60	18.90	25.71	17.89	9.38	7.22	5.96	7.20	6.04	104271.02
BAK-1401	7	0.00	0.02	0.15	0.09	0.00	0.38	1.59	5.67	12.63	15.38	16.20	14.20	15.80	11.68	108177.65
BAK-1401	6	0.01	0.18	0.16	0.25	0.82	1.08	2.59	4.54	8.10	12.36	17.00	20.05	23.85	17.18	98847.37
BAK-1401	5	0.03	0.08	0.27	0.29	0.81	1.12	2.43	5.81	11.36	11.49	9.82	7.91	7.55	5.52	99562.70
BAK-1401	3	0.00	0.02	0.12	0.15	0.14	0.16	0.88	3.41	8.43	11.06	11.20	10.07	10.25	8.20	106043.37
BAK-1401	1	0.00	1.15	0.24	0.49	4.36	8.82	26.61	49.09	67.07	79.75	88.39	91.28	118.06	104.55	82862.28
BAK-1401	12	0.00	0.04	0.16	0.13	0.32	1.09	4.23	12.32	17.98	12.90	9.27	7.14	8.05	6.44	102902.00
BAK-1401	14	0.00	0.12	0.15	0.00	0.82	3.40	13.43	28.82	35.45	22.94	13.61	9.27	8.79	6.36	101059.40
BAK-1401	15	0.00	0.16	0.15	0.21	1.03	2.19	6.64	13.49	19.86	19.15	14.87	10.07	10.07	7.64	101030.54
BAK-1401	16	0.00	0.10	0.12	0.10	0.60	1.72	6.60	16.84	25.79	21.99	15.19	9.48	9.22	7.09	105231.71
BAK-1401	16	0.00	0.01	0.12	0.08	0.17	0.25	0.80	2.84	6.38	8.21	8.24	7.50	7.14	5.72	110485.19
BAK-1401	17	0.00	0.47	0.09	0.22	1.87	4.71	12.74	19.94	16.98	10.48	7.97	7.16	8.05	7.71	102825.59
BAK-1401	20	0.00	0.27	0.13	0.16	1.43	3.83	11.21	17.91	18.15	12.87	9.43	7.30	7.22	5.98	105609.48
BAK-1401	24	0.00	1.19	0.19	0.30	3.70	6.95	19.23	31.35	40.47	44.79	51.50	58.00	73.67	70.23	85335.66
BAK-1401	26	0.01	0.11	0.11	0.12	1.03	2.37	8.28	13.39	13.20	8.58	6.72	5.73	6.21	4.95	107026.02
BAK-1401	27	0.04	0.18	0.20	0.25	1.70	4.34	16.29	37.25	49.19	33.97	19.24	11.02	9.04	6.45	97270.99
BAK-1401	29	0.00	0.02	0.11	0.13	0.16	0.18	0.52	1.09	3.48	5.01	5.32	5.16	5.65	4.01	111713.42
BAK-1401	30	0.00	1.29	0.16	0.28	2.88	4.96	14.99	30.18	49.10	63.99	79.48	88.50	119.33	119.13	97297.02
BAK-1401	30	0.07	1.32	0.20	0.37	2.90	5.35	16.40	32.17	52.89	69.55	86.78	97.53	129.49	130.78	96466.94
BAK-1401	34	0.00	0.14	0.08	0.09	1.03	2.97	10.92	25.59	30.78	21.18	14.98	11.79	12.74	10.84	101766.52
BAK-1401	37	0.00	0.02	0.11	0.07	0.00	0.59	1.78	4.79	9.34	10.49	9.66	7.34	6.57	5.03	105814.95
BAK-1401	38	0.00	1.72	0.20	0.53	7.05	16.45	47.59	77.35	105.81	119.08	136.89	145.60	183.62	169.30	93466.29
BAK-1401	38	0.00	1.79	0.24	0.41	8.56	17.03	44.46	73.84	108.19	118.86	137.17	149.33	188.37	173.45	93735.93
BAK-1401	39	0.00	0.40	0.11	0.17	2.24	6.16	18.04	24.24	16.83	8.97	6.68	6.20	7.32	5.98	103409.37
BAK-1401	40	0.00	0.01	0.11	0.11	0.13	0.22	1.29	5.27	11.41	12.66	11.00	8.87	8.41	7.16	104629.65
BAK-1401	43	0.00	0.95	0.08	0.00	2.34	4.44	14.66	26.94	41.36	51.79	60.59	66.63	86.81	77.76	76854.18
BAK-1401	43	0.00	0.70	0.08	0.26	2.06	3.82	11.76	17.90	26.80	29.36	31.86	34.68	40.42	37.52	83738.12
BAK-1401	46	0.05	0.09		0.14	0.72	1.47	6.05	18.76	36.79	35.36	25.20	17.48	16.83	11.29	100385.92

APPENDIX D: ID-TIMS U-PB DATES

MIC-1301																							
Fraction	206Pb /238U <Th>	2σ abs	207Pb/ 235U	2σ abs	207Pb/ 206Pb	2σ abs	Corr coeff	% disc	Mass U(pg)	Th/ U	Pb* (pg)	Pb c (pg)	Pb* /Pbc	206Pb/ 204Pb	206Pb /238U	2σ %	207Pb/ 235U	2σ %	207Pb/ 206Pb	2σ %	Corr coef
F1	411	10	559	120	1217	530	0.84	66.2	24	0.1	1.5	4.68	0	40	0.066	2.6	0.73	29	0.081	27	0.8
F2	422	13	457	190	636	1100	0.88	33.6	32	0.1	2.1	8.97	0	34	0.068	3.3	0.57	53	0.061	50	0.9
F4	414.3	4.4	443	60	595	350	0.86	30.4	75	0	4.6	6.41	1	68	0.066	1.1	0.547	17	0.06	16	0.1
BAK-1302																					
Fraction	206Pb /238U <Th>	2σ abs	207Pb/ 235U	2σ abs	207Pb/ 206Pb	2σ abs	Corr coeff	% disc	Mass U(pg)	Th/ U	Pb* (pg)	Pb c (pg)	Pb* /Pbc	206Pb/ 204Pb	206Pb /238U	2σ %	207Pb/ 235U	2σ %	207Pb/ 206Pb	2σ %	Corr coef
F1	466	21	446	140	345	850	0.52	-35	5	0	0.3	0.93	0	45	0.075	4.6	0.55	40	0.053	37	0.5
F3	292	28	286	220	231	2000	0.57	-27	2	0.1	0.1	0.59	0	31	0.046	9.9	0.32	90	0.051	85	0.6

APPENDIX E: LASS-ICMPS U-PB DATES

Sample/ Zircon #	206Pb/ 238U	2σ	207Pb/ 235U	2σ	207Pb/ 206Pb	2σ	Corr coeff	Approx U ppm	2σ	Approx Th ppm	2σ	Approx Pb ppm	2σ	Th/U	206Pb/ 204Pb	2σ	207Pb/ 235U	2σ	206Pb/ 238U	2σ	208Pb/ 232U	2σ	207Pb/20 6Pb	2σ %	Corr coef
BAK1301 z03	470	23	491	25	513	90	-0.23295	3.42	0.16	0.16	0.54	0.0216	0.0052	0.047	115.36	73.45	0.623	0.041	0.0758	0.0039	0.0006	0.0023	0.0581	0.0024	0.8101
BAK1301 z03	455	16	471	18	510	95	0.20338	3.91	0.13	0.53	0.39	0.0978	0.0071	0.136	86.88	29.90	0.595	0.029	0.0731	0.0026	0.0071	0.0038	0.0583	0.0025	0.7954
BAK1301 z03	485	10	481	11	489	61	0.24214	9.26	0.15	0.42	0.42	0.078	0.0062	0.045	153.43	43.41	0.608	0.018	0.0782	0.0017	0.0068	0.0095	0.0570	0.0015	0.5039
BAK1301 z04	463	9	453	11	416	57	0.15769	8.2	0.16	0.07	0.37	0.0106	0.0042	0.009	237.40	123.51	0.561	0.017	0.0744	0.0015	-0.0002	0.0008	0.0555	0.0014	0.4924
BAK1301 z05	600	170	510	110	470	290	0.41820	0.91	0.26	0.06	0.87	0.0093	0.0068	0.066	27.58	25.33	0.530	0.370	0.0900	0.0570	0.0004	0.0008	0.0588	0.0097	0.8987
BAK1301 z05	558	34	614	33	830	100	0.11025	2.66	0.17	0.21	0.41	0.099	0.01	0.079	35.03	9.27	0.839	0.060	0.0907	0.0058	0.0004	0.0035	0.0677	0.0033	0.8448
BAK1301 z06	457	20	459	20	549	80	0.16736	3.58	0.15	0.15	0.47	0.0089	0.0041	0.042	124.30	74.60	0.577	0.032	0.0731	0.0033	0.0005	0.0007	0.0591	0.0022	0.7208
BAK1301 z06	457	17	468	19	530	81	0.08698	4.21	0.14	0.23	0.49	0.0733	0.0053	0.055	108.04	60.05	0.587	0.030	0.0735	0.0029	-0.0001	0.0025	0.0580	0.0022	0.7487
BAK1301 z06	524	28	1037	42	2365	68	0.02214	2.77	0.15	0.27	0.46	0.549	0.03	0.097	33.55	7.03	1.790	0.120	0.0840	0.0046	0.0010	0.0160	0.1533	0.0059	0.7542
BAK1301 z07	446	31	481	32	670	110	0.08625	2.13	0.13	0.38	0.45	0.0484	0.0064	0.178	75.84	55.90	0.620	0.052	0.0718	0.0051	0.0006	0.0032	0.0628	0.0031	0.8177
BAK1301 z07	508	55	480	42	560	150	0.15360	1.87	0.16	0.02	0.47	0.0196	0.0056	0.011	102.54	102.56	0.689	0.098	0.0826	0.0095	0.0007	0.0025	0.0610	0.0043	0.9622
BAK1301 z08	459	10	456	13	459	65	0.10618	10.8	0.19	0.48	0.54	0.0834	0.0073	0.044	317.08	211.45	0.568	0.021	0.0738	0.0017	-0.0024	0.0050	0.0565	0.0017	0.4621
BAK1301 z08	580	190	532	81	780	170	-0.19408	1.11	0.15	-0.25	0.49	0.0217	0.0051	-0.225	24.06	10.89	0.710	0.200	0.0740	0.0190	0.0000	0.0012	0.0645	0.0059	0.9044
BAK1301 z10	477	27	595	32	1138	93	0.00552	3.26	0.16	0.26	0.46	0.161	0.015	0.080	76.70	33.26	0.811	0.057	0.0769	0.0046	0.0010	0.0130	0.0784	0.0035	0.8003
BAK1301 z10	456	7	449	7	400	40	0.28632	34.59	0.55	0.27	0.53	0.0642	0.0066	0.008	1278.95	875.36	0.557	0.010	0.0732	0.0012	-0.0017	0.0033	0.0547	0.0010	0.5380
BAK1301 z11	420	240	520	120	590	250	0.18544	0.8	0.16	-0.05	0.57	0.0053	0.0043	-0.063	15.62	5.52	0.620	0.470	0.0850	0.0550	0.0001	0.0006	0.0645	0.0084	0.8502
BAK1301 z13	427	13	449	19	500	100	0.02559	5.24	0.18	0.46	0.45	0.0365	0.0065	0.088	158.68	93.81	0.557	0.029	0.0685	0.0021	-0.0001	0.0012	0.0583	0.0028	0.5681
BAK1301 z14	463	12	469	13	518	72	0.10224	8.98	0.19	0.5	0.54	0.1073	0.009	0.056	137.66	41.08	0.589	0.021	0.0744	0.0020	0.0011	0.0059	0.0572	0.0019	0.6375
BAK1301 z14	455	9	445	11	414	52	0.08759	15.74	0.26	0.6	0.41	0.1248	0.0097	0.038	544.00	380.86	0.551	0.017	0.0731	0.0015	0.0054	0.0062	0.0549	0.0013	0.6908
BAK1301 z14	453	12	458	15	481	70	0.06549	6.54	0.15	0.05	0.37	0.0586	0.0068	0.008	208.09	132.47	0.573	0.024	0.0729	0.0020	-0.0046	0.0034	0.0568	0.0018	0.5706
BAK1301 z15	441	41	476	48	620	160	-0.18249	1.72	0.13	0.18	0.56	0.034	0.0086	0.105	42.54	21.30	0.653	0.097	0.0711	0.0068	0.0002	0.0016	0.0634	0.0048	0.5769
BAK1301 z15	414	41	410	45	420	200	0.01875	1.55	0.16	-0.24	0.5	0.0152	0.004	-0.155	56.00	36.27	0.590	0.110	0.0740	0.0110	-0.0001	0.0018	0.0558	0.0054	0.9943
BAK1301 z16	462	11	456	14	418	64	0.05698	9.74	0.21	-0.16	0.53	0.0199	0.005	-0.016	199.71	88.18	0.570	0.022	0.0743	0.0018	-0.0006	0.0009	0.0556	0.0016	0.6400
BAK1301 z16	445	13	456	16	516	82	0.13821	6.08	0.17	0.27	0.49	0.0847	0.0075	0.044	258.63	210.17	0.563	0.024	0.0715	0.0021	0.0013	0.0062	0.0585	0.0022	0.6143
BAK1301 z16	446	12	481	19	649	76	-0.15986	6.83	0.18	-0.27	0.47	0.078	0.01	-0.040	245.05	180.60	0.604	0.030	0.0717	0.0020	-0.0036	0.0071	0.0616	0.0022	0.6802
BAK1301 z18	400	200	528	96	840	230	-0.13018	0.7	0.13	0.04	0.5	0.0118	0.0082	0.057	16.74	8.70	0.620	0.470	0.0620	0.0370	0.0120	0.0250	0.0740	0.0110	0.5561
BAK1301 z18	560	120	547	95	790	190	0.07011	1.11	0.16	-0.13	0.44	0.0273	0.0059	-0.117	34.57	24.72	0.820	0.270	0.0850	0.0250	-0.0023	0.0060	0.0671	0.0060	0.9584
BAK1301 z18	270	220	420	130	770	310	0.06418	0.58	0.17	0.12	0.36	0.008	0.0053	0.207	9.83	3.56	0.460	0.430	0.0690	0.0500	0.0000	0.0014	0.0710	0.0110	0.9692
BAK1301 z18	474	59	501	56	610	130	-0.13824	2	0.19	0.13	0.5	0.042	0.012	0.065	29.89	8.49	0.760	0.160	0.0880	0.0160	-0.0003	0.0025	0.0621	0.0040	0.9109
BAK1301 z19	449	16	473	21	502	89	0.09509	5.06	0.16	0.03	0.49	0.0189	0.0072	0.006	39.31	6.58	0.591	0.033	0.0721	0.0027	0.0004	0.0012	0.0580	0.0025	0.6470
BAK1301 z19	464	20	477	21	568	93	0.19191	3.78	0.16	-0.12	0.38	0.0393	0.0083	-0.032	110.12	52.89	0.605	0.033	0.0748	0.0034	-0.0030	0.0033	0.0603	0.0026	0.4453
BAK1301 z19	458	11	468	14	562	60	0.03824	7.81	0.2	-0.2	0.47	0.0155	0.004	-0.026	169.55	56.57	0.585	0.021	0.0736	0.0019	-0.0004	0.0005	0.0592	0.0016	0.6717
BAK1301 z22	462	6	461	6	445	23	0.09992	48	2	2.88	0.44	0.67	0.026	0.060	1927.78	1287.88	0.575	0.010	0.0743	0.0010	0.0310	0.0480	0.0559	0.0006	0.7652
BAK1301 z22	462	6	461	5	439	16	0.13658	131.4	4.3	8.8	0.46	1.733	0.051	0.067	2350.00	767.18	0.575	0.008	0.0743	0.0010	0.0214	0.0011	0.0557	0.0004	0.8657
BAK1301 z24	449	13	441	17	391	78	-0.02880	6.14	0.16	-0.38	0.52	0.0182	0.004	-0.062	285.80	228.69	0.547	0.026	0.0722	0.0022	-0.0007	0.0006	0.0549	0.0020	0.7085
BAK1301 z24	455	14	449	16	419	67	-0.01254	6.22	0.19	-0.13	0.49	0.0351	0.0057	-0.021	188.57	106.62	0.556	0.025	0.0731	0.0023	-0.0003	0.0018	0.0555	0.0016	0.7820
BAK1301 z24	454	14	458	15	448	63	0.04356	6.75	0.17	0.26	0.42	0.0648	0.0066	0.039	158.80	74.16	0.570	0.024	0.0731	0.0024	0.0017	0.0029	0.0561	0.0015	0.6259
BAK1301 z24	830	290	1770	120	3357	52	0.16454	1.25	0.18	0.22	0.48	0.898	0.027	0.176	19.59	3.66	4.600	2.100	0.1320	0.0500	-0.0180	0.0390	0.2781	0.0094	0.9912
BAK1301 z26	453	10	447	12	442	60	0.03199	9.58	0.16	0.99	0.4	0.144	0.0076	0.103	390.06	321.27	0.552	0.018	0.0728	0.0017	0.0011	0.0078	0.0557	0.0015	0.6498
BAK1301 z26	443	25	501	33	720	130	0.08729	2.48	0.14	0.51	0.48	0.0861	0.0089	0.206	45.35	17.20	0.653	0.056	0.0713	0.0042	0.0007	0.0025	0.0658	0.0039	0.7213
~~BAK1301 z28~~	~~107~~	~~2~~	~~108~~	~~2~~	~~129~~	~~14~~	~~0.02252~~	~~966~~	~~15~~	~~382.5~~	~~5~~	~~19.61~~	~~0.33~~		~~5733.33~~	~~2868.56~~	~~0.112~~	~~0.002~~	~~0.0167~~	~~0.0002~~	~~0.0052~~	~~0.0001~~	~~0.0486~~	~~0.0003~~	~~0.9282~~
~~BAK1301 z28~~	~~101~~	~~2~~	~~102~~	~~2~~	~~115~~	~~16~~	~~0.10624~~	~~638.2~~	~~9.5~~	~~322.6~~	~~3.2~~	~~15.63~~	~~0.22~~		~~6842.86~~	~~4888.64~~	~~0.105~~	~~0.002~~	~~0.0158~~	~~0.0003~~	~~0.0052~~	~~0.0001~~	~~0.0484~~	~~0.0003~~	~~0.9187~~
BAK1301 z30	458	11	458	14	435	57	-0.03128	10.06	0.2	0.46	0.37	0.0863	0.006	0.046	320.45	174.88	0.570	0.021	0.0736	0.0018	-0.0023	0.0072	0.0556	0.0014	0.6971
BAK1301 z31	449	10	453	12	503	53	-0.14128	10.23	0.19	0.12	0.5	0.0476	0.0057	0.012	387.22	279.72	0.563	0.018	0.0721	0.0017	-0.0001	0.0015	0.0575	0.0014	0.7696
BAK1301 z31	443	10	452	12	483	45	0.13062	13.72	0.24	0.37	0.5	0.0254	0.0046	0.027	661.43	614.27	0.561	0.018	0.0712	0.0017	0.0003	0.0011	0.0569	0.0012	0.7106
BAK1301 z31	460	13	454	15	430	63	0.01235	9.61	0.21	0.28	0.48	0.0492	0.0054	0.029	606.36	716.69	0.566	0.023	0.0740	0.0022	0.0023	0.0046	0.0555	0.0015	0.7320
BAK1301 z32	450	11	467	14	529	53	-0.06410	11.45	0.21	-0.09	0.45	0.0295	0.0051	-0.008	130.83	24.08	0.584	0.021	0.0721	0.0017	0.0006	0.0015	0.0584	0.0014	0.7310
BAK1301 z32	459	12	489	11	609	50	0.29123	12.06	0.21	0.37	0.42	0.081	0.01	0.031	-209.00	-62.84	0.620	0.018	0.0738	0.0019	0.0016	0.0063	0.0606	0.0014	0.5937
BAK1301 z33	490	40	518	37	680	100	-0.00978	3.12	0.18	-0.02	0.41	0.0273	0.0074	-0.006	42.56	11.96	0.686	0.065	0.0794	0.0069	0.0004	0.0014	0.0630	0.0029	0.9995
BAK1301 z33	450	13	477	15	607	60	-0.00082	8.72	0.2	0.32	0.51	0.0811	0.0088	0.037	422.86	422.94	0.600	0.025	0.0723	0.0021	0.0053	0.0041	0.0600	0.0018	0.6601
BAK1301 z34	250	180	360	160	840	340	0.06522	0.5	0.16	-0.13	0.44	0.0165	0.0078	-0.260	-1605.0	########	0.400	0.450	0.0260	0.0320	-0.0019	0.0040	0.0730	0.0140	0.8873
BAK1301 z35	465	15	563	35	900	140	-0.10527	7.69	0.23	0.34	0.57	0.276	0.061	0.044	205.77	118.79	0.759	0.064	0.0749	0.0025	0.0057	0.0076	0.0728	0.0054	0.4512
BAK1301 z35	463	16	497	19	700	73	0.11411	6.04	0.17	0.03	0.56	0.11	0.012	0.005	122.06	50.31	0.637	0.031	0.0744	0.0027	0.0002	0.0025	0.0625	0.0020	0.6839

Sample/ Zircon #	206Pb/ 238U	2σ	207Pb/ 235U	2σ	207Pb/ 206Pb	2σ	Corr coeff	Approx U ppm	2σ	Approx Th ppm	2σ	Approx Pb ppm	2σ	Th/U	206Pb/ 204Pb	2σ	207Pb/ 235U	2σ	206Pb/ 238U	2σ	208Pb/ 232U	2σ	207Pb/20 6Pb	2σ %	Corr coef
BAK1301 z08	484	11	483	10	489	30	0.15256	24.52	0.71	0.31	0.31	0.1107	0.0067	0.013	1232.94	870.89	0.609	0.016	0.0780	0.0019	0.0003	0.0061	0.0570	0.0008	0.8409
BAK1301 z35	453	7	458	8	522	40	0.06662	22.51	0.37	1.92	0.37	0.443	0.01	0.085	607.33	263.33	0.570	0.013	0.0729	0.0012	0.0320	0.0150	0.0580	0.0010	0.6275
BAK1301 z37	463	9	461	9	447	45	0.18676	15.87	0.36	-0.01	0.41	0.0191	0.0041	-0.001	403.33	122.54	0.575	0.014	0.0744	0.0015	-0.0002	0.0011	0.0557	0.0011	0.6371
BAK1301 z17	456	10	464	11	505	51	0.23929	9.52	0.23	0.57	0.46	0.0424	0.0049	0.060	336.09	190.05	0.576	0.016	0.0733	0.0017	-0.0002	0.0019	0.0575	0.0013	0.6611
BAK1301 z21	467	9	470	12	472	61	0.12274	8.75	0.17	-0.12	0.28	0.0541	0.0051	-0.014	251.03	103.96	0.590	0.019	0.0751	0.0015	-0.0036	0.0026	0.0570	0.0016	0.5180
BAK1301 z37	456	9	456	12	481	44	0.10782	8.32	0.16	-0.03	0.38	0.0295	0.0045	-0.004	325.71	186.20	0.569	0.019	0.0732	0.0015	0.0006	0.0016	0.0567	0.0011	0.6806
BAK1301 z24	457	10	468	14	487	68	-0.07089	7.89	0.16	0.14	0.36	0.1464	0.0075	0.018	281.30	171.30	0.585	0.023	0.0735	0.0017	0.0050	0.0130	0.0575	0.0018	0.6547
BAK1301 z26	458	9	459	13	477	60	0.07410	7.74	0.15	0.2	0.43	0.0944	0.0055	0.026	334.21	211.16	0.569	0.020	0.0737	0.0015	0.0034	0.0042	0.0569	0.0015	0.6644
BAK1301 z09	461	10	490	13	623	57	0.21996	6.98	0.15	-0.13	0.32	0.056	0.0053	-0.019	410.86	381.57	0.620	0.021	0.0741	0.0017	-0.0011	0.0025	0.0606	0.0017	0.5547
BAK1301 z19	458	14	469	14	512	61	0.12181	6.69	0.2	0.79	0.33	0.2088	0.0095	0.118	236.96	144.33	0.584	0.022	0.0737	0.0024	0.0130	0.0120	0.0578	0.0016	0.6935
BAK1301 z15	458	11	472	14	547	60	0.01333	6.6	0.13	0.01	0.41	0.0557	0.0047	0.002	256.57	171.11	0.591	0.022	0.0737	0.0018	-0.0020	0.0024	0.0582	0.0015	0.6148
BAK1301 z06	467	14	470	16	465	71	0.04277	6.07	0.14	-0.11	0.45	0.0094	0.0041	-0.018	365.29	339.25	0.589	0.025	0.0751	0.0023	0.0000	0.0009	0.0563	0.0018	0.6797
BAK1301 z19	457	12	438	13	363	59	0.06964	5.95	0.14	0.48	0.39	0.0659	0.0049	0.081	181.04	73.82	0.542	0.019	0.0736	0.0019	-0.0029	0.0051	0.0537	0.0014	0.6573
BAK1301 z39	460	11	447	15	397	91	0.13381	5.81	0.14	-0.17	0.41	0.0361	0.0041	-0.029	244.00	134.29	0.556	0.024	0.0740	0.0018	-0.0007	0.0012	0.0546	0.0023	0.4086
BAK1301 z15	454	13	459	14	474	61	0.09203	5.7	0.16	-0.09	0.43	0.0385	0.0041	-0.016	179.88	96.91	0.575	0.022	0.0730	0.0021	0.0001	0.0012	0.0568	0.0015	0.6961
BAK1301 z29	458	11	460	16	482	72	-0.07382	5.58	0.15	0.19	0.4	0.0407	0.0038	0.034	213.33	142.29	0.572	0.025	0.0736	0.0018	0.0021	0.0020	0.0569	0.0019	0.7647
BAK1301 z26	453	14	459	16	477	76	-0.02186	5.51	0.17	0.29	0.4	0.0452	0.0039	0.053	372.33	403.41	0.572	0.025	0.0729	0.0023	0.0017	0.0031	0.0573	0.0019	0.7202
BAK1301 z32	463	13	454	15	418	77	0.06084	5.39	0.17	0.27	0.47	0.0404	0.0047	0.050	170.58	78.79	0.567	0.023	0.0745	0.0022	0.0001	0.0020	0.0550	0.0018	0.6069
BAK1301 z25	464	14	470	19	511	72	-0.09202	5.13	0.14	0.13	0.38	0.0429	0.0042	0.025	221.89	163.55	0.594	0.030	0.0748	0.0024	0.0010	0.0030	0.0574	0.0018	0.7417
BAK1301 z22	469	16	472	15	495	64	0.21791	4.85	0.14	0.12	0.43	0.0562	0.0047	0.025	313.15	313.20	0.592	0.024	0.0755	0.0026	-0.0010	0.0043	0.0576	0.0017	0.6634
BAK1301 z23	461	16	472	21	535	93	0.00019	4.82	0.13	0.23	0.43	0.0312	0.0049	0.048	134.03	75.99	0.597	0.034	0.0742	0.0026	0.0013	0.0020	0.0586	0.0024	0.6564
BAK1301 z23	467	16	469	21	488	80	0.02681	4.76	0.14	0.13	0.4	0.0081	0.0039	0.027	153.27	88.47	0.591	0.032	0.0751	0.0027	0.0011	0.0012	0.0572	0.0020	0.7133
BAK1301 z36	447	15	459	19	481	76	0.02800	4.53	0.15	0.34	0.39	0.0547	0.0055	0.075	40.80	5.94	0.572	0.029	0.0719	0.0025	0.0002	0.0024	0.0569	0.0020	0.6987
BAK1301 z05	469	18	468	17	510	74	0.18801	4.37	0.15	-0.34	0.43	0.0098	0.0037	-0.078	140.27	70.18	0.589	0.027	0.0755	0.0030	-0.0006	0.0016	0.0579	0.0020	0.7503
BAK1301 z11	463	16	469	19	497	79	-0.03125	4.22	0.13	0.52	0.38	0.0492	0.0047	0.123	156.32	99.53	0.588	0.031	0.0745	0.0026	0.0005	0.0017	0.0577	0.0020	0.7993
BAK1301 z31	448	12	449	19	454	91	0.03567	4.15	0.12	0.1	0.36	0.0389	0.0038	0.024	126.08	72.77	0.561	0.030	0.0721	0.0021	0.0010	0.0021	0.0563	0.0024	0.5992
BAK1301 z22	467	16	462	17	430	69	0.09759	4.08	0.13	-0.06	0.36	0.0328	0.0046	-0.015	197.71	127.97	0.581	0.026	0.0752	0.0027	-0.0032	0.0038	0.0558	0.0018	0.6900
BAK1301 z09	468	17	475	19	517	84	-0.01014	3.87	0.13	0.21	0.36	0.0369	0.0047	0.054	205.00	166.63	0.592	0.030	0.0750	0.0029	-0.0005	0.0026	0.0580	0.0023	0.7333
BAK1301 z05	454	20	457	21	521	72	-0.01067	3.78	0.14	0.17	0.44	0.0079	0.0035	0.045	278.82	354.90	0.573	0.032	0.0731	0.0033	-0.0003	0.0008	0.0576	0.0020	0.8415
BAK1301 z12	463	17	478	18	542	86	0.21288	3.73	0.14	0.13	0.4	0.0649	0.0056	0.035	125.84	55.40	0.602	0.030	0.0745	0.0029	0.0021	0.0036	0.0586	0.0023	0.7068
BAK1301 z04	459	19	458	22	475	88	-0.07095	3.64	0.13	0.02	0.39	0.0071	0.0041	0.005	136.55	86.94	0.576	0.034	0.0740	0.0032	-0.0027	0.0050	0.0561	0.0021	0.7523
BAK1301 z06	483	23	489	24	567	84	0.09610	3.51	0.13	-0.02	0.36	0.0157	0.0039	-0.006	142.38	88.19	0.628	0.039	0.0779	0.0039	-0.0001	0.0011	0.0590	0.0024	0.9184
BAK1301 z08	460	17	477	20	490	92	0.06026	3.45	0.12	-0.01	0.35	0.0368	0.0041	-0.003	122.13	63.76	0.596	0.032	0.0740	0.0028	-0.0022	0.0023	0.0573	0.0023	0.6588
BAK1301 z05	470	21	465	24	464	96	-0.08678	3.13	0.13	-0.06	0.37	0.0063	0.0035	-0.019	#######	########	0.589	0.038	0.0758	0.0035	0.0004	0.0021	0.0563	0.0024	0.7881
BAK1301 z04	472	26	465	29	420	100	-0.03335	2.43	0.12	-0.05	0.37	0.0178	0.0038	-0.021	62.47	31.27	0.586	0.044	0.0750	0.0042	0.0014	0.0014	0.0563	0.0026	0.7482
BAK1301 z04	453	28	512	30	760	130	0.22409	2.25	0.14	0.12	0.37	0.0288	0.0058	0.053	109.06	83.43	0.668	0.049	0.0729	0.0046	-0.0019	0.0037	0.0654	0.0039	0.6471
BAK1301 z34	484	30	478	29	490	110	0.21445	2.21	0.13	0.32	0.39	0.0068	0.0043	0.145	86.05	46.97	0.612	0.046	0.0782	0.0051	0.0000	0.0006	0.0571	0.0029	0.8228
BAK1301 z33	477	28	487	34	560	140	-0.02703	2.19	0.13	0.04	0.41	0.0108	0.0038	0.018	96.89	66.32	0.622	0.054	0.0770	0.0047	-0.0001	0.0009	0.0600	0.0040	0.6907
BAK1301 z28	467	33	478	29	620	110	0.21705	2.19	0.12	-0.25	0.42	0.0108	0.0037	-0.114	144.25	144.28	0.638	0.058	0.0754	0.0056	-0.0001	0.0006	0.0615	0.0030	0.9402
BAK1301 z33	483	30	477	33	440	120	-0.04098	2.16	0.14	-0.22	0.41	0.0108	0.0041	-0.102	78.96	48.10	0.614	0.054	0.0780	0.0051	-0.0003	0.0008	0.0561	0.0033	0.7220
BAK1301 z20	457	29	455	29	460	140	0.13264	2.15	0.13	0.1	0.35	0.0104	0.0047	0.047	35.10	9.85	0.576	0.044	0.0736	0.0048	0.0017	0.0015	0.0574	0.0038	0.6131
BAK1301 z20	464	29	472	37	510	120	-0.07285	2.05	0.13	0.17	0.36	0.0201	0.0048	0.083	57.89	26.91	0.609	0.061	0.0749	0.0049	-0.0005	0.0027	0.0583	0.0036	0.7691
BAK1301 z16	468	25	491	34	540	120	-0.18612	2.02	0.1	-0.16	0.29	0.0085	0.0037	-0.079	70.04	37.96	0.638	0.056	0.0754	0.0041	-0.0010	0.0022	0.0597	0.0034	0.8584
BAK1301 z30	491	36	509	33	620	120	0.19553	1.85	0.14	0.56	0.42	0.0277	0.0043	0.303	79.15	47.52	0.650	0.054	0.0795	0.0060	-0.0002	0.0011	0.0604	0.0033	0.7512
BAK1301 z07	480	37	491	41	570	130	0.01941	1.67	0.12	-0.05	0.35	0.0274	0.0032	-0.030	61.36	36.29	0.645	0.071	0.0776	0.0062	0.0001	0.0017	0.0604	0.0037	0.9449
BAK1301 z13	480	120	501	54	500	140	0.06506	1.22	0.13	-0.34	0.51	0.0185	0.0043	-0.279	40.32	24.23	0.650	0.120	0.0800	0.0170	0.0001	0.0007	0.0574	0.0045	0.9659
BAK1301 z34	590	110	540	57	680	160	-0.17052	0.92	0.11	-0.11	0.37	0.0085	0.0039	-0.120	45.22	37.70	0.830	0.160	0.0980	0.0190	-0.0004	0.0019	0.0645	0.0048	0.9794
~~BAK1301 z38~~	~~540~~	~~210~~	~~467~~	~~99~~	~~560~~	~~180~~	~~0.01978~~	~~0.9~~	~~0.15~~	~~0.12~~	~~0.4~~	~~0.0047~~	~~0.0036~~		~~19.90~~	~~8.36~~	~~1.010~~	~~0.510~~	~~0.0980~~	~~0.0400~~	~~-0.0003~~	~~0.0010~~	~~0.0590~~	~~0.0056~~	~~0.7703~~
~~BAK1301 z28~~	~~340~~	~~120~~	~~380~~	~~110~~	~~460~~	~~560~~	~~-0.02704~~	~~0.51~~	~~0.15~~	~~-0.09~~	~~0.36~~	~~0.0066~~	~~0.0031~~		~~14.54~~	~~5.74~~	~~0.440~~	~~0.170~~	~~0.0490~~	~~0.0230~~	~~0.0008~~	~~0.0008~~	~~0.0590~~	~~0.0180~~	~~0.7922~~
~~BAK1301 z07~~	~~70~~	~~270~~	~~40~~	~~320~~	~~740~~	~~600~~	~~-0.20501~~	~~0.47~~	~~0.15~~	~~-0.07~~	~~0.47~~	~~0.006~~	~~0.0045~~		~~14.07~~	~~7.06~~	~~-0.030~~	~~0.380~~	~~0.0140~~	~~0.0430~~	~~0.0012~~	~~0.0011~~			

Sample/ Zircon #	206Pb/ 238U	2σ	207Pb/ 235U	2σ	207Pb/ 206Pb	2σ	Corr coeff	Approx U ppm	2σ	Approx Th ppm	2σ	Approx Pb ppm	2σ	Th/U	206Pb/ 204Pb	2σ	207Pb/ 235U	2σ	206Pb/ 238U	2σ	208Pb/ 232U	2σ	207Pb/20 6Pb	2σ %	Corr coef
MIC1301 z12	389.7	9.4	399	11	453	52	0.03300	25	0.65	0.9	1.1	0.114	0.016	0.036	-28.2	-14.1	0.481	0.016	0.062	0.002	-0.0007	0.0033	0.0559	0.0013	0.6937
MIC1301 z15	411.0	32.0	579	44	1390	130	0.18277	7.69	0.64	0.4	1.2	0.382	0.032	0.052	26.7	58.3	0.784	0.080	0.066	0.005	-0.0030	0.0100	0.0880	0.0055	0.8277
MIC1301 z03	402.0	15.0	424	21	543	88	-0.04076	11.75	0.69	0.9	1.2	0.125	0.013	0.077	5.8	1.3	0.515	0.031	0.065	0.003	0.0011	0.0026	0.0587	0.0023	0.7716
MIC1301 z01	401.0	23.0	419	27	440	120	0.09165	2.64	0.15	0.13	0.45	0.0209	0.0054	0.049	76.3	41.6	0.520	0.042	0.064	0.004	0.0011	0.0020	0.0569	0.0032	0.6800
MIC1301 z33	413.0	36.0	472	44	760	150	0.21080	4.63	0.37	0.5	1.1	0.113	0.017	0.108	7.4	7.0	0.596	0.068	0.066	0.006	0.0015	0.0016	0.0656	0.0050	0.8612
MIC1301 z08	411.0	12.0	444	15	581	74	0.08418	6.38	0.23	0.49	0.43	0.0384	0.0056	0.077	203.5	132.4	0.548	0.022	0.066	0.002	0.0022	0.0022	0.0596	0.0019	0.6180
MIC1301 z05	412.0	20.0	446	32	540	130	-0.12677	2.66	0.14	0.62	0.39	0.1065	0.0086	0.233	74.4	43.0	0.548	0.050	0.066	0.003	-0.0010	0.0100	0.0595	0.0036	0.7443
MIC1301 z04	411.0	11.0	410	12	450	65	0.26313	15.37	0.6	1.92	0.89	0.158	0.017	0.125	29.5	32.0	0.499	0.018	0.066	0.002	0.0020	0.0024	0.0561	0.0017	0.6117
MIC1301 z05	419.0	16.0	476	25	760	100	-0.06848	6.17	0.22	2.51	0.77	0.72	0.039	0.407	141.2	81.4	0.603	0.040	0.067	0.003	0.0270	0.0130	0.0649	0.0032	0.6886
MIC1301 z33	424.0	20.0	467	26	780	110	0.06096	11.32	0.51	1.92	0.98	0.961	0.045	0.170	11.0	4.4	0.590	0.041	0.067	0.004	0.0190	0.0310	0.0661	0.0034	0.8148
MIC1301 z04	415.0	48.0	433	50	600	180	0.07394	3.94	0.35	0.5	1.1	0.015	0.011	0.127	6.3	5.5	0.560	0.083	0.067	0.008	0.0011	0.0029	0.0605	0.0055	0.9270
MIC1301 z01	418.0	21.0	445	21	555	91	0.02706	3.46	0.16	-0.11	0.42	0.0214	0.0036		65.8	22.0	0.550	0.033	0.067	0.003	0.0001	0.0016	0.0590	0.0024	0.7511
MIC1301 z19	420.0	16.0	461	18	627	71	0.17620	14.41	0.46	1.3	0.94	0.106	0.015	0.090	12.3	5.6	0.578	0.029	0.067	0.003	0.0027	0.0020	0.0608	0.0021	0.7530
MIC1301 z05	430.0	28.0	536	36	1070	110	0.02932	2.01	0.13	0.07	0.39	0.087	0.0069	0.035	47.2	23.6	0.714	0.062	0.069	0.005	-0.0019	0.0029	0.0739	0.0040	0.7298
MIC1301 z31	427.0	20.0	494	22	789	65	0.06138	11.44	0.48	-0.4	1.3	0.123	0.015		-8.4	-4.0	0.612	0.032	0.069	0.003	-0.0022	0.0031	0.0657	0.0020	0.8469
MIC1301 z05	424.0	18.0	444	19	566	79	0.20612	4.22	0.18	0.9	0.42	0.2137	0.0089	0.213	90.1	36.1	0.548	0.028	0.068	0.003	-0.0020	0.0100	0.0599	0.0022	0.6596
MIC1301 z36	428.0	19.0	481	23	750	87	-0.01310	13.82	0.68	1.1	1.3	0.144	0.024	0.080	8.2	2.8	0.612	0.037	0.069	0.003	-0.0025	0.0065	0.0643	0.0027	0.7287
MIC1301 z31	427.0	14.0	454	17	551	78	-0.11247	14.3	0.45	0.41	0.96	0.095	0.018	0.029	-29.9	-36.8	0.567	0.026	0.069	0.002	0.0006	0.0052	0.0594	0.0021	0.4752
MIC1301 z01	427.0	22.0	437	27	570	100	-0.06918	2.9	0.19	-0.06	0.37	0.0246	0.004		78.9	35.2	0.547	0.042	0.069	0.004	0.0001	0.0023	0.0603	0.0028	0.8637
MIC1301 z03	433.4	8.1	524	10	935	44	0.22412	12.9	0.23	0.55	0.43	0.173	0.011	0.043	257.6	98.6	0.673	0.017	0.070	0.001	0.0014	0.0048	0.0700	0.0015	0.5816
MIC1301 z18	439.0	30.0	559	37	1030	110	0.04196	14.39	0.88	1.1	1.6	0.374	0.038	0.076	-16.4	-12.6	0.741	0.063	0.071	0.005	-0.0090	0.0140	0.0726	0.0041	0.7734
MIC1301 z37	441.0	24.0	549	28	992	89	0.10470	8.42	0.4	1.8	1.1	0.24	0.032	0.214	3.1	0.5	0.721	0.051	0.071	0.004	0.0023	0.0047	0.0731	0.0030	0.8355
MIC1301 z09	437.0	13.0	475	15	653	52	-0.09464	8.91	0.23	0.14	0.43	0.0989	0.0081	0.016	232.3	107.3	0.596	0.026	0.070	0.002	-0.0060	0.0170	0.0618	0.0015	0.6795
MIC1301 z32	437.0	18.0	481	20	693	81	0.18056	14.37	0.48	1	1.2	0.234	0.029	0.070	-17.0	-10.7	0.611	0.032	0.070	0.003	0.0080	0.0110	0.0628	0.0025	0.7518
MIC1301 z37	437.0	43.0	478	53	640	140	-0.22563	5.63	0.56	-0.7	1.2	0.07	0.014		14.6	19.9	0.626	0.092	0.070	0.007	-0.0003	0.0022	0.0614	0.0037	0.9127
MIC1301 z26	450.0	21.0	597	27	1234	68	0.07249	10.39	0.42	-0.3	1	0.042	0.013		20.6	12.0	0.813	0.051	0.072	0.004	0.0002	0.0012	0.0826	0.0028	0.8595
MIC1301 z36	437.0	22.0	440	18	526	87	0.27977	11.03	0.54	0.3	1	0.088	0.014	0.027	13.5	8.0	0.545	0.027	0.070	0.004	0.0008	0.0020	0.0584	0.0023	0.7278
MIC1301 z32	445.0	27.0	511	30	793	83	0.14228	8.24	0.43	0.72	0.89	0.067	0.016	0.087	24.7	29.7	0.668	0.051	0.072	0.005	0.0006	0.0025	0.0661	0.0025	0.8727
MIC1301 z09	444.6	8.9	461	11	528	46	-0.01476	13.11	0.27	0.21	0.48	0.06	0.0075	0.016	572.5	501.0	0.574	0.018	0.071	0.002	0.0100	0.0120	0.0581	0.0013	0.6128
MIC1301 z17	444.0	37.0	444	35	560	140	0.08610	5.63	0.49	0	1.1	0.064	0.016	0.000	-7.3	-5.5	0.560	0.056	0.072	0.006	0.0002	0.0022	0.0582	0.0038	0.8470
MIC1301 z01	442.0	26.0	421	27	330	120	0.03900	2.27	0.14	0.06	0.34	0.0118	0.0041	0.026	44.1	16.6	0.518	0.041	0.071	0.004	0.0002	0.0010	0.0525	0.0030	0.7062
MIC1301 z02	447.0	49.0	436	42	540	150	0.04291	1.93	0.18	0.03	0.48	0.0137	0.0052	0.016	80.4	75.1	0.579	0.079	0.072	0.008	0.0005	0.0013	0.0606	0.0042	0.9072
MIC1301 z35	459.0	28.0	569	32	1040	100	0.11976	7.69	0.38	-0.5	1.2	0.112	0.017		13.6	8.8	0.765	0.055	0.074	0.005	-0.0001	0.0015	0.0744	0.0037	0.8755
MIC1301 z28	455.0	46.0	466	42	590	180	0.36545	7.3	0.74	2.3	1.7	0.501	0.049	0.315	2.2	0.6	0.594	0.068	0.073	0.008	-0.0020	0.0180	0.0615	0.0051	0.8039
MIC1301 z01	458.0	11.0	469	10	519	20	0.03950	66.7	1.7	-0.09	0.41	0.1856	0.007		1139.6	357.3	0.588	0.015	0.074	0.002	0.0018	0.0090	0.0577	0.0005	0.9318
MIC1301 z06	462.0	33.0	485	31	680	81	-0.09191	6.86	0.43	-1.26	0.92	0.023	0.013		-2.2	-0.3	0.625	0.052	0.075	0.006	0.0007	0.0009	0.0627	0.0023	0.9127
MIC1301 z03	495.0	22.0	821	39	1854	94	-0.12519	3.37	0.16	0.04	0.52	0.347	0.028	0.012	87.4	35.0	1.272	0.088	0.080	0.004	0.0030	0.0130	0.1146	0.0055	0.7182
MIC1301 z01	477.0	67.0	589	72	1000	150	0.12299	1.39	0.18	0.11	0.44	0.0316	0.0071	0.079	39.6	26.9	0.800	0.130	0.077	0.011	-0.0009	0.0025	0.0731	0.0051	0.9106
MIC1301 z002	472.0	52.0	528	47	820	130	0.15622	1.62	0.16	0.28	0.47	0.0246	0.0038	0.173	24.0	6.9	0.716	0.087	0.077	0.009	-0.0011	0.0019	0.0680	0.0042	0.8967
MIC1301 z19	459.0	52.0	486	50	720	150	0.09062	3.83	0.38	0.13	0.77	0.026	0.011	0.034	3.5	1.7	0.760	0.160	0.077	0.011	-0.0006	0.0009	0.0653	0.0046	0.9438
MIC1301 z30	477.0	14.0	487	16	516	61	0.02397	18.59	0.54	-0.2	1.3	0.032	0.012		18.0	8.4	0.612	0.026	0.077	0.002	0.0003	0.0007	0.0581	0.0016	0.7464
MIC1301 z15	486.0	72.0	560	63	1090	160	0.08500	4.72	0.61	0.9	1.3	0.221	0.022	0.191	5.3	2.5	0.760	0.120	0.079	0.012	0.0020	0.0044	0.0773	0.0056	0.9146
MIC1301 z03	488.0	29.0	471	29	460	110	0.05384	2.66	0.17	0.12	0.43	0.0075	0.0041	0.045	68.5	29.7	0.601	0.047	0.079	0.005	0.0007	0.0008	0.0570	0.0030	0.7922
MIC1301 z36	502.0	32.0	614	52	1060	170	-0.22082	5	0.29	0.1	1.1	0.22	0.026	0.020	18.0	27.8	0.890	0.120	0.081	0.005	0.0036	0.0077	0.0743	0.0055	0.9063
MIC1301 z14	492.0	60.0	474	54	370	140	0.09825	4.44	0.46	1.4	1.1	0.033	0.012	0.315	572.0	40040.0	0.635	0.098	0.080	0.010	0.0005	0.0030	0.0552	0.0038	0.9324
MIC1301 z01	520.0	71.0	532	50	720	130	0.02831	1.56	0.14	-0.24	0.54	0.0076	0.0043		90.8	98.4	0.725	0.090	0.082	0.011	-0.0006	0.0011	0.0635	0.0042	0.8818
MIC1301 z27	531.0	56.0	507	53	440	170	0.10689	4.39	0.44	0	1.2	0.088	0.014	0.000	5.7	3.9	0.688	0.095	0.089	0.011	0.0009	0.0018	0.0573	0.0046	0.9382
MIC1301 z36	680.0	110.0	600	65	760	130	-0.01023	2.9	0.39	-0.4	1	0.025	0.011		1.6	0.3	1.110	0.280	0.121	0.025	0.0000	0.0009	0.0653	0.0038	0.9792
MIC1301 z18	586.0	87.0	678	80	1210	150	0.05353	2.76	0.35	1.29	0.86	0.054	0.013	0.467	8.7	8.7	1.040	0.230	0.094	0.022	0.0013	0.0009	0.0825	0.0061	0.9840

Sample/ Zircon #	206Pb/ 238U	2σ	207Pb/ 235U	2σ	207Pb/ 206Pb	2σ	Corr coeff	Approx U ppm	2σ	Approx Th ppm	2σ	Approx Pb ppm	2σ	Th/U	206Pb/ 204Pb	2σ	207Pb/ 235U	2σ	206Pb/ 238U	2σ	208Pb/ 232U	2σ	207Pb/20 6Pb	2σ %	Corr coef
MIC1301 z18	570.0	120.0	527	76	730	170	0.05827	2.47	0.35	-1	1.1	0.032	0.014		2.5	1.1	0.750	0.220	0.089	0.026	-0.0001	0.0009	0.0640	0.0052	0.9477
MIC1301 z35	500.0	190.0	700	110	1150	240	-0.15878	2.23	0.44	0.29	0.93	0.115	0.019	0.130	1.3	0.4	1.000	0.290	0.087	0.032	0.0052	0.0082	0.0794	0.0093	0.9384
MIC1301 z28	520.0	130.0	499	80	740	190	-0.06916	3.21	0.53	-0.5	1.3	0.26	0.027		-9.5	-18.1	0.600	0.210	0.069	0.022	-0.0270	0.0450	0.0652	0.0057	0.9746
MIC1301 z26	520.0	150.0	461	70	510	170	0.08205	3.5	0.49	0.1	1.1	0.082	0.015	0.029	3.4	2.3	0.670	0.320	0.078	0.036	-0.0015	0.0028	0.0581	0.0049	0.9792
MIC1301 z04	430.0	120.0	460	75	380	210	-0.21389	2.49	0.39	1.5	0.85	0.041	0.011	0.602	5.8	6.9	0.450	0.240	0.068	0.032	-0.0001	0.0008	0.0543	0.0060	0.9569
MIC1301 z05	~~490.0~~	~~58.0~~	~~452~~	~~52~~	~~400~~	~~160~~	~~0.09444~~	~~1.24~~	~~0.15~~	~~-0.05~~	~~0.37~~	~~0.0486~~	~~0.0048~~		~~22.8~~	~~5.9~~	~~0.470~~	~~0.190~~	~~0.069~~	~~0.036~~	~~0.0015~~	~~0.0032~~	~~0.0545~~	~~0.0044~~	~~0.9476~~
MIC1301 z12	460.0	230.0	490	130	970	340	-0.03568	1.7	0.48	-0.5	1.4	0.014	0.017		3.3	4.4	0.750	0.540	0.072	0.045	-0.0007	0.0014	0.0750	0.0120	0.9557
MIC1301 z37	260.0	180.0	530	130	1060	270	-0.07576	1.75	0.45	-0.7	1.2	0.075	0.017		2.4	1.4	0.560	0.330	0.046	0.028	0.0018	0.0026	0.0769	0.0099	0.6731
MIC1301 z03	310.0	180.0	404	85	390	270	-0.01380	2.17	0.47	-0.2	1.1	0.025	0.01		0.6	0.1	0.320	0.260	0.048	0.031	0.0002	0.0018	0.0569	0.0077	0.9650
MIC1301 z11	180.0	140.0	110	230	2100	1100	-0.88888	0.13	0.63	-0.5	1.5	0.013	0.014		0.4	0.2	0.150	0.340	0.031	0.024	-0.0011	0.0020	0.1730	0.0780	0.5329
MIC1301 z17	220.0	230.0	370	170	940	360	-0.02013	0.94	0.36	0.3	1.1	0.0114	0.0089	0.319	-0.8	-0.4	0.580	0.500	0.040	0.050	0.0017	0.0023	0.0760	0.0150	0.9889
MIC1301 z10	160.0	270.0	560	290	1640	450	-0.45659	0.79	0.58	-0.6	2.2	0.025	0.012		-1.1	-0.9	0.380	0.670	0.030	0.045	-0.0006	0.0008	0.1060	0.0270	0.8777
MIC1301 z09	100.0	180.0	1310	240	3970	120	-0.18975	0.51	0.42	-0.2	1	0.032	0.013		9.8	8.6	1.100	1.900	0.030	0.053	-0.0003	0.0008	0.4250	0.0350	0.9480
MIC1301 z09	240.0	170.0	500	160	960	320	0.16398	1.07	0.35	0.3	1.1	0.003	0.012	0.280	-4.5	-5.8	0.410	0.300	0.022	0.035	-0.0009	0.0019	0.0790	0.0120	0.9400
MIC1301 z02	80.0	160.0	210	130	940	340	0.15139	0.39	0.16	0.1	0.44	0.0085	0.004	0.256	9.7	5.0	0.150	0.540	0.018	0.026	0.0003	0.0010	0.0820	0.0140	0.9243
MIC1301 z11	130.0	160.0	90	150	330	570	0.23906	0.52	0.56	-0.8	1.3	0.01	0.015		-36.2	-1085.1	0.000	0.300	0.011	0.025	-0.0009	0.0005	0.0610	0.0200	0.6030
MIC1301 z30	36.0	63.0	650	310	4910	310	-0.50782	0.3	0.49	0.5	1.1	0.063	0.015	1.667	3.8	2.8	0.460	0.660	0.006	0.010	-0.0005	0.0025	0.8100	0.1200	0.9741
MIC1301 z03	30.0	160.0	170	150	2190	320	0.14282	0.91	0.53	-1.2	1.5	0.039	0.011		1.9	1.7	-0.070	0.320	0.001	0.020	-0.0002	0.0011	0.1480	0.0240	0.8208
MIC1301 z35	340.0	630.0	870	270	1520	220	-0.10988	1	0.43	0.4	1.7	0.128	0.022	0.400	4.1	3.3	-1.000	3.200	-0.010	0.210	0.0038	0.0035	0.1000	0.0110	0.9978
MIC1301 z06	-22.0	69.0	20	170	1110	690	0.06034	-0.24	0.41	-1.4	1.2	0.011	0.011	5.833	0.3	0.1	-0.060	0.200	-0.003	0.011	-0.0005	0.0032	0.1130	0.0360	0.7021
MIC1301 z13	-35.0	80.0	140	150	1990	680	0.05893	0.47	0.38	-1.68	0.89	0.036	0.013		0.6	0.4	0.000	0.240	-0.005	0.012	0.0010	0.0036	0.1560	0.0530	0.6695
MIC1301 z17	-210.0	340.0	-20	190	1700	1500	0.38010	0.69	0.54	0.3	2	0.015	0.016	0.435	0.4	0.4	-0.500	0.480	-0.048	0.060	0.0002	0.0009	0.1280	0.0970	-0.1808
MIC1301 z37	49.0	97.0	220	320	900	2200	0.00398	-0.06	0.59	-0.1	1.6	0.06	0.022	1.667	0.7	0.5	0.210	0.450	0.000	0.020	0.0001	0.0014	0.1200	0.1700	0.7915

Sample/ Zircon #	206Pb/ 238U	2σ	207Pb/ 235U	2σ	207Pb/ 206Pb	2σ	Corr coeff	Approx U ppm	2σ	Approx Th ppm	2σ	Approx Pb ppm	2σ	Th/U	206Pb/ 204Pb	2σ	207Pb/ 235U	2σ	206Pb/ 238U	2σ	208Pb/ 232U	2σ	207Pb/20 6Pb	2σ %	Corr coef
BAK1302 z27	67	98	60	190	1960	540	-0.6309	0.24	0.48	-1.40	1.20	0.06	0.01	-0.040	1.2524	0.9514	0.000	0.370	0.012	0.016	0.0000	0.0008	0.139	0.040	0.7409
BAK1302 z27	-10	120	230	130	710	540	0.3141	0.40	0.38	-0.90	1.10	0.02	0.01	0.150	-0.9458	-0.6451	-0.020	0.330	-0.006	0.033	0.0003	0.0007	0.073	0.022	0.8786
BAK1302 z27	20	240	180	270	1900	310	0.0325	0.30	0.43	1.60	1.00	0.07	0.02	0.020	-0.6333	-0.2114	-0.700	1.300	-0.020	0.073	-0.0013	0.0027	0.121	0.022	0.9782
BAK1302 z27	40	140	40	170	870	500	-0.1723	0.21	0.38	1.40	1.20	0.04	0.01	0.360	1.6000	1.6409	-0.170	0.260	-0.004	0.029	-0.0001	0.0013	0.086	0.022	0.2812
BAK1302 z26	430	210	400	190	890	290	-0.0305	1.05	0.45	0.90	1.10	0.04	0.01	0.270	1.1486	0.4446	0.570	0.490	0.068	0.040	0.0010	0.0010	0.070	0.011	0.9910
BAK1302 z26	-1	62	-80	220	2590	940	0.0097	0.23	0.38	0.90	1.10	0.03	0.01	-0.210	0.3480	0.1418	0.020	0.500	0.000	0.009	-0.0001	0.0018	0.236	0.088	0.7081
BAK1302 z26	90	160	300	480	-5200	4700	-0.6617	-0.10	1.10	0.90	1.90	0.03	0.03	0.420	-0.0183	-0.1570	0.200	0.570	0.014	0.027	0.0021	0.0020	-0.040	0.160	0.1521
BAK1302 z18	60	160	170	150	550	490	-0.1039	0.62	0.44	0.11	0.91	0.03	0.01	-0.090	0.3783	0.1189	0.220	0.250	0.007	0.022	0.0005	0.0013	0.071	0.019	0.4424
BAK1302 z18	490	110	538	81	1070	190	0.1367	2.34	0.36	-0.85	0.95	0.11	0.02	-0.170	6.8000	11.1430	0.940	0.280	0.090	0.027	-0.0001	0.0033	0.078	0.007	0.9817
BAK1302 z18	55	49	170	150	800	1300	0.5287	0.75	0.48	0.50	1.40	0.05	0.01	0.240	-0.4000	-0.2069	0.200	0.250	0.009	0.008	-0.0004	0.0011	0.160	0.083	0.8268

REFERENCES

Abbott, R., and Greenwood, J., 2001, Retrograde metamorphism of eclogite in the southern Appalachian Mountains, USA–A case involving seamount subduction?: Journal of Metamorphic Geology, v. 19, p. 433–443.

Abbott, R.N., and Raymond, L.A., 1984, The Ashe Metamorphic Suite, Northwest North Carolina: Metamorphism and Observations on Geologic History: American Journal of Science, v. 284, p. 350–375.

Abbott, R.N., and Raymond, L.A., 1997, Petrology of Pelitic and Mafic Rocks in the Ashe and Alligator Back Metamorphic Suites, Northeast of the Grandfather Mountain Window: Paleozoic Structure, Metamorphism, and Tectonics of the Blue Ridge of Western North Carolina, in Stewart, K.G., et al., eds., Paleozoic structure, metamorphism, and tectonics of the Blue Ridge of western North Carolina: Chapel Hill, North Carolina, Carolina Geological Society 1997 Field Trip Guidebook, p. 49–66.

Adams, M.G., 1995, The tectonothermal evolution of part of the Blue Ridge thrust complex, northwestern North Carolina [Ph.D. thesis]: Chapel Hill, University of North Carolina, 193 p.

Adams, M.G., Stewart, K.G., Trupe, C.H., and Willard, R.A., 1995, Tectonic significance of high-pressure metamorphic rocks and dextral strike-slip faulting in the southern Appalachians, in Hibbard, J., et al., eds., Current perspectives in the Appalachian-Caledonian orogen: St. John's, Newfoundland, Geological Association of Canada Special Paper 41, p. 21–42

Adams, M.G., Trupe, C.H., 1997, Conditions and Timing of Metamorphism in the Blue Ridge Thrust Complex, Northwestern North Carolina and Eastern Tennessee, in Stewart, K.G., et al., eds., Paleozoic structure, metamorphism, and tectonics of the Blue Ridge of western North Carolina: Chapel Hill, North Carolina, Carolina Geological Society 1997 Field Trip Guidebook, p. 49–66.

Anderson, C.B., 1994, Petrology and geochemistry of the Ordovician Blountian and Taconic foreland basin sequences: Implications for terrane accretionary history [Ph.d thesis] Syracuse University, 218 p.

Anderson, E., and Moecher, D., 2007, Omphacite breakdown reactions and relation to eclogite exhumation rates: Contributions to Mineralogy and Petrology, v. 154, no. 3, p. 253–277, doi: 10.1007/s00410-007-0192-x.

Baldwin, J.A., Brown, M., Schmitz, M.D., 2007, First application of titanium-in-zircon thermometry to ultrahigh-temperature metamorphism: Geology, v. 35, no. 4, p.295–298.

Borella, J., 2000, The Crabtree-Penland Fault Zone; Investigating a New Control on the Macroscopic Brittle-Ductile Transition through Mapping and Related Structural Studies [M.S. thesis]: Chapel Hill, University of North Carolina at Chapel Hill, 79 p.

Brobst, D.A., 1962, Geology of the Spruce Pine district, Avery, Mitchell, and Yancey Counties, North Carolina: Reston, Virginia, U.S. Geological Survey Bulletin, 1122-A, 26 p.

Brueckner, H.K., and Cuthbert, S.J., 2013, Extension, disruption, and translation of an orogenic wedge by exhumation of large ultrahigh-pressure terranes: Examples from the Norwegian Caledonides: Lithosphere, v. 5, no. 3, p. 277–289, doi: 10.1130/L256.1.

Bryant, B., and Reed, J. C., Jr., 1970, Geology of the Grandfather Mountain window and vicinity, North Carolina and Tennessee: U.S. Geol. Survey Prof. Paper 615, 190 p.

Camacho, A., and McDougall, I., 2000, Intracratonic, strike-slip partitioned transpression and the formation and exhumation of eclogite facies rocks: An example from the Musgrave Block, central Australia: Tectonics, v. 19, no. 5, p. 978-996.

Cloos, M., 1982, Flow melanges: Numerical modeling and geologic constraints on their origin in the Franciscan subduction complex, California: Geological Society of America Bulletin, v. 93, no. April, p. 330–345.

Cloos, M. and Shreve, R. L., 1988, Subduction-channel model of prism accretion, melange formation, sediment subduction, and subduction erosion at convergent plate margins; Part II, Implications and discussion: Pure and Applied Geophysics, v. 128, p. 501–545.

Coleman, R.G., Lanphere, M.A., 1971, Distribution and age of high-grade blueschists associated eclogites, and amphibolites from Oregon and California: Geological Society of America Bulletin, v. 82, p.2397–2412.

Coleman, R.G., Lee, D.E., Beatty, L.B., Brannock, W.W., 1965, Eclogites and eclogites: their differences and similarities: Geological Society of America Bulletin, v.76, p 486–508.

Corfu, F., Hanchar, J.M., Hoskin, P.W.O., Kinny, P.D., 2003, Atlas of zircon textures: Reviews in Mineralogy and Geochemistry, v. 53, p. 469-500.

Dallmeyer, R.D., Wright, J.E., Secor, D.T., Jr., and Snoke, A.W., 1986, Character of the Alleghanian orogeny in the Southern Appalachians: Part II. Geochronological constraints on the tectonothermal evolution of the eastern Piedmont in South Carolina: Geological Society of America Bulletin, v. 97, no. 11, p. 1329–1344, doi: 10.1130/0016-7606(1986)97<1329:COTAOI>2.0.CO;2.

Dennis, A.J., 2007, Cat Square basin, Catskill clastic wedge: Silurian-Devonian orogenic events in the central Appalachians and the crystalline southern Appalachians, in Sears, J.W., Harms, T.A., and Evenchick, C.A., eds., Whence the Mountains? Inquiries into the Evolution of Orogenic Systems: A Volume in Honor of Raymond A. Price: Geological Society of America Special Paper 433, p. 313–329, doi: 10.1130/2007.2433(15).

Dilts, S. L., 2006, Zircon inclusion suite analysis of the Ashe metamorphic suite, North Carolina: Implications for exhumation history of eclogite, [M.S. thesis]: Chapel Hill, University of North Carolina at Chapel Hill, 133 p.

Dunning, G.R., O'Brien, S.J., Colman-Sadd, S.P., Blackwood, R.F., Dickson, W.L., O'Neill, P.P., and Krogh, T.E., 1990, Silurian Orogeny in the Newfoundland Appalachians: The Journal of Geology, v. 98, no. 6, p. 895–913, doi: 10.1086/629460.

Ernst, W.G., 1984, Californian blueschists, subduction, and the significance of tectonostratigraphic terranes, Geology, v. 12, p. 436-440.

Ernst, W.G., and Liou, J.G., 2008, High- and ultrahigh-pressure metamorphism: Past results and future prospects: American Mineralogist, v. 93, p. 1771–1786, doi: 10.2138/am.2008.2940.

Ernst, W.G., Maruyama, S., and Wallis, S., 1997, Buoyancy-driven, rapid exhumation of ultrahigh-pressure metamorphosed continental crust.: Proceedings of the National Academy of Sciences of the United States of America, v. 94, no. September, p. 9532–9537, doi: 10.1073/pnas.94.18.9532.

Ettensohn, F.R., 2004, Modeling the nature and development of major Paleozoic clastic wedges in the Appalachian Basin, USA: Journal of Geodynamics, v. 37, p. 657-681, doi:10.1016/j.jog.2004.02.009.

Ettensohn, F.R., Brett, C.E., 2002, Stratigraphic evidence from the Appalachian Basin for continuation of the Taconian Orogeny into Early Silurian time. In: Mitchell, C.E., Jacobi, R. (Eds.), Taconic Convergence: Orogen, Foreland Basin, and Craton.Physics and Chemistry of the Earth, v. 27, p. 279–288.

Ewing, T.A., Hermann, J., and Rubatto, D., 2013, The robustness of the Zr-in-rutile and Ti-in-zircon thermometers during high-temperature metamorphism (Ivrea-Verbano Zone, northern Italy): Contributions to Mineralogy and Petrology, v. 165, p. 757–779, doi: 10.1007/s00410-012-0834-5.

Ferriss, E.D.A., Essene, E.J., Becker, U., 2008, Computational Study of the Effect of Pressure on the Ti-in-zircon Geothermometer: European Journal of Mineralogy, v. 20, p. 745-755.

Ferry, J.M., and Watson, E.B., 2007, New thermodynamic models and revised calibrations for the Ti-in-zircon and Zr-in-rutile thermometers: Contributions to Mineralogy and Petrology, v. 154, p. 429–437, doi: 10.1007/s00410-007-0201-0.

Fetter, A.H., and Goldberg, S.A., 1995, Age and Geochemical Characteristics of Bimodal Magmatism in the Neoproterozoic Grandfather Mountain Rift Basin: The Journal of Geology, v. 103, no. 3, p. 313–326, doi: 10.1086/629749.

Fullagar, P.D., 2002, Evidence for Early Mesoproterozoic (and Older?) Crust in the Southern and Central Appalachians of North America: Gondwana Research, v. 5, no. 1, p. 197–203.

Goldberg, S., and Dallmeyer, R., 1997, Chronology of Paleozoic metamorphism and deformation in the Blue Ridge thrust complex, North Carolina and Tennessee: American Journal of Science, v. 297, p. 488–526.

Guillot, S., Hattori, K.H., de Sigoyer, J., Nagler, T., Auzende, A.L., 2001, Evidence of hydration of the mantle wedge and its role in the exhumation of eclogites, Earth and Planetary Science Letters, v. 193, p. 115-127.

Harley, S.L., and Carswell, D. a., 1995, Ultradeep crustal metamorphism: A prospective view: Journal of Geophysical Research, v. 100, no. B5, p. 8367-8380, doi: 10.1029/94JB02421.

Harley, S.L., Kelly, N.M., Möller, A., 2007, Zircon Behaviour and the Thermal Histories of Mountain Chains: Elements, v. 3, p. 25-30.

Hatcher, R.D., Jr., 2002, An Inner Piedmont primer, in Hatcher, R.D., Jr., and Bream, B.R., eds., Inner Piedmont geology in the South Mountains-Blue Ridge Foothills and the southwestern Brushy Mountains, central-western North Carolina: North Carolina Geological Survey, Carolina Geological Society annual field trip guidebook, p. 1-18.

Hatcher, R.D., Jr., 2010, The Appalachian orogen: A brief summary, in Tollo, R.P., Bartholomew, M.J., Hibbard, J.P., and Karabinos, P.M., eds., From Rodinia to Pangea: The Lithotectonic Record of the Appalachian Region: Geological Society of America Memoir 206, p. 1-19, doi: 10.1130/2010.1206(01).

Hewitt, L.K., 1999, The thermobarometric history along a transect of the Ashe Metamorphic Suite, southwest of the Grandfather Mountain window, northwestern North Carolina [M.S. thesis]: Chapel Hill, University of North Carolina, 162 p.

Hibbard, J.P., 2000, Docking Carolina: Mid Paleozoic accretion in the southern Appalachians: Geology, v. 28,p. 127–130, doi: 10.1130/0091-7613(2000)028<0127:DCMPAI>2.3.CO;2.

Hibbard, J.P., Miller, B. V., Hames, W.E., Standard, I.D., Allen, J.S., Lavallee, S.B., and Boland, I.B., 2012, Kinematics, U-Pb geochronology, and 40Ar/39Ar thermochronology of the Gold Hill shear zone, North Carolina: The Cherokee orogeny in Carolinia, Southern Appalachians: Bulletin of the Geological Society of America, v. 124, no. 5, p. 643–656, doi: 10.1130/B30579.1.

Hibbard, J.P., van Staal, C.R., and Rankin, D.W., 2010, Comparative analysis of the geological evolution of the northern and southern Appalachian orogen: Late Ordovician–Permian, in Tollo, R.P., Bartholomew, M.J., Hibbard, J.P., and Karabinos, P.M., eds., From Rodinia to Pangea: The Lithotectonic Record of the Appalachian Region: Geological Society of America Memoir 206, p. 51–69, doi: 10.1130/2010.1206(03).

Hibbard, J.P., van Staal, C.R., and Rankin, D.W., 2007, A comparative analysis of pre-Silurian crustal building blocks of the northern and the southern Appalachian orogen: American Journal of Science, v. 307, p. 23–45, doi: 10.2475/01.2007.02.

Hibbard, J.P., Waldron, J.W.F., 2009, Truncation and translation of Appalachian promontories: Mid-Paleozoic strike-slip tectonics and basin initiation: Geology, v. 37; no. 6; p. 487–490; doi: 10.1130/G25614A.1

Horton, J. W., Jr.; Drake, A. A., Jr.; and Rankin, D. W, 1989, Tectonostratigraphic terranes and their Paleozoic boundaries in the central and southern Appalachians. In Dallmeyer, D., ed. Terranes in the circum- Atlantic Paleozoic orogens. Geological Society of America Special Paper v. 230, p.213–245.

Hoskin, P.W.O., and Ireland, T.R., 2000, Rare earth element chemistry of zircon and its use as a provenance indicator: Geology, v. 28, no. 7, p. 627, doi: 10.1130/0091-7613(2000)28<627:REECOZ>2.0.CO;2.

Hoskin, P., and Schaltegger, U., 2003, The composition of zircon and igneous and metamorphic petrogenesis: Reviews in Mineralogy and Geochemistry, v. 1, p. 27–62, doi: 10.2113/0530027.

Janák, M., Cornell, D., Froitzheim, N., De Hoog, J.C.M., Broska, I., Vrabec, M., and Hurai, V., 2009, Eclogite-hosting metapelites from the Pohorje Mountains (Eastern Alps): P-T evolution, zircon geochronology and tectonic implications: European Journal of Mineralogy, v. 21, no. 6, p. 1191–1212, doi: 10.1127/0935-1221/2009/0021-1966.

Johnson, B.S., Miller, B.V., Stewart, K.G., 2001, The nature and timing of Acadian deformation in the southern Appalachian Blue Ridge constrained by the Spruce Pine Plutonic Suite, western North Carolina: Geological Society of America Abstracts with Programs, v. 33 A30

Kish, S.A., 1983, A geochronological study of deformation and metamorphism in the Blue Ridge and Piedmont of the Carolinas: Ph.D. Dissertation, University of North Carolina, Chapel Hill, 220p.

Krogh, E.J., 1988, The garnet-clinopyroxene Fe-Mg geothermometer — a reinterpretation of existing experimental data: Contributions to Mineralogy and Petrology, v. 99, p. 44-48.

Kylander-Clark, A.R.C., Hacker, B.R., and Cottle, J.M., 2013, Laser-ablation split-stream ICP petrochronology: Chemical Geology, v. 345, p. 99–112, doi:10.1016/j.chemgeo.2013.02.019.

Kylander-Clark, A.R.C., Hacker, B.R., and Mattinson, C.G., 2012, Size and exhumation rate of ultrahigh-pressure terranes linked to orogenic stage: Earth and Planetary Science Letters, v. 321-322, p. 115-120.

Liu, S., Li, J., Santosh, M., 2010, First application of the revised Ti-in-zircon geothermometer to Paleoproterozoic ultrahigh-temperature granulites of Tuguiwula, Inner Mongolia, North China Craton: Contributions to Mineralogy and Petrology, v. 159, no. 2, p.225–235.

Maresch, W.V., Kluge, R., Baumann, A., Krückhans-Lueder, G., Pindell, J.L., Stanek, K-P., Stöckhert, B., 2009, The occurrence and timing of high-pressure metamorphism on

Margarita Island, Venezuela: a constraint on Caribbean–South America interaction, In: James K H, Lorente M A, Pindell J L, editors. The Origin and Evolution of the Caribbean Plate. Geological Society, London, Special Publications, v. 328, p.705-741.

McDonough, M.F., and Sun, S.S., 1995, The Composition of the Earth: Chemical Geology, v. 120, p. 223–253.

McSween, H., Abbott, R., and Raymond, L., 1989, Metamorphic conditions in the Ashe Metamorphic Suite, North Carolina Blue Ridge: Geology, v. 17, no. December, p. 1140–1143.

Miller, B. V., Stewart, K.G., Miller, C. F.; and Thomas, C. W., 2000a, U-Pb Ages from the Bakersville, North Carolina Eclogite: Taconian Eclogite Metamorphism Followed by Acadian and Alleghenian Cooling: GSA Abstracts with Programs, p. A–62.

Miller, C.F., Hatcher, R.D., Jr., Ayers, J.C., Coath, C.D., and Harrison, T.M., 2000b, Age and zircon inheritance of eastern Blue Ridge plutons, southwestern North Carolina and northeastern Georgia, with implications for magma history and evolution of the Southern Appalachian Orogen: American Journal of Science, v. 300, p. 142-172.

Miller, B. V., Fetter, A. H., and Stewart, K. G., 2006, Plutonism in three orogenic pulses, eastern Blue Ridge Province, southern Appalachians, Geological Society of America Bulletin, v. 118, p. 171–184.

Miller, B.V., Stewart, K.G., and Whitney, D.L., 2010, Three tectonothermal pulses recorded in eclogite and amphibolite of the Eastern Blue Ridge, Southern Appalachians, in Tollo, R.P., Bartholomew, M.J., Hibbard, J.P., and Karabinos, P.M., eds., From Rodinia to Pangea: The Lithotectonic Record of the Appalachian Region: Geological Society of America Memoir 206, p. 701–724, doi: 10.1130/2010.1206(27).

Misra, K.C., and Conte, J.A., 1991, Amphibolites of the Ashe and Alligator Back Formations, North Carolina: Samples of Late Proterozoic–Early Paleozoic oceanic crust: Geological Society of America Bulletin, v. 103, p. 737–750.

Moecher, D.P., Hietpas, J., Samson, S., Chakraborty, S., 2011, Insights into southern Appalachian tectonics from ages of detrital monazite and zircon in modern alluvium: Geosphere, v. 7, p. 494-512, doi: 10.1130/GES00615.1.

Moecher, D.P., Samson, S.D., and Miller, C.F., 2004, Precise Time and Conditions of Peak Taconian Granulite Facies Metamorphism in the Southern Appalachian Orogen, U.S.A., with Implications for Zircon Behavior during Crustal Melting Events: The Journal of Geology, v. 112, no. 3, p. 289–304, doi: 10.1086/382760.

Möller, A., O'Brien, P.J., Kennedy, A., Kröner, A., 2002, Polyphase zircon in ultrahigh-temperature granulites (Rogaland, SW Norway): constraints for Pb diffusion in zircon: Journal of Metamorphic Geology, v.20, p. 727–740, doi:10.1046/j.1525-1314.2002.00400.x

Mysen, B., and Griffin, W.L., 1973, Pyroxene stoichiometry and the breakdown of omphacite: American Mineralogist, v. 58, p.60–63.

Page, F.Z., Essene, E.J., and Mukasa, S.B, 2003, Prograde and retrograde history of eclogites from the eastern Blue Ridge, North Carolina, USA: Journal of Metamorphic Geology, v. 21, p. 685−698.

Platt, J.P., 1993, Exhumation of high-pressure rocks: a review of concepts and processes: Terra Nova, v. 5, no. 2, p. 119–133, doi: 10.1111/j.1365-3121.1993.tb00237.x.

Rankin, D.W., 1970, Stratigraphy and structure of Precambrian rocks in northwestern North Carolina, in Fisher, G.W., et al., eds., Studies of Appalachian geology—Central and southern: New York, Wiley Interscience, p. 227–245.

Rankin, D.W., Coish, R.A., Tucker, R.D., Peng, Z.X., Wilson, S.A., Rouff, A.A., 2007, Silurian Extension in the Upper Connecticut Valley, United States and the Origin of Middle Paleozoic Basins in the Québec Embayment: American Journal of Science, v. 307, p. 216–264, doi: 10.2475/01.2007.07.

Raymond, L.A., Yurkovich, S.P., and McKinney, M., 1989, Block-in-matrix structures in the North Carolina Blue Ridge belt and their significance for the tectonic history of the southern Appalachian orogen, in Horton, J.W., Jr., and Rast, N., eds., Mélanges and olistostromes of the U.S. Appalachians: Boulder, Colorado, Geological Society of America Special Paper 228, p. 195–215.

Rubatto, D., 2002, Zircon trace element geochemistry: partition with garnet and the link between U-Pb ages and metamorphism: Chemical Geology, v. 184, p. 123–138.

Săbău, G., and Massonne, H.J., 2003, Relationships Among Eclogite Bodies and Host Rocks in the Lotru Metamorphic Suite (South Carpathians, Romania): Petrological Evidence for Multistage Tectonic Emplacement of Eclogites in a Medium-Pressure Terrain: International Geology Review, v. 45, p. 225–262, doi: 10.2747/0020-6814.45.3.225.

Schwartz, S., Allemand, P., Guillot, S., 2001, Numerical model of the effect of serpentinites on the exhumation of eclogitic rocks: insights from the Monviso ophiolitic massif (Western Alps): Tectonophysics, v. 342, p. 193-206.

Skublov, S.G., Berezin, A.V., Berezhnaya, N.G., 2012, General Relations in the Trace-Element Composition of Zircons from Eclogites with Implications for the Age of Eclogites in the Belomorian Mobile Belt: Petrology, v. 20, no. 5, p. 427-449.

Stewart, K.G., Adams, M.G., and Trupe, C.H., 1997, Paleozoic structural evolution of the Blue Ridge thrust complex, western North Carolina, in, Stewart, K.G., et al., eds., Paleozoic structure, metamorphism, and tectonics of the Blue Ridge of western North Carolina: Chapel Hill, North Carolina, Carolina Geological Society 1997 Field Trip Guidebook, p. 21–32.

Swanson, S. E., and Raymond, L. A., 2010, Petrogenesis of chromite in metaultramafic rocks of the Spruce Pine area, North Carolina, Southeastern Geology, v. 47, p. 147-172.

Syvertsen, K.A., 2006, Electron backscatter analyses of omphacite to constrain eclogite exhumation in the Blue Ridge of western North Carolina. [M.S. Thesis]: Chapel Hill, University of North Carolina, 137 p.

Thompson, A.B., Schulmann, K., and Jezek, J., 1997, Thermal evolution and exhumation in obliquely convergent (transpressive) orogens: Tectonophysics, v. 280, p. 171–184, doi: 10.1016/S0040-1951(97)00144-3.

Tomkins, H.S., Powell, R., and Ellis, D.J., 2007, The pressure dependence of the zirconium-in-rutile thermometer: Journal of Metamorphic Geology, v. 25, no. 6, p. 703–713, doi: 10.1111/j.1525-1314.2007.00724.x.

Tremblay, A., Castonguay, S., 2002, Structural evolution of the Laurentian margin revisited (southern Quebec Appalachians): Implications for the Salinian orogeny and successor basins: Geology, v. 30, no. 1, p. 79-82.

Trupe, C.H., Stewart, K.G., Adams, M.G., and Foudy, J.P., 2004, Deciphering the Grenville of the southern Appalachians through evaluation of the post-Grenville tectonic history in northwestern North Carolina: Geological Society of America Memoirs, v. 197, p. 679–695, doi: 10.1130/0-8137-1197-5.679.

Trupe, C.H., Stewart, K.G., Adams, M.G., Waters, C.L., Miller, B. V., and Hewitt, L.K., 2003, The Burnsville fault: Evidence for the timing and kinematics of southern Appalachian Acadian dextral transform tectonics: Geological Society of America Bulletin, v. 115, p. 1365–1376, doi: 10.1130/B25256.1.

Turcotte, D.L, Schubert, G., 1982, Geodynamics, Wiley, New York, 450 pp.

Vermeesch, P., 2006, Tectonic discrimination diagrams revisted: Geochemistry Geophysics Geosystems, v. 7, n. 6, p. 1-55, doi: 10.1029/2005GC001092.

Warner, R., Poterala, S., Fleisher, C., 2008, A Note on Uranium Minerals from the Spruce Pine Area, in, Glover, A., Taylor, K., eds., Spruce Pine Mining District, North Carolina, Carolina Geological Society Annual Field Trip, p. 29-52.

Warren, C.J., 2013, Exhumation of (ultra-) high-pressure terranes: concepts and mechanisms: Solid Earth, v. 4 , p. 75–92, doi: 10.5194/se-4-75-2013.

Warren, C.J., Beaumont, C., and Jamieson, R.A., 2008, Modelling tectonic styles and ultra-high pressure (UHP) rock exhumation during the transition from oceanic subduction to continental collision: Earth Planetary Science Letters, v. 267, p. 129–145, doi: 10.1016/j.epsl.2007.11.025.

Waters, C.L., 1999, Mapping and Related Studies of Pre-Alleghanian Tectonic Features within the Blue Ridge Thrust Complex of Western North Carolina, Micaville Quadrangle [M.S. thesis]: Chapel Hill, University of North Carolina at Chapel Hill, 90 p.

Waters-Tormey, C., and Stewart, K.G., 2010, Heterogeneous wrench-dominated transpression in the deep crust recorded by the Burnsville fault and related structures , Blue Ridge , North Carolina : Implications for the Acadian orogeny in the Southern Appalachians: Geological Society of America Memoirs, v. 206, p. 917-934, doi: 10.1130/2010.1206(35).

Watson, E.B., Wark, D. a., and Thomas, J.B., 2006, Crystallization thermometers for zircon and rutile: Contributions to Mineralogy and Petrology, v. 151, no. 4, p. 413–433, doi: 10.1007/s00410-006-0068-5.

Whalen, J.B., McNicoll, V.J., van Staal, C.R., Lissenberg, C.J., Longstaffe, F.J., Jenner, G. a., and van Breeman, O., 2006, Spatial, temporal and geochemical characteristics of Silurian collision-zone magmatism, Newfoundland Appalachians: An example of a rapidly evolving magmatic system related to slab break-off: Lithos, v. 89, no. 3-4, p. 377–404, doi: 10.1016/j.lithos.2005.12.011.

Willard, R.A., and Adams, M.G., 1994, Newly discovered eclogite in the southern Appalachian orogen, northwestern North Carolina: Earth and Planetary Science Letters, v. 123, p. 61–70.

Williams, I.S., Buick, I.S. & Cartwright, I., 1996. An extended episode of early Mesoproterozoic metamorphic fluid flow in the Reynolds Range, Central Australia: Journal of Metamorphic Geology, v. 14, p. 29–47.

Wilson, R.A., Kamo, S.L., 2012, The Salinic Orogeny in northern New Brunswick: geochronological constraints and implications for Silurian stratigraphic nomenclature: Canadian Journal of Earth Science, v. 49, p. 222-238, doi:10.1139/E11-041.